CHAPTER 3: STRUCTURAL EVALUATION†

In this chapter, the structural components of the HI-STORM 100 System that are important to safety (ITS) are identified and described. The objective of the structural analyses is to ensure that the integrity of the HI-STORM 100 System is maintained under all credible loads for normal, off-normal, and design basis accident/natural phenomena. The chapter results support the conclusion that the confinement, criticality control, radiation shielding, and retrievability criteria set forth by 10CFR72.236(l), 10CFR72.124(a), 10CFR72.104, 10CFR72.106, and 10CFR72.122(l) are met. In particular, the design basis information contained in the previous two chapters and in this chapter provides sufficient data to permit structural evaluations to demonstrate compliance with the requirements of 10CFR72.24. To facilitate regulatory review, the assumptions and conservatism's inherent in the analyses are identified along with a complete description of the analytical methods, models, and acceptance criteria. A summary of other material considerations, such as corrosion and material fracture toughness is also provided. Design calculations for the HI-TRAC transfer cask are included where appropriate to comply with the guidelines of NUREG-1536.

~~Detailed numerical computations supporting the conclusions in the main body of this chapter are presented in a series of appendices. Where appropriate, the subsections make reference to results in the appendices. Section 3.6.3 contains the complete list of appendices that support this chapter.~~

The organization of technical information in this chapter follows the format and content guidelines of USNRC Regulatory Guide 3.61 (February 1989). The FSAR ensures that the responses to the review requirements listed in NUREG-1536 (January 1997) are complete and comprehensive. The areas of NRC staff technical inquiries, with respect to structural evaluation in NUREG-1536, span a wide array of technical topics within and beyond the material in this chapter. To facilitate the staff's review to ascertain compliance with the stipulations of NUREG-1536, Table 3.0.1 "Matrix of NUREG-1536 Compliance - Structural Evaluation", is included in this chapter. A comprehensive cross-reference of the topical areas set forth in NUREG-1536, and the location of the required compliance information is contained in Table 3.0.1.

Section 3.7 describes in detail HI-STORM 100 System's compliance to NUREG-1536 Structural Evaluation Requirements.

---

† This chapter has been prepared in the format and section organization set forth in Regulatory Guide 3.61. However, the material content of this chapter also fulfills the requirements of NUREG-1536. Pagination and numbering of sections, figures, and tables are consistent with the convention set down in Chapter 1, Section 1.0, herein. Finally, all terms-of-art used in this chapter are consistent with the terminology of the glossary (Table 1.0.1) and component nomenclature of the Bill-of-Materials (Section 1.5).

The HI-STORM 100 System matrix of compliance table given in this section is developed with the supposition that the storage overpack is designated as a steel structure which falls within the purview of subsection 3.V.3 "Other Systems Components Important to Safety" (page 3-28 of NUREG-1536), and therefore, does not compel the use of reinforced concrete. (Please refer to Table 1.0.3 for an explicit statement of exception on this matter). The concrete mass installed in the HI-STORM 100 overpack is accordingly equipped with "plain concrete" for which the sole applicable industry code is ACI 318.1 (92). Plain concrete, in contrast to reinforced concrete, is the preferred shielding material HI-STORM 100 because of three key considerations:

(i) Plain concrete is more amenable to a void free pour than reinforced concrete in narrow annular spaces typical of ventilated vertical storage casks.

(ii) The tensile strength bearing capacity of reinforced concrete is not required to buttress the steel weldment of the HI-STORM 100 overpack.

(iii) The compression and bearing strength capacity of plain concrete is unaffected by the absence of rebars. A penalty factor, on the compression strength, pursuant to the provisions of ACI-318.1 is, nevertheless, applied to insure conservatism. However, while plain concrete is the chosen shielding embodiment for the HI-STORM 100 storage overpack, all necessary technical, procedural Q.C., and Q.A. provisions to insure nuclear grade quality will be implemented by utilizing the relevant sections from ACI-349 (85) as specified in Appendix 1.D.

In other words, guidelines of NUREG 1536 pertaining to reinforced concrete are considered to insure that the material specification, construction quality control and quality assurance of the shielding concrete comply with the provisions of ACI 349 (85). These specific compliance items are listed in the compliance matrix.

TABLE 3.0.1 MATRIX OF NUREG-1536 COMPLIANCE ITEMS – STRUCTURAL EVALUATION †

PARAGRAPH IN NUREG-1536	NUREG-1536 COMPLIANCE ITEM	LOCATION IN FSAR CHAPTER 3	LOCATION OUTSIDE OF FSAR CHAPTER 3
IV.1.a	ASME B&PV Compliance		
	NB	3.1.1	Tables 2.2.6,2.2.7
	NG	3.1.1	Tables 2.2.6,2.2.7
IV.2	Concrete Material Specification		Appendix 1.D
IV.4	Lifting Devices	3.1; 3.4~~;3.D;3.E;3.AC~~	
V.	Identification of SSC that are ITS		Table 2.2.6
"	Applicable Codes/Standards	3.6.1	Table 2.2.6
"	Loads		Table 2.2.13
"	Load Combinations	3.1.2.1.2; Tables 3.1.1-3.1.5	Table 2.2.14
"	Summary of Safety Factors	3.4.3; 3.4.4.2; 3.4.4.3.1-3 3.4.6-3.4.9; Tables 3.4.3-3.4.9	
"	Design/Analysis Procedures	Chapter 3~~ plus Appendices~~	
"	Structural Acceptance Criteria		Tables 2.2.10-2.2.12

Table continued on following page

TABLE 3.0.1 (CONTINUED)

"	Material/QC/Fabrication	Table 3.4.2	Chap. 9; Chap. 13
"	Testing/In-Service Surveillance		Chap. 9; Chap. 12
"	Conditions for Use		Table 1.2.6; Chaps. 8,9,12
V.1.a	Description of SSC	3.1.1	1.2
V.1.b.i.(2)	Identification of Codes & Standards		Tables 2.2.6, 2.2.7
V.1.b.ii	Drawings/Figures		1.5
"	Identification of Confinement Boundary		1.5; 2.3.2; 7.1; Table 7.1.1
"	Boundary Weld Specifications	3.3.1.4	1.5; Table 7.1.2
"	Boundary Bolt Torque	NA	
"	Weights and C.G. Location	Tables 3.2.1-3.2.4	
"	Chemical/Galvanic Reactions	3.4.1; Table 3.4.2	
V.1.c	Material Properties	3.3; Tables 3.3.1-3.3.5	1.A; 1.C; 1.D
"	Allowable Strengths	Tables 3.1.6-3.1.17	Tables 2.2.10-2.2.12; 1.D
"	Suitability of Materials	3.3; Table 3.4.2	1.A; 1.B; 1.D
"	Corrosion	3.3	
"	Material Examination before Fabrication		9.1.1

Table continued on following page

TABLE 3.0.1 (CONTINUED)

"	Material Testing and Analysis		9.1; Table 9.1.1;1.D
"	Material Traceability		9.1.1
"	Material Long Term Performance	3.3; 3.4.11; 3.4.12	9.2
"	Materials Appropriate to Load Conditions		Chap. 1
"	Restrictions on Use		Chap. 12
"	Temperature Limits	Table 3.1.17	Table 2.2.3
"	Creep/Slump	3.4.4.3.3.2~~; 3.F~~	
"	Brittle Fracture Considerations	3.1.2.3; Table 3.1.18	
"	Low Temperature Handling		2.2.1.2
V.1.d.i.(1)	Normal Load Conditions		2.2.1; Tables 2.2.13,2.2.14
"	Fatigue	3.1.2.4	
"	Internal Pressures/Temperatures for Hot and Cold Conditions	3.4.4.1	2.2.2; Tables 2.2.1,2.2.3
"	Required Evaluations		
"	Weight+Pressure	3.4.4.3.1.2	
"	Weight/Pressure/Temp.	3.4.4.3.1.2	
"	Free Thermal Expansion	3.4.4.2~~; 3.U; 3.W; 3.I;3.AF~~	Tables 4.4.15, 4.5.4

Table continued on following page

TABLE 3.0.1 (CONTINUED)

V.1.d.i.(2)	Off-Normal Conditions		2.2.2; Tables 2.2.13, 2.2.14; 11.1
V.1.d.i.(3)	Accident Level Events and Conditions	Tables 3.1.1, 3.1.2	2.2.3; Tables 2.2.13, 2.2.14; 11.2
V.1.d.i.(3).(a)	Storage Cask Vertical Drop	3.1.2.1.1.2; 3.4.10; 3.A	2.2.3.1
"	Storage Cask Tipover	3.1.2.1.1.1; 3.4.10; 3.A	2.2.3.2
"	Transfer Cask Horizontal Drop	3.4.9~~; 3.Z; 3.AL~~	2.2.3.1
V.1.d.i.(3).(b)	Explosive Overpressure	3.1.2.1.1.4~~;3AK~~	2.2.3.10
V.1.d.i.(3).(c)	Fire		
"	Structural Evaluations	3.4.4.2	2.2.3.3
"	Material Properties		11.2
"	Material Suitability	3.1.2.2; 3.3.1.1	Table 2.2.3;11.2
V.1.d.i.(3).(d)	Flood		
"	Identification	3.1.2.1.1.3; 3.4.6	2.2.3.6
"	Cask Tipover	3.4.6	
"	Cask Sliding	3.4.6	
"	Hydrostatic Loading	3.1.2.1.1.3; 3.4.6	72-1008(3.H)
"	Consequences		11.2
V.1.d.i.(3).(e)	Tornado Winds		
"	Specification	3.1.2.1.1.5	2.2.3.5; Table 2.2.4
"	Drag Coefficients	3.4.8~~; 3.C~~	
"	Load Combination	3.4.8~~; 3.C~~	

Table continued on following page

TABLE 3.0.1 (CONTINUED)

"	Overturning	*3.4.8*~~3.C~~	
"	Overturning –Transfer	NA	
V.1.d.i.(3).(f)	Tornado Missiles		
"	Missile Parameters	3.1.2.1.1.5	Table 2.2.5
"	Tipover	3.4.8~~; 3.C~~	
"	Damage	*3.4.8.1; 3.4.8.2*~~3.B; 3.G; 3.H; 3Z; 3.AM~~	
"	Consequences	3.4.8.1; 3.4.8.2	11.2
V.1.d.i.(3).(g)	Earthquakes		
"	Definition of DBE	3.1.2.1.1.6; 3.4.7	2.2.3.7; Table 2.2.8
"	Sliding	3.4.7	
"	Overturning	3.4.7	
"	Structural Evaluations	3.4.7~~; 3B~~	11.2
V.1.d.i.(4).(a)	Lifting Analyses		
"	Trunnions		
"	Requirements	3.1.2.1.2; 3.4.3.1;3.4.3.2	72-1008(3.4.3);2.2.1.2
"	Analyses	3.4.3.1; 3.4.3.2~~; 3.D;3.E; 3.AC; 3.AE~~	72-1008(3.4.3)
"	Other Lift Analyses	3.4.3.7-3.4.3.9~~; 3.D; 3.AB; 3.AC; 3.AE; 3.AD; 3.AI; 3.AJ~~	
V.1.d.i.(4).(b)	Fuel Basket		
"	Requirements	3.1.2.1.2; Table 3.1.3	
"	Specific Analyses	3.4.4.2; 3.4.4.3; 3.6.3~~; 3.U; 3.W; 3.I; 3.N 3.T; 3.Y~~	72-1008(3.4.4.3.1.2; 3.4.4.3.1.6; 3.AA; 3.M; 3.H; 3.I)
"	Dynamic Amplifiers	*3.4.4.4.1*~~3.X~~	

Table continued on following page

TABLE 3.0.1 (CONTINUED)

"	Stability	3.4.4.3; 3.4.4.4~~; 3.AK~~	72-1008(Figures 3.4.27-32)
V.1.d.i.(4).(c)	Confinement Closure Lid Bolts		
"	Pre-Torque	NA	
"	Analyses	NA	
"	Engagement Length	NA	
"	Miscellaneous Bolting		
"	Pre-Torque	*3.4.3.7; 3.4.3.8~~3.AC~~*	
"	Analyses	*3.4.4.3.2.2~~3.L~~*	
"	Engagement Length	*3.4.3.5; 3.4.3.7; 3.4.3.8~~3.AC; 3.D~~*	
V.1.d.i.(4)	Confinement		
"	Requirements	3.1.2.1.2; Table 3.1.4	Chap. 7
"	Specific Analyses	3.6.3; Tables 3.4.3, 3.4.4~~; 3.D; 3.N 3.T~~	72-1008(3.E; 3.K; 3.I; 3.AA 3.4.4.3.1.5)
"	Dynamic Amplifiers	~~3.X;~~ 3.4.4.1	
"	Stability	3.4.4.3.1	72-1008(3.H)
"	Overpack		
"	Requirements	3.1.2.1.2; Tables 3.1.1, 3.1.5	
"	Specific Analyses	3.6.3; ~~3.B; 3.D; 3.L; 3.M; 3.AC; 3.D;~~ 3.4.4.3~~; 3.K; 3.AK~~	

Table continued on following page

TABLE 3.0.1 (CONTINUED)

"	Dynamic Amplifiers	3.4.4.3.2~~; 3.X~~	
"	Stability	3.4.4.3; Table 3.1.1; 3.4.4.5~~; 3.AK~~	
"	Transfer Cask		
"	Requirements	3.1.2.1.2; Table 3.1.5	
"	Specific Analyses	3.4.4.3; 3.6.3~~; 3.E; 3.H; 3.I; 3.Z; 3.AD; 3.AE; 3.AA; 3.AI; 3.AB; 3.AD; 3.AG; 3.F; 3.AH; 3.AJ; 3.AL; 3.AM~~	
"	Dynamic Amplifiers	*3.4.4.4.13*~~.X~~	
"	Stability	NA	2.2.3.1

† Legend for Table 3.0.1

Per the nomenclature defined in Chapter 1, the first digit refers to the chapter number, the second digit is the section number within the chapter; an alphabetic character in the second place means it is an appendix to the chapter.

72-1008	HI-STAR 100 Docket Number where the referenced item is located
NA	Not Applicable for this item

3.4 GENERAL STANDARDS FOR CASKS

3.4.1 Chemical and Galvanic Reactions

In this section, it is shown that there is no credible mechanism for chemical or galvanic reactions in the HI-STORM 100 System (including HI-STORM 100S and HI-STORM 100SA).

The MPC, which is filled with helium, provides a nonaqueous and inert environment. Insofar as corrosion is a long-term time-dependent phenomenon, the inert gas environment in the MPC precludes the incidence of corrosion during storage on the ISFSI. Furthermore, the only dissimilar material groups in the MPC are: (1) *the neutron absorber material* ~~Boral~~™ and stainless steel and (2) aluminum and stainless steel. *Neutron absorber materials* ~~Boral~~ and stainless steel*s* have been used in close proximity in wet storage for over 30 years. Many spent fuel pools at nuclear plants contain fuel racks, which are fabricated from *neutron absorber materials* ~~Boral~~ and stainless steel materials, with geometries similar to the MPC. Not one case of chemical or galvanic degradation has been found in fuel racks built by Holtec. This experience provides a sound basis to conclude that corrosion will not occur in these materials. Additionally, the aluminum conduction inserts and stainless steel basket are very close on the galvanic series chart. Aluminum, like other metals of its genre (e.g., titanium and magnesium) rapidly passivates in an aqueous environment, leading to a thin ceramic (Al_2O_3) barrier, which renders the material essentially inert and corrosion-free over long periods of application. The physical properties of the material, e.g., thermal expansion coefficient, diffusivity, and thermal conductivity, are essentially unaltered by the exposure of the aluminum metal stock to an aqueous environment. In order to eliminate the incidence of aluminum water reaction inside the MPC during fuel loading operation (when the MPC is flooded with pool water) *all* aluminum surfaces will be pre-passivated or anodized before installation of *the neutron absorber material* ~~Boral~~ or *the* conduction inserts in the MPC.

The HI-STORM 100 storage overpack and the HI-TRAC transfer cask each combine low alloy and nickel alloy steels, carbon steels, neutron and gamma shielding materials, and bolting materials. All of these materials have a long history of nongalvanic behavior within close proximity of each other. The internal and external steel surfaces of each of the storage overpacks are sandblasted and coated to preclude surface oxidation. The HI-TRAC coating does not chemically react with borated water. Therefore, chemical or galvanic reactions involving the storage overpack materials are highly unlikely and are not expected.

In accordance with NRC Bulletin 96-04 [3.4.7], a review of the potential for chemical, galvanic, or other reactions among the materials of the HI-STORM 100 System, its contents and the operating environments, which may produce adverse reactions, has been performed. Table 3.4.2 provides a listing of the materials of fabrication for the HI-STORM 100 System and evaluates the performance of the material in the expected operating environments during short-term loading/unloading operations and long-term storage operations. As a result of this review, no operations were identified which could produce adverse reactions beyond those conditions already analyzed in this FSAR.

3.4.2 Positive Closure

There are no quick-connect/disconnect ports in the confinement boundary of the HI-STORM 100 System. The only access to the MPC is through the storage overpack lid, which weighs over 23,000 pounds (see Table 3.2.1). The lid is fastened to the storage overpack with large bolts. Inadvertent opening of the storage overpack is not feasible; opening a storage overpack requires mobilization of special tools and heavy-load lifting equipment.

3.4.3 Lifting Devices

As required by Reg. Guide 3.61, in this subsection, analyses for all lifting operations applicable to the deployment of a member of the HI-STORM 100 family are presented to demonstrate compliance with applicable codes and standards.

The HI-STORM 100 System has the following components and devices participating in lifting operations: lifting trunnions located at the top of the HI-TRAC transfer cask, lid lifting connections for the HI-STORM 100 lid and for other lids in the HI-TRAC transfer cask, connections for lifting and carrying a loaded HI-STORM 100 vertically, and lifting connections for the loaded MPC.

Analyses of HI-STORM 100 storage overpack and HI-TRAC transfer cask lifting devices are *reported*~~provided~~ in this submittal. Analyses of MPC lifting operations are presented in the HI-STAR 100 FSAR (Docket Number 72-1008, Subsection 3.4.3) and are also applicable here.

The evaluation of the adequacy of the lifting devices entails careful consideration of the applied loading and associated stress limits. The load combination D+H, where H is the "handling load", is the generic case for all lifting adequacy assessments. The term D denotes the dead load. Quite obviously, D must be taken as the bounding value of the dead load of the component being lifted. In all lifting analyses considered in this document, the handling load H is assumed to be 0.15D. In other words, the inertia amplifier during the lifting operation is assumed to be equal to 0.15g. This value is consistent with the guidelines of the Crane Manufacturer's Association of America (CMAA), Specification No. 70, 1988, Section 3.3, which stipulates a dynamic factor equal to 0.15 for slowly executed lifts. Thus, the "apparent dead load" of the component for stress analysis purposes is $D^* = 1.15D$. Unless otherwise stated, all lifting analyses in this report use the "apparent dead load", D^*, as the lifted load.

Analysis methodology to evaluate the adequacy of the lifting device may be analytical or numerical. For the analysis of the trunnion, an accepted conservative technique for computing the bending stress is to assume that the lifting force is applied at the tip of the trunnion "cantilever" and that the stress state is fully developed at the base of the cantilever. This conservative technique, recommended in NUREG-1536, is applied to all trunnion analyses presented in this SAR and has also been applied to the trunnions analyzed in the HI-STAR 100 FSAR.

In general, the stress analysis to establish safety pursuant to NUREG-0612, Regulatory Guide 3.61, and the ASME Code, requires evaluation of three discrete zones which may be referred to as (i) the

trunnion, (ii) the trunnion/component interface, hereinafter referred to as Region A, and (iii) the rest of the component, specifically the stressed metal zone adjacent to Region A, herein referred to as Region B. During this discussion, the term "trunnion" applies to any device used for lifting (i.e., trunnions, lift bolts, etc.)

Stress limits germane to each of the above three areas are discussed below:

i. Trunnion: NUREG-0612 requires that under the "apparent dead load", D^*, the maximum primary stress in the trunnion be less than 10% of the trunnion material ultimate strength *and* less than 1/6th of the trunnion material yield strength. Because of the materials of construction selected for trunnions in all HI-STORM 100 System components, the ultimate strength-based limit is more restrictive in every case. Therefore, all trunnion safety factors reported in this document pertain to the ultimate strength-based limit.

ii. Region A: Trunnion/Component Interface: Stresses in Region A must meet ASME Code Level A limits under applied load D*. Additionally, Regulatory Guide 3.61 requires that the primary stress under 3D*, associated with the cross-section, be less than the yield strength of the applicable material. In cases involving section bending, the developed section moment may be compared against the plastic moment at yield. The circumferential extent of the characteristic cross-section at the trunnion/component interface is calculated based on definitions from ASME Section III, Subsection NB and is defined in terms of the shell thickness and radius of curvature at the connection to the trunnion block. By virtue of the construction geometry, only the mean shell stress is categorized as "primary" for this evaluation.

iii. Region B: Typically, the stresses in the component in the vicinity of the trunnion/component interface are higher than elsewhere. However, exceptional situations exist. For example, when lifting a loaded MPC, the MPC baseplate, which supports the entire weight of the fuel and the fuel basket, is a candidate location for high stress even though it is far removed from the lifting location (which is located in the top lid).

Even though the baseplate in the MPC would normally belong to the Region B category, for conservatism it was considered as Region A in the HI-STAR 100 SAR. The pool lid and the transfer lid of the HI-TRAC transfer cask also fall into this dual category. In general, however, all locations of high stress in the component under D^* must also be checked for compliance with ASME Code Level A stress limits.

Unless explicitly stated otherwise, all analyses of lifting operations presented in this report follow the load definition and allowable stress provisions of the foregoing. Consistent with the practice adopted throughout this chapter, results are presented in dimensionless form, as safety factors, defined as

$$\text{Safety Factor, } \beta = \frac{\text{Allowable Stress in the Region Considered}}{\text{Computed Maximum Stress in the Region}}$$

The safety factor, defined in the manner of the above, is the added margin over what is mandated by the applicable code (NUREG-0612 or Regulatory Guide 3.61).

In the following subsections, we briefly describe each of the lifting analyses performed to demonstrate compliance with regulations. Summary results are presented for each of the analyses.

It is recognized that stresses in Region A are subject to two distinct criteria, namely Level A stress limits under D* and yield strength at 3D*. We will identify the applicable criteria in the summary tables, under the column heading "Item", using the "3D*" identifier.

All of the lifting analyses reported on in this Subsection are designated as Load Case 01 in Table 3.1.5.

3.4.3.1 125 Ton HI-TRAC Lifting Analysis - Trunnions

The lifting device in the 125-ton HI-TRAC cask is presented in Holtec Drawing 1880 (Section 1.5 herein). The two lifting trunnions for HI-TRAC are spaced at 180 degrees. The trunnions are designed for a two-point lift in accordance with the aforementioned NUREG-0612 criteria. Figure 3.4.21 shows the overall lifting configuration. ~~Appendix 3.E contains the lifting trunnion stress analysis for the 125 Ton HI-TRAC. Figures within that appendix provide details to support the analysis.~~ *The lifting analysis demonstrates* ~~It is demonstrated in Appendix 3.E~~ that the stresses in the trunnions, computed using the conservative methodology described previously, comply with NUREG-0612 provisions.

Specifically, the following results are obtained:

125 Ton HI-TRAC Lifting Trunnions†		
	Value (ksi)	**Safety Factor**
Bending stress	16.98	1.07
Shear stress	7.23	1.5

† The lifted load is 245,000 lb.(a value that bounds the actual lifted weight from the pool after the lift yoke weight is eliminated per Table 3.2.4).

Note that the safety factor presented in the previous table represents the *additional* margin beyond the mandated limit of 6 on yield strength and 10 on tensile strength.

3.4.3.2 125 Ton HI-TRAC Lifting - Trunnion Lifting Block Welds, Bearing, and Thread Shear Stress (Region A)

~~Appendix 3.E contains calculations that analyze~~ *As part of the Region A evaluation,* the weld group connecting the lifting trunnion block to the inner and outer shells, and to the HI-TRAC top flange, *is analyzed.* Conservative analyses are also performed to determine safety factors for bearing stress and for thread shear stress at the interface between the trunnion and the trunnion block. The following results are obtained:

125 Ton HI-TRAC Lifting Trunnion Block (Region A Evaluation)			
Item	**Value (ksi)**	**Allowable (ksi)**	**Safety Factor**
Trunnion Block Bearing Stress	5.94	11.4	1.92
Trunnion Block Thread Shear Stress	5.19	6.84	1.32
Weld Shear Stress (3D*)	8.03†	11.4	1.42

† A quality factor of 0.45 has been applied to the weld group. We have followed the guidance of ASME Code, Section III, Subsection NG-3352-1 (other referenced codes such as Subsection NF or NUREG-0612 do not apply penalty factors to the structural welds).

3.4.3.3 125 Ton HI-TRAC Lifting - Structure near Trunnion (Region B/Region A)

~~Appendix 3.AE contains results of a finite element analysis of the region in the 125 Ton HI-TRAC structure adjacent to the lifting trunnions. Appendix 3.AE shows that the primary stresses in the 125 Ton HI-TRAC structure comply with the Level A stress limits for Subsection NF structures.~~

A three-dimensional elastic model of the 125 Ton HI-TRAC metal components is analyzed using the ANSYS finite element code. ~~Figure 3.AE.1 shows details of the one-quarter symmetry model using a color-coding to identify the various modeled parts.~~ The structural model includes, in addition to the trunnion and the trunnion block, a portion of the inner and outer HI-TRAC shells and the HI-TRAC top flange. ~~In Appendix 3.AE, s~~Stress results over the characteristic interface section are summarized and compared with allowable strength limits per ASME Section III, Subsection NF, and per Regulatory Guide 3.61. *The results show that the primary stresses in the 125 Ton HI-TRAC structure comply with the Level A stress limits for Subsection NF structures.*

The results from the analysis ~~in Appendix 3.AE~~ are summarized below:

125 Ton HI-TRAC Trunnion Region (Regions A and B)			
Item	**Value (ksi)**	**Allowable (ksi)**	**Safety Factor**
Membrane Stress	6.1859	17.5	2.83
Membrane plus Bending Stress	8.1919	26.25	3.2
Membrane Stress (3D*)	18.56	34.6	1.86

3.4.3.4 100 Ton HI-TRAC Lifting Analysis

The lifting trunnions and the trunnion blocks for the 100 Ton HI-TRAC are identical to the trunnions analyzed ~~in Appendices 3.E and 3.AE~~ for the 125 Ton HI-TRAC. However, the outer shell geometry (outer diameter) is different. A calculation performed in the spirit of strength-of-materials provides justification that, despite the difference in local structure at the attachment points, the stresses in the body of the HI-TRAC 100 Ton unit meet the allowables set forth in Subsection 3.1.2.2.

Figure 3.4.10 illustrates the differences in geometry, loads, and trunnion moment arms between the body of the 125-Ton HI-TRAC and the body of the 100-Ton HI-TRAC. It is reasonable to assume that the level of stress in the 100 Ton HI-TRAC body, in the immediate vicinity of the interface (Section X-X in Figure 3.4.10), is proportional to the applied force and the bending moment applied. In what follows, the subscripts 1 and 0 refer to 100 Ton and 125 Ton casks, respectively. Figure 3.4.10 shows the location of the area centroid (with respect to the outer surface) and the loads and moment arms associated with each construction. Conservatively, neglecting all other interfaces between the top of the trunnion block and the top flange and between the sides of the trunnion block and the shells, equilibrium is maintained by developing a force and a moment in the section comprised of the two shell segments interfacing with the base of the trunnion block.

The most limiting stress state is in the outer shell at the trunnion block base interface. The stress level in the outer shell at Section X-X is proportional to P/A + Mc/I. Evaluating the stress for a unit width of section permits an estimate of the stress state in the HI-TRAC 100 outer shell if the corresponding stress state in the HI-TRAC 125 is known (the only changes are the applied load, the moment arm and the geometry). Using the geometry shown in Figure 3.4.10 gives the result as:

Stress (HI-TRAC 100 outer shell) = 1.236 x Stress (HI-TRAC 125 outer shell)

The tabular results in the previous subsection can be adjusted accordingly and are reported below:

100 Ton HI-TRAC Near Trunnion (Region A and Region B)	
Item	**Safety Factor**
Membrane Stress	2.29
Membrane plus Bending Stress	2.59
Membrane Stress (3D*)	1.50

3.4.3.5 HI-STORM 100 Lifting Analyses

There are two vertical lifting scenarios for the HI-STORM 100 storage overpack carrying a fully loaded MPC. Figure 3.4.17 shows a schematic of these lifting scenarios. Both lifting scenarios are examined ~~in Appendix 3.D~~ using finite element models that focus on the local regions near the lift points. The analysis ~~in Appendix 3.D~~ is based on the geometry of the HI-STORM 100; ~~T~~*t*he alterations to the lid and to the length of the overpack barrel to configure the HI-STORM 100S have no effect on the conclusions reached in the area of the baseplate. Therefore, there is no separate analysis for ~~the analysis of~~ the baseplate, inboard of the inner shell, for the HI-STORM 100S as the results are identical to or bounded by the results *presented here*~~documented in Appendix 3.D~~. Since the upper portion of the HI-STORM 100S, the HI-STORM 100S lid, and the radial ribs and anchor block have a different configuration than the HI-STORM 100, separate calculations have been performed for these areas of the HI-STORM 100S.

Scenario #1 considers a "bottom lift" where the fully loaded HI-STORM 100 storage overpack is lifted vertically by four synchronized hydraulic jacks each positioned at one of the four inlet air vents. This lift allows for installation and removal of "air pads" which may be used for horizontal positioning of HI-STORM 100 at the ISFSI pad.

Scenario #2, labeled the "top lift scenario" considers the lifting of a fully loaded HI-STORM 100 vertically through the four lifting lugs located at the top end.

No structural credit is assumed for the HI-STORM concrete in either of the two lifting scenarios except as a vehicle to transfer compressive loads.

For the bottom lift, a three-dimensional one-quarter symmetry finite element model of the bottom region of the HI-STORM 100 storage overpack is constructed. The model includes the inner shell, the outer shell, the baseplate, the inlet vent side and top plates, and the radial plates connecting the inner and outer shells. ~~Further details of the model are provided in Appendix 3.D. The key results are contained in Figure 3.D.3 that shows the stress intensity distribution on the HI-STORM 100 storage overpack.~~

For the analysis of the "top lift" scenario, a three-dimensional 1/8-symmetry finite element model of the top segment of HI-STORM 100 storage overpack is constructed. The metal HI-STORM 100 material is modeled (shells, radial plates, lifting block, ribs, vent plates, etc.) using shell or solid elements. ~~Color-coded views of the model are given in Figure 3.D.2.~~ Lumped weights are used to ensure that portions of the structure not modeled are, in fact, properly represented as part of a lifted load. The model is supported vertically at the lifting lug.

~~Figures 3.D.4(a) through 3.D.4(c) and Figure 3.D.5(a) through 3.D.5(c) show the stress intensity results under the lifted load and in the baseplate region, respectively.~~

To provide an alternate calculation to demonstrate that the bolt anchor blocks are adequate, we compute the average normal stress in the net metal area of the block under three times the lifted load. Further conservatism is introduced by including an additional 15% for dynamic amplification, i.e., the total load is equal to 3D*.

The average normal load in one bolt anchor block is

Load = 3 x 1.15 x 360,000 lb./4 = 310,500 lb. (Weight comes from Table 3.2.1)

The net area of the bolt anchor block is

Area = 5" x 5" – (3.14159/4)/4 x (3.25" x 3.25") = 16.70 sq. inch (Dimensions from BM-1575)

Therefore, the safety factor (yield strength at 350 degrees F/calculated stress from Table 3.3.3) is

SF = 32,700 psi/ (Load/Area) = 1.76

~~Appendix 3.D also examines t~~*The* shear stress in the threads of the lifting block *is also examined.* This analysis considers a cylindrical area of material under an axial load resisting the load by shearing action. The diameter of the area is the basic pitch diameter of the threads, and the length of the cylinder is the thread engagement length.

The analysis ~~Appendix 3.D~~ also examines the capacity of major welds in the load path and the compression capacity of the pedestal shield and pedestal shield shell.

The table below summarizes key results obtained from the analyses *described above* ~~reported in detail in Appendix 3.D~~ for the HI-STORM 100.

HI-STORM 100 Top and Bottom Lifting Analyses†‡			
Item	**Value (ksi)**	**Allowable (ksi)**	**Safety Factor**
Primary Membrane plus Bending - Bottom Lift - Inlet Vent Plates - Region B	8.0	26.3	3.28
Primary Membrane - Top Lift - Radial Rib Under Lifting Block - Region B	6.67	17.5	2.63
Primary Membrane plus Bending – Top Lift - Baseplate – Region B	7.0	26.3	3.75
Primary Membrane Region A (3D*)	19.97	33.15	1.66
Primary Membrane plus Bending Region A (3D*)	24.02	33.15	1.38
Lifting Block Threads - Top Lift –Region A (3D*)	10.67	19.62	1.84
Lifting Stud - Top Lift –Region A (3D*)	43.733	108.8	2.49
Welds – Anchor Block-to-Radial Rib Region B	5.74	19.695	3.43
Welds – Anchor Block-to-Radial Rib Region A (3D*)	17.21	19.62	1.14
Weld – Baseplate-to Inner Shell Region A (3D*)	1.56	19.89	12.78
Weld – Baseplate-to-Inlet Vent Region A (3D*)	15.05	19.89	1.32
Pedestal Shield Concrete (3D*)	0.096	1.535	16.03
Pedestal Shell (3D*)	3.263	33.15	10.16

† Regions A and B are defined at beginning of Subsection 3.4.3

‡ The lifted load is 360000 lb. and an inertia amplification of 15% is included.

It is concluded that all structural integrity requirements are met during a lift of the HI-STORM 100 storage overpack under either the top lift or the bottom lift scenario. All factors of safety are greater than 1.0 using criteria from the ASME Code Section III, Subsection NF for Class 3 plate and shell supports and from USNRC Regulatory Guide 3.61.

Similar calculations have been performed for the HI-STORM 100S where differences in configuration warrant. The results are summarized in the table below:

HI-STORM 100S Top and Bottom Lifting Analyses†‡			
Item	**Value (ksi)**	**Allowable (ksi)**	**Safety Factor**
Primary Membrane plus Bending - Bottom Lift - Inlet Vent Plates - Region A (3D*)	9.824	33.15	3.374
Lifting Block Threads - Top Lift –Region A (3D*)	5.540	18.840	3.40
Lifting Stud - Top Lift –Region A (3D*)	49.199	83.7	1.70
Welds – Anchor Block-to-Radial Rib Region B	5.483	21.0	3.83
Welds – Anchor Block-to-Radial Rib Region A (3D*)	16.469	18.84	1.144
Weld – Baseplate-to Inner Shell Region A (3D*)	1,592	19.89	12.49
Weld – Baseplate-to-Inlet Vent Region A (3D*)	8.982	19.89	2.214
Radial Rib Membrane Stress – Bottom Lift Region A (3D*)	10.58	33.15	3.132
Pedestal Shield Concrete (3D*)	0.095	1.535	16.17
Pedestal Shell (3D*)	3.235	33.15	10.24

† Regions A and B are defined at beginning of Subsection 3.4.3

‡ The lifted load is 405,000 lb. and an inertia amplification of 15% is included. The increased weight (over the longer HI-STORM 100) comes from conservatively assuming an increase in concrete weight density in the HI-STORM 100S overpack and lid to provide additional safety margin.

It is concluded that all structural integrity requirements are met during a lift of the HI-STORM 100 and HI-STORM 100S storage overpacks under either the top lift or the bottom lift scenario. All factors of safety are greater than 1.0 using criteria from the ASME Code Section III, Subsection NF for Class 3 plate and shell supports and from USNRC Regulatory Guide 3.61.

3.4.3.6 MPC Lifting Analysis

The MPC lifting analyses are found in the HI-STAR 100 FSAR (Docket-72-1008). Some results of the analyses in that document (Appendices 3.K, 3.E, 3.I and 3.Y Docket-72-1008) are summarized here for completeness.

Summary of MPC Lifting Analyses			
Item	**Thread Engagement Safety Factor (NUREG- 0612)**	**Region A Safety Factor**	**Region B Safety Factor†**
MPC	1.08	1.09	1.56

† The factor reported here is for the MPC baseplate considered under a load equal to 3D*.

3.4.3.7 Miscellaneous Lid Lifting Analyses

~~Appendix 3.AC contains analyses of lifting attachments for various lid lifting operations.~~

The HI-STORM 100 lid lifting analysis is performed to ensure that the threaded connections provided in the lid are adequately sized. The lifting analysis of the top lid is based on a vertical orientation of loading from an attached lifting device. The top lid of the HI-STORM 100 storage overpack is lifted using four lugs that are threaded into holes in the top plate of the lid (Holtec Drawing 1495, Section 1.5). It is noted that failure of the lid attachment would not result in any event of safety consequence because a free-falling HI-STORM 100 lid cannot strike a stored MPC (due to its size and orientation). Operational limits on the carry height of the HI-STORM 100 lid above the top of the storage overpack containing a loaded MPC preclude any significant lid rotation out of the horizontal plane in the event of a handling accident. Therefore, contact between the top of the MPC and the edge of a dropped lid due to uncontrolled lowering of the lid during the lid placement operation is judged to be a non-credible scenario. ~~Appendix 3.AC provides an example of a commercially available item that has the appropriate safety factors to serve as a lifting device for the HI-STORM 100 overpack top lid.~~ Except for location of the lift points, the lifting device for the HI-STORM 100S lid is the same as for the regular HI-STORM 100 lid. Since the lid weight for the HI-STORM 100S bounds the HI-STORM 100, the calculated safety factors for the lifting of the HI-STORM 100S lid are reduced and are also reported in the summary table below.

In addition to the HI-STORM 100 top lid lifting analysis, ~~Appendix 3.AC also contains details of~~ the strength qualification of *the* ~~other~~ lid lifting holes, and associated lid lifting devices, *for the HI-TRAC pool lid and top lid has been performed.* The qualification is based on the Regulatory Guide 3.61 requirement that a load factor of 3 results in stresses less than the yield stress. ~~Lifting of the HI-TRAC pool lid and top lid are considered in Appendix 3.AC.~~ Example commercially available lifting structures are considered ~~in Appendix 3.AC~~ and it is shown that thread engagement lengths are acceptable. Loads to lifting devices are permitted to be at a maximum angle of 45 degrees from vertical. A summary of results ~~from Appendix 3.AC~~, pertaining to the various lid lifting operations, is given in the table below:

Summary of HI-STORM 100 Lid Lifting Analyses

Item	Dead Load (lb)	Minimum Safety Factor
HI-STORM 100 (100S) Top Lid Lifting	23,000 (25,500)	2.731 (2.464)
HI-TRAC Pool Lid Lifting	12,500	4.73
HI-TRAC Top Lid Lifting	2,750	11.38

The analysis ~~Appendix 3.AC~~ demonstrates that thread engagement is sufficient for the threaded holes used solely for lid lifting and that commercially available lifting devices engaging the threaded holes, are available. We note that all reported safety factors are based on an allowable strength equal to 33.3% of the yield strength of the lid material when evaluating shear capacity of the internal threads and based on the working loads of the commercially available lifting devices associated with the respective threaded holes.

3.4.3.8 HI-TRAC Pool Lid Analysis - Lifting MPC From the Spent Fuel Pool (Load Case 01 in Table 3.1.5)

During lifting of the MPC from the spent fuel pool, the HI-TRAC pool lid supports the weight of a loaded MPC plus water (see Figure 3.4.21). ~~Appendix 3.AB details the c~~*C*alculations *are* performed to show structural integrity under this condition for both 100 Ton and 125 Ton HI-TRAC transfer casks. In accordance with the general guidelines set down at the beginning of Subsection 3.4.3, the pool lid is considered as both Region A and Region B for evaluating safety factors. The analysis ~~in Appendix 3.AB~~ shows that the stress in the pool lid top plate is less than the Level A allowable stress under pressure equivalent to the heaviest MPC, contained water, and lid self weight (Region B evaluation). Stresses in the lids and bolts are also shown to be below yield under three times the applied lifted load (Region A evaluation using Regulatory Guide 3.61 criteria). The threaded holes in the HI-TRAC pool lid are also examined for acceptable engagement length under the condition of lifting the MPC from the pool. ~~This analysis is performed in Appendix 3.AC.~~ It is demonstrated ~~in Appendix 3.AC~~ that the pool lid peripheral bolts have adequate engagement length into the pool lid to permit the transfer of the required load. The safety factor is defined based on the strength limits imposed by Regulatory Guide 3.61.

The following table summarizes the results of the analyses *for the HI-TRAC pool lid*~~performed in Appendix 3.AB and the thread engagement calculation in Appendix 3.AC~~. Results given in the following table compare calculated stress and allowable stress except for the final table item, ~~that compares thread engagement analysis~~ where a comparison is made *between* ~~of~~ calculated load~~:~~ and allowable load. In all cases, the safety factor is defined as the allowable value divided by the calculated value.

HI-TRAC Pool Lid Lifting a Loaded MPC Evaluation†			
Item	**Value (ksi)**	**Allowable (ksi)**	**Safety Factor**
Lid Bending Stress -125 ton HI-TRAC - Region B Analysis - Pool Lid Top Plate	10.1	26.3	2.604
Lid Bending Stress -125 ton HI-TRAC - Region B Analysis - Pool Lid Bottom Plate	5.05	26.3	5.208
Lid Bending Stress -100 ton HI-TRAC - Region B Analysis- Pool Lid Top Plate	10.06	26.3	2.614
Lid Bending Stress -100 ton HI-TRAC - Region B Analysis- Pool Lid Bottom Plate	6.425	26.3	4.093
Lid Bolt Stress -125 ton HI-TRAC – (3D*)	18.92	95.0	5.02
Lid Bolt Stress -100 ton HI-TRAC – (3D*)	18.21	95.0	5.216
Lid Bending Stress -125 ton HI-TRAC - Region A Analysis - Pool Lid Top Plate (3D*)	30.3	33.15	1.094
Lid Bending Stress -125 ton HI-TRAC - Region A Analysis - Pool Lid Bottom Plate (3D*)	15.15	33.15	2.188
Lid Bending Stress –100 ton HI-TRAC – Region A Analysis- Pool Lid Top Plate (3D*)	30.19	33.15	1.098
Lid Bending Stress –100 ton HI-TRAC – Region A Analysis- Pool Lid Bottom Plate (3D*)	19.28	33.15	1.72
Lid Thread Engagement Length (125 ton HI-TRAC)	137.5‡	324.6‡	2.362

† Region A and B defined at beginning of Subsection 3.4.3.
‡ Calculated and allowable value for this item in (kips).

3.4.3.9 HI-TRAC Transfer Lid Analysis - Lifting MPC Away from Spent Fuel Pool (Load Case 01 in Table 3.1.5)

During transfer to or from a storage overpack, the HI-TRAC transfer lid supports the weight of a loaded MPC. Figure 3.4.21 illustrates the lift operation. In accordance with the general lifting analysis guidelines, the transfer lid should be considered as both a Region A (Regulatory Guide 3.61 criteria) and a Region B location (ASME Section III, Subsection NF for Class 3 plate and shell structures) for evaluation of safety factors. ~~Appendices 3.AD and 3.AJ present analyses and results for t~~*T*he 125 Ton HI-TRAC transfer lid and the 100 Ton HI-TRAC transfer lid *are analyzed separately because of differences in geometry*~~, respectively~~.

It is shown ~~in the above mentioned appendices~~ that the transfer lid doors can support a loaded MPC together with the door weight without exceeding ASME NF stress limits and the more conservative limits of Regulatory Guide 3.61. It is also shown that the connecting structure transfers the load to the cask body without overstress. The following tables summarize the results for both HI-TRAC casks:

125 Ton HI-TRAC Transfer Lid – Lifting Evaluation†			
Item	**Value (ksi)**	**Allowable (ksi)**	**Safety Factor**
125 Ton HI-TRAC - Door Plate – (3D*)	9.381	32.7	3.486
125 Ton HI-TRAC - Door Plate – Region B	3.127	26.25	8.394
125 Ton HI-TRAC – Wheel Track (3D*)	26.91	36.0	1.338
125 Ton HI-TRAC - Door Housing Bottom Plate- Region B	7.701	26.25	3.409
125 Ton HI-TRAC - Door Housing Bottom Plate- (3D*)	23.103	32.7	1.415
125 Ton HI-TRAC - Door Housing Stiffeners- (3D*)	4.131	32.7	7.913
125 Ton HI-TRAC - Housing Bolts-Region B	29.96	57.5	1.919
125 Ton HI-TRAC – Housing Bolts (3D*)	89.88	95.0	1.057
125 Ton HI-TRAC – Lid Top Plate (3D*)	30.907	32.7	1.058

† Region A and B defined at beginning of Subsection 3.4.3

100 Ton HI-TRAC Transfer Lid – Lifting Evaluation†			
Item	**Value (ksi)**	**Allowable (ksi)**	**Safety Factor**
100 Ton HI-TRAC - Door Plate – (3D*)	20.697	32.7	1.58
100 Ton HI-TRAC - Door Plate – Region B	6.899	26.25	3.805
100 Ton HI-TRAC – Wheel Track (3D*)	26.03	36.0	1.383
100 Ton HI-TRAC – Door Housing Bottom Plate- Region B	7.447	26.25	3.525
100 Ton HI-TRAC – Door Housing Bottom Plate- (3D*)	22.336	32.7	1.464
100 Ton HI-TRAC – Door Housing Stiffeners- (3D*)	4.917	32.7	6.65
100 Ton HI-TRAC - Housing Bolts- Region B	22.478	57.5	2.558
100 Ton HI-TRAC – Housing Bolts (3D*)	67.423	95.0	1.409
100 Ton HI-TRAC – Lid Top Plate (3D*)	19.395	32.7	1.686

† Region A and B defined at beginning of Subsection 3.4.3

3.4.3.10 HI-TRAC Bottom Flange Evaluation during Lift (Load Case 01 in Table 3.1.5)

During a lifting operation, the HI-TRAC transfer cask body supports the load of a loaded MPC, and the transfer lid (away from the spent fuel pool) or the pool lid plus contained water (lifting from the spent fuel pool). In either case, the load is transferred to the bottom flange of HI-TRAC through the bolts and a state of stress in the flange and the supporting inner and outer shells is developed. Figure 3.4.21 illustrates the lifting operation. ~~Appendix 3.AE provides the evaluation of t~~*T*his area of the HI-TRAC *is analyzed* to demonstrate that *the* required limits on stress are maintained for both ASME and Regulatory Guide 3.61. The bottom flange is considered as an annular plate subject to a total bolt load acting at the bolt circle and supported by reaction loads developed in the inner and outer shells of HI-TRAC. The solution for maximum flange bending stress is found in the classical literature and stresses and corresponding safety factors developed for the bottom flange and for the outer and inner shell direct stress. The loaded welds are full penetration in this area so they do not require separate investigation. The table below summarizes the results of the evaluation ~~in Appendix 3.AE~~.

Safety Factors in HI-TRAC Bottom Flange During a Lift Operation			
Item	**Value(ksi)**	**Allowable(ksi)**	**Safety Factor**
Bottom Flange – Region B	7.798	26.25	3.37
Bottom Flange (3D*)	23.39	33.15	1.42
Outer Shell (3D*)	3.117	33.15	10.63

3.4.3.11 Conclusion

Synopses of lifting device, device/component interface, and component stresses, under all contemplated lifting operations for the HI-STORM 100 System have been presented in the foregoing. The HI-STORM storage overpack and the HI-TRAC transfer cask have been evaluated for limiting stress states. The results show that all factors of safety are greater than 1.

3.4.4 Heat

The thermal evaluation of the HI-STORM 100 System is reported in Chapter 4.

3.4.4.1 Summary of Pressures and Temperatures

Design pressures and design temperatures for all conditions of storage are listed in Tables 2.2.1 and 2.2.3, respectively.

3.4.4.2 Differential Thermal Expansion

Consistent with the requirements of Reg. Guide 3.61, Load Cases F1 (Table 3.1.3) and E4 (Table 3.1.4) are defined to study the effect of differential thermal expansion among the constituent components in the HI-STORM 100 System. Tables 4.4.9, 4.4.10, 4.4.26, 4.4.27, and 4.4.36 provide the temperatures necessary to perform the differential thermal expansion analyses for the MPC in the HI-STORM 100 and HI-TRAC casks, respectively. The material presented in the remainder of this paragraph demonstrates that a physical interference between discrete components of the HI-STORM 100 System (e.g. storage overpack and enclosure vessel) will not develop due to differential thermal expansion during any operating condition.

3.4.4.2.1 Normal Hot Environment

Closed form calculations are performed to demonstrate that initial gaps between the HI-STORM 100 storage overpack or the HI-TRAC transfer cask and the MPC canister, and between the MPC canister and the fuel basket, will not close due to thermal expansion of the system components under loading conditions, defined as F1 and E4 in Tables 3.1.3 and 3.1.4, respectively. To assess this in the most conservative manner, the thermal solutions computed in Chapter 4, including the thermosiphon effect, are surveyed for the following information.

- The radial temperature distribution in each of the fuel baskets at the location of peak center metal temperature.

- The highest and lowest mean temperatures of the canister shell for the hot environment condition.

- The inner and outer surface temperature of the HI-STORM 100 storage overpack and the HI-TRAC transfer cask at the location of highest and lowest surface temperature (which will produce the lowest mean temperature).

Tables 4.4.9, 4.4.10, 4.4.26, *and* 4.4.27~~, and 4.4.36~~ present the resulting temperatures used in the evaluation of the MPC expansion in the HI-STORM 100 storage overpack. Table 4.5.2 presents similar results for the MPC in the HI-TRAC transfer cask. *The long-term normal storage temperatures for the HI-STORM overpack are provided in Table 4.4.36. For conservatism, lower bound temperatures (i.e., temperatures less than the values reported in Tables 4.4.36 and 4.5.2) are used as input for the HI-STORM overpack and HI-TRAC transfer cask in the calculations to increase the potential for interference.*

Using the temperature information in the above-mentioned tables, simplified thermoelastic solutions of equivalent axisymmetric problems are used to obtain conservative estimates of gap closures. The following procedure, which conservatively neglects axial variations in temperature distribution, is utilized.

1. Use the surface temperature information for the fuel basket to define a parabolic distribution in the fuel basket that bounds (from above) the actual temperature distribution. Using this result, generate a conservatively high estimate of the radial and axial growth of the different fuel baskets using classical closed form solutions for thermoelastic deformation in cylindrical bodies.

2. Use the temperatures obtained for the canister to predict an estimate of the radial and axial growth of the canister to check the canister-to-basket gaps.

3. Use the temperatures obtained for the canister to predict an estimate of the radial and axial growth of the canister to check the canister-to-storage overpack and canister-to-HI-TRAC gaps.

4. Use the storage overpack and HI-TRAC surface temperatures to construct a logarithmic temperature distribution (characteristic of a thick walled cylinder) at the location used for canister thermal growth calculations; and use this distribution to predict an estimate of storage overpack or HI-TRAC (as applicable) radial and axial growth.

5. For given initial clearances, compute the operating clearances.

~~The calculation procedure outlined above is used in Appendix 3.I (HI-TRAC), and in Appendices 3.U, 3.V, 3.W, and 3.AQ (HI-STORM 100 storage overpack with MPC-24, MPC-32, MPC-68, and 24E respectively).~~ The results are summarized in the tables given below for normal storage conditions. The worst-case MPC is evaluated in the HI-TRAC transfer cask, in lieu of all MPC designs. In all cases, the minimal initial radial gap between MPC and overpack is used as the initial point.

THERMOELASTIC DISPLACEMENTS IN THE MPC AND HI-STORM 100 STORAGE OVERPACK UNDER HOT TEMPERATURE ENVIRONMENT CONDITION

CANISTER – FUEL BASKET

	Radial Direction (in.)		Axial Direction (in.)	
Unit	Initial Clearance	Final Clearance	Initial Clearance	Final Clearance
MPC-24	0.1875	0.1048	1.8125	1.404
MPC-24E	0.1875	0.104	1.8125	1.404
MPC-32	0.1875	0.103	1.8125	1.398
MPC-68	0.1875	0.091	1.8125	1.336

CANISTER – STORAGE OVERPACK

Unit	Radial Direction (in.)		Axial Direction (in.)	
	Initial Clearance	Final Clearance	Initial Clearance	Final Clearance
MPC-24	0.5	0.435	1.0	0.633
MPC-24E	0.5	0.434	1.0	0.628
MPC-32	0.5	0.433	1.0	0.621
MPC-68	0.5	0.434	1.0	0.628

THERMOELASTIC DISPLACEMENTS IN THE MPC AND HI-TRAC UNDER HOT TEMPERATURE ENVIRONMENT CONDITION

CANISTER - FUEL BASKET

	Radial Direction (in.)		Axial Direction (in.)	
Unit	Initial Clearance	Final Clearance	Initial Clearance	Final Clearance
MPC (worst case)	0.1875	0.083	1.8125	1.305

CANISTER - HI-TRAC

	Radial Direction (in.)		Axial Direction (in.)	
Unit	Initial Clearance	Final Clearance	Initial Clearance	Final Clearance
MPC (worst case)	0.125	0.123	0.75	0.735

It can be verified by referring to the Design Drawings provided in Section 1.5 of this report and the foregoing table, that the clearances between the MPC basket and canister structure, as well as that between the MPC shell and storage overpack or HI-TRAC inside surface, are sufficient to preclude a temperature induced interference from differential thermal expansions under normal operating conditions.

3.4.4.2.2 Fire Accident

It is shown in Chapter 11 that the fire accident has a small effect on the MPC temperatures because of the short duration of the fire accidents and the large thermal inertia of the storage overpack. Therefore, a structural evaluation of the MPC under the postulated fire event is not required. The conclusions reached in Subsection 3.4.4.2.1 are also appropriate for the fire accident with the MPC housed in the storage overpack. Analysis of fire accident temperatures of the MPC housed within the HI-TRAC for thermal expansion is unnecessary, as the HI-TRAC, directly exposed to the fire, expands to increase the gap between the HI-TRAC and MPC.

As expected, the external surfaces of the HI-STORM 100 storage overpack that are directly exposed to the fire event experience maximum rise in temperature. The outer shell and top plate in the top lid are the external surfaces that are in direct contact with heated air from fire. The table below, extracted from data provided in Chapter 11, provides the maximum temperatures attained at the key locations in HI-STORM 100 storage overpack under the postulated fire event.

Component	Maximum Fire Condition Temperature (Deg. F)
Storage Overpack Inner Shell	300
Storage Overpack Radial Concrete Mid-Depth	173
Storage Overpack Outer Shell	570
Storage Overpack Lid	<570

The following conclusions are readily reached from the above table.

- The maximum metal temperature of the carbon steel shell most directly exposed to the combustion air is well below 600°F (Table 2.2.3 applicable short-term temperature limit). 600°F is well below the permissible temperature limit in the ASME Code for the outer shell material.

- The bulk temperature of concrete is well below the normal condition temperature limit of 200°F specified in Table 2.2.3 and Appendix 1.D. ACI-349 permits 350°F as the short-term temperature limit; the shielding concrete in the HI-STORM 100 Overpack, as noted in Appendix 1.D, will comply with the specified compositional and manufacturing provisions of ACI-349. As the detailed information in Section 11.2 shows, the radial extent in the concrete where the local temperature exceeds 350°F begins at the outer shell/concrete interface and ends in less than one-

inch. Therefore, the potential loss in the shielding material's effectiveness is less than 4% of the concrete shielding mass in the overpack annulus.

- The metal temperature of the inner shell does not exceed 300°F at any location, which is below the normal condition temperature limit of 350°F specified in Table 2.2.3 for the inner shell.

- The presence of a stitch weld between the overpack inner shell and the overpack top plate ensures that there will be no pressure buildup in the concrete annulus due to the concrete losing water that then turns to steam.

The above summary confirms that the postulated fire event will not jeopardize the structural integrity of the HI-STORM 100 Overpack or significantly diminish its shielding effectiveness.

The above conclusions, as relevant, also apply to the HI-TRAC fire considered in Chapter 11. Water jacket over-pressurization is precluded by the safety valve set point. The non-structural effects of loss of water have been evaluated in Chapter 5 and shown to meet regulatory limits. Therefore, it is concluded that the postulated fire event will not cause significant loss in storage overpack or HI-TRAC shielding function.

3.4.4.3 Stress Calculations

This subsection presents calculations of the stresses in the different components of the HI-STORM 100 System from the effects of mechanical load case assembled in Section 3.1. Loading cases for the MPC fuel basket, the MPC enclosure vessel, the HI-STORM 100 storage overpack and the HI-TRAC transfer cask are listed in Tables 3.1.3 through 3.1.5, respectively. The load case identifiers defined in Tables 3.1.3 through 3.1.5 denote the cases considered.

The purpose of the analyses is to provide the necessary assurance that there will be no unacceptable risk of criticality, unacceptable release of radioactive material, unacceptable radiation levels, or impairment of ready retrievability of fuel from the MPC and the MPC from the HI-STORM 100 storage overpack or from the HI-TRAC transfer cask.

For all stress evaluations, the allowable stresses and stress intensities for the various HI-STORM 100 System components are based on bounding high metal temperatures to provide additional conservatism (Table 3.1.17 for the MPC basket, for example).

In addition to the loading cases germane to stress evaluations mentioned above, three cases pertaining to the stability of HI-STORM 100 are also considered (Table 3.1.1).

The results of various stress calculations on components are reported. The calculations are either performed directly as part of the text, or *carried out in a separate calculation report* ~~are summarized in an appendix (see the list of all supporting appendices provided in Section 3.6)~~ that provides details of strength of materials evaluations or finite element numerical analysis. The specific calculations reported in this subsection are:

1. MPC stress calculations
2. HI-STORM 100 storage overpack stress calculations
3. HI-TRAC stress calculations

The MPC calculations reported in this document are complemented by analyses in the HI-STAR 100 Dockets. As noted earlier in this chapter, calculations for MPC components that are reported in HI-STAR 100 FSAR and SAR (Docket Numbers 72-1008 or 71-9261) are not repeated here unless geometry or load changes warrant reanalysis. For example, analysis of the MPC lid is not included in this submittal since neither the MPC lid loading nor geometry is affected by the MPC being placed in HI-TRAC or HI-STORM 100. MPC stress analyses reported herein focus on the basket and canister stress distributions due to the design basis (45g) lateral deceleration imposed by a non-mechanistic tip-over of the HI-STORM 100 storage overpack or a horizontal drop of HI-TRAC. In the submittals for the HI-STAR 100 FSAR and SAR (Docket Numbers 72-1008 and 71-9261, for storage and transport, respectively), the design basis deceleration was 60g. In this submittal the design basis deceleration is 45g. However, since the geometry of the MPC external boundary condition, viz. canister-to-storage overpack gap, has changed, a reanalysis of the MPC stresses under the lateral deceleration loads is required. This analysis is performed and the results are summarized in this subsection.

The HI-STORM 100 storage overpack and the HI-TRAC transfer cask have been evaluated for certain limiting load conditions that are germane to the storage and operational modes specified for the system in Tables 3.1.1 and 3.1.5. The determination of component safety factors at the locations considered in the HI-STORM 100 storage overpack and in the HI-TRAC transfer cask is based on the allowable stresses permitted by the ASME Code Section III, Subsection NF for Class 3 plate and shell support structures.

3.4.4.3.1 MPC Stress Calculations

The structural function of the MPC in the storage mode is stated in Section 3.1. The calculations presented here demonstrate the ability of the MPC to perform its structural function. The purpose of the analyses is to provide the necessary assurance that there will be no unacceptable risk of criticality, unacceptable release of radioactive material, or impairment of ready retrievability.

3.4.4.3.1.1 Analysis of Load Cases E.3.b, E.3.c (Table 3.1.4) and F.3.b, F.3.c (Table 3.1.3)

Analyses are performed for each of the MPC designs. The following subsections describe the model, individual loads, load combinations, and analysis procedures applicable to the MPC. Unfortunately, unlike vertical loading cases, where the analyses performed in the HI-STAR 100 dockets remain fully applicable for application in HI-STORM 100, the response of the MPC to a horizontal loading event is storage overpack-geometry dependent. Under a horizontal drop event, for example, the MPC and the fuel basket structure will tend to flatten. The restraint to this flattening offered by the storage overpack will clearly depend on the difference in the diameters of the storage overpack internal cavity and that of the outer surface of the MPC. In the HI-STORM 100 storage overpack, the

diameter difference is larger than that in HI-STAR 100; therefore, the external restraint to MPC ovalization under a horizontal drop event is less effective. For this reason, the MPC stress analysis for lateral loading scenarios must be performed anew for the HI-STORM 100 storage overpack; the results from the HI-STAR 100 analyses will not be conservative. The HI-TRAC transfer casks and HI-STAR 100 overpack inner diameters are identical. Therefore, the analysis of the MPC in the HI-STAR 100 overpack under 60g's for the side impact (Docket 72-1008) bounds the analysis of the MPC in the HI-TRAC under 45g's.

Description of Finite Element Models of the MPCs Under Lateral Loading

A finite element model of each MPC is used to assess the effects of the accident loads. The models are constructed using ANSYS [3.4.1], and they are identical to the models used in Holtec's HI-STAR 100 submittals in Docket Numbers 72-1008 and 71-9261. The following model description is common to all MPCs.

The MPC structural model is two-dimensional. It represents a one-inch long cross section of the MPC fuel basket and MPC canister.

The MPC model includes the fuel basket, the basket support structures, and the MPC shell. A basket support is defined as any structural member that is welded to the inside surface of the MPC shell. A portion of the storage overpack inner surface is modeled to provide the correct restraint conditions for the MPC. Figures 3.4.1 through 3.4.9 show typical MPC models.

The fuel basket support structure shown in the figures is a multi-plate structure consisting of solid shims or support members having two separate compressive load supporting members. For conservatism in the finite element model some dual path compression members (i.e., "V" angles) are simulated as single columns. Therefore, the calculated stress intensities in the fuel basket angle supports from the finite element solution are conservatively overestimated in some locations.

The ANSYS model is not intended to resolve the detailed stress distributions in weld areas. Individual welds are not included in the finite element model. A separate analysis for basket welds and for the basket support "V" angles is *performed outside of ANSYS* ~~contained in Appendix 3.Y~~.

No credit is taken for any load support offered by the *neutron absorber* ~~Boral~~ panels, sheathing, and the aluminum heat conduction elements. Therefore, these so-called non-structural members are not represented in the model. The bounding MPC weight used, however, does include the mass contributions of these non-structural components.

The model is built using five ANSYS element types: BEAM3, PLANE82, CONTAC12, CONTAC26, and COMBIN14. The fuel basket and MPC shell are modeled entirely with two-dimensional beam elements (BEAM3). Plate-type basket supports are also modeled with BEAM3 elements. Eight-node plane elements (PLANE82) are used for the solid-type basket supports. The gaps between the fuel basket and the basket supports are represented by two-dimensional point-to-point contact elements (CONTAC12). Contact between the MPC shell and the storage overpack is

modeled using two-dimensional point-to-ground contact elements (CONTAC26) with an appropriate clearance gap.

Two orientations of the deceleration vector are considered. The 0-degree drop model includes the storage overpack-MPC interface in the basket orientation illustrated in Figure 3.1.2. The 45-degree drop model represents the storage overpack-MPC interface with the basket oriented in the manner of Figure 3.1.3. The 0-degree and the 45-degree drop models are shown in Figures 3.4.1 through 3.4.6. Table 3.4.1 lists the element types and number of elements for current MPC's.

A contact surface is provided in the model ~~is~~ used for drop analyses to represent the storage overpack channels. As the MPC makes contact with the storage overpack, the MPC shell deforms to mate with the channels that are welded at equal intervals around the storage overpack inner surface. The nodes that define the elements representing the fuel basket and the MPC shell are located along the centerline of the plate material. As a result, the line of nodes that forms the perimeter of the MPC shell is inset from the real boundary by a distance that is equal to half of the shell thickness. In order to maintain the specified MPC shell/storage overpack gap dimension, the radius of the storage overpack channels is decreased by an equal amount in the model.

The three discrete components of the HI-STORM 100 System, namely the fuel basket, the MPC shell, and the storage overpack or HI-TRAC transfer cask, are engineered with small diametral clearances which are large enough to permit unconstrained thermal expansion of the three components under the rated (maximum) heat duty condition. A small diametral gap under ambient conditions is also necessary to assemble the system without physical interference between the contiguous surfaces of the three components. The required gap to ensure unrestricted thermal expansion between the basket and the MPC shell is small and will further decrease under maximum heat load conditions, but will introduce a physical nonlinearity in the structural events involving lateral loading (such as side drop of the system) under ambient conditions. It is evident from the system design drawings that the fuel basket that is non-radially symmetric is in proximate contact with the MPC shell at a discrete number of locations along the circumferences. At these locations, the MPC shell, backed by the channels attached to the storage overpack, provides a support line to the fuel basket during lateral drop events. Because the fuel basket, the MPC shell, and the storage overpack or HI-TRAC are all three-dimensional structural weldments, their inter-body clearances may be somewhat uneven at different azimuthal locations. As the lateral loading is increased, clearances close at the support locations, resulting in the activation of the support from the storage overpack or HI-TRAC.

The bending stresses in the basket and the MPC shell at low lateral loading levels which are too small to close the support location clearances are secondary stresses since further increase in the loading will activate the storage overpack's or HI-TRAC's transfer cask support action, mitigating further increase in the stress. Therefore, to compute primary stresses in the basket and the MPC shell under lateral drop events, the gaps should be assumed to be closed. However, in the analyses, we have conservatively assumed that an initial gap of 0.1875" exists, in the direction of the applied deceleration, at all support locations between the fuel basket and the MPC shell and that the clearance gap between the shell and the storage overpack at the support locations is 3/16". In the

evaluation of safety factors for the MPC-24, MPC-32, and MPC-68, the total stress state produced by the applied loading on these configurations is conservatively compared with primary stress levels, even though the self-limiting stresses should be considered secondary in the strict definition of the Code. To illustrate the conservatism we have eliminated the secondary stress (that develops to close the clearances) in the comparison with primary stress allowable values and report safety factors for the MPC-24E that are based only on primary stresses necessary to maintain equilibrium with the inertia forces.

ANSYS requires that for a static solution all bodies be constrained to prevent rigid body motion. Therefore, in the 0 degree and 45 degree drop models, two-dimensional linear spring elements (COMBIN14) join the various model components, i.e., fuel basket and enclosure vessel, at the point of initial contact. This provides the necessary constraints for the model components in the direction of the impact. By locating the springs at the points of initial contact, where the gaps remain closed, the behavior of the springs is identical to the behavior of a contact element. Linear springs and contact elements that connect the same two components have equal stiffness values.

Description of Individual Loads and Boundary Conditions Applied to the MPCs

The method of applying each individual load to the MPC model is described in this subsection. The individual loads are listed in Table 2.2.14. A free-body diagram of the MPC corresponding to each individual load is given in Figures 3.4.7-3.4.9. In the following discussion, reference to vertical and horizontal orientations is made. Vertical refers to the direction along the cask axis, and horizontal refers to a radial direction.

Quasi-static structural analysis methods are used. The effects of any dynamic load factors (DLFs) are included in the final evaluation of safety factors. All analyses are carried out using the design basis decelerations in Table 3.1.2.

The MPC models used for side drop evaluations are shown in Figures 3.4.1 through 3.4.6. In each model, the fuel basket and the enclosure vessel are constrained to move only in the direction that is parallel to the acceleration vector. The storage overpack inner shell, which is defined by three nodes needed to represent the contact surface, is fixed in all degrees of freedom. The fuel basket, enclosure vessel, and storage overpack inner shell are all connected at one location by linear springs, as described in Subsection 3.4.4.3.1.1 (see Figure 3.4.1, for example). Detailed side drop evaluations here focus on an MPC within a HI-STORM 100 storage overpack. Since the analyses performed in Docket Number 72-1008 for the side drop condition in the HI-STAR 100 storage overpack demonstrates a safe condition under a 60g deceleration, no new analysis is required for the MPC and contained fuel basket and fuel during a side drop in the HI-TRAC, which is limited to a 45g deceleration (HI-TRAC and HI-STAR 100 overpacks have the same inside dimensions).

Accelerations

During a side impact event, the stored fuel is directly supported by the cell walls in the fuel basket. Depending on the orientation of the drop, 0 or 45 degrees (see Figures 3.4.8 and 3.4.9), the fuel is

supported by either one or two walls. In the finite element model this load is effected by applying a uniformly distributed pressure over the full span of the supporting walls. The magnitude of the pressure is determined by the weight of the fuel assembly (Table 2.1.6), the axial length of the fuel basket support structure, the width of the cell wall, and the impact acceleration. It is assumed that the load is evenly distributed along an axial length of basket equal to the fuel basket support structure. For example, the pressure applied to an impacted cell wall during a 0-degree side drop event is calculated as follows:

$$p = \frac{a_n W}{L c}$$

where:

p = pressure

a_n = ratio of the impact acceleration to the gravitational acceleration

W = weight of a stored fuel assembly

L = axial length of the fuel basket support structure

c = width of a cell wall

For the case of a 45-degree side drop the pressure on any cell wall equals p (defined above) divided by the square root of 2.

It is evident from the above that the effect of deceleration on the fuel basket and canister metal structure is accounted for by amplifying the gravity field in the appropriate direction.

Internal Pressure

Design internal pressure is applied to the MPC model. The inside surface of the enclosure vessel shell is loaded with pressure. The magnitude of the internal pressure applied to the model is taken from Table 2.2.1.

For this load condition, the center node of the fuel basket is fixed in all degrees of freedom to numerically satisfy equilibrium.

Temperature

Temperature distributions are developed in Chapter 4 and applied as nodal temperatures to the finite element model of the MPC enclosure vessel (confinement boundary). Maximum design heat load has

been used to develop the temperature distribution used to demonstrate compliance with ASME Code stress intensity levels.

Analysis Procedure

The analysis procedure for this set of load cases is as follows:

1. The stress intensity and deformation field due to the combined loads is determined by the finite element solution. Results are postprocessed and tabulated in the calculation package associated with this FSAR.

2. The results for each load combination are compared to allowables. The comparison with allowable values is made in Subsection 3.4.4.4.

3.4.4.3.1.2 Analysis of Load Cases E1.a and E1.c (Table 3.1.4)

Since the MPC shell is a pressure vessel, the classical Lame's calculations should be performed to demonstrate the shell's performance as a pressure vessel. We note that dead load has an insignificant effect on this stress state. We first perform calculations for the shell under internal pressure. Subsequently, we examine the entire confinement boundary as a pressure vessel subject to both internal pressure and temperature gradients. Finally, we perform confirmatory hand calculations to gain confidence in the finite element predictions.

The stress from internal pressure is found for normal and accident pressures conditions using classical formulas:

Define the following quantities:

P = pressure, r = MPC radius, and t = shell thickness.

Using classical thin shell theory, the circumferential stress, $\sigma_1 = Pr/t$, the axial stress $\sigma_2 = Pr/2t$, and the radial stress $\sigma_3 = -P$ are computed for both normal and accident internal pressures. The results are given in the following table (conservatively using the outer radius for r):

Classical Shell Theory Results for Normal and Accident Internal Pressures				
Item	**σ_1 (psi)**	**σ_2 (psi)**	**σ_3 (psi)**	**$\sigma_1 - \sigma_3$ (psi)**
P= 100 psi	6838	3419	-100	6938
P= 200 psi	13675	6838	-200	13875

Finite Element Analysis (Load Case E1.a and E1.c of Table 3.1.4)

The MPC shell, the top lid, and the baseplate together form the confinement boundary (enclosure vessel) for storage of spent nuclear fuel. In this section, we evaluate the operating condition consisting of dead weight, internal pressure, and thermal effects for the hot condition of storage. The top and bottom plates of the MPC enclosure vessel (EV) are modeled using plane axisymmetric elements, while the shell is modeled using the axisymmetric thin shell element. The thickness of the top lid varies in the different MPC types; for conservative results, the minimum thickness top lid is modeled. The temperature distributions for all MPC constructions are nearly identical in magnitude and gradient and reflect the thermosiphon effect inside the MPC. Temperature differences across the thickness of both the baseplate and the top lid exist during HI-STORM 100's operations. There is also a thermal gradient from the center of the top lid and baseplate out to the shell wall. The metal temperature profile is essentially parabolic from the centerline of the MPC out to the MPC shell. There is also a parabolic temperature profile along the length of the MPC canister. Figure 3.4.11 shows a sketch of the confinement boundary structure with identifiers A-I locating points where temperature input data is used to represent a continuous temperature distribution for analysis purposes. The overall dimensions of the confinement boundary are also shown in the figure.

The desired temperatures for confinement thermal stress analysis are determined from Tables 4.4.9, 4.4.10, 4.4.19, 4.4.26, and 4.4.27 in Chapter 4. The MPC-68 is identified to have the maximum through thickness thermal gradients. Detailed stress analyses are performed only for the MPC-68; these results are representative for all MPCs.

Figure 3.4.12 shows details of the finite element model of the top lid, canister shell, and baseplate. The top lid is modeled with 40 axisymmetric quadrilateral elements; the weld connecting the lid to the shell is modeled by a single element solely to capture the effect of the top lid attachment to the canister offset from the middle surface of the top lid. The MPC canister is modeled by 50 axisymmetric shell elements, with 20 elements concentrated in a short length of shell appropriate to capture the so-called "bending boundary layer" at both the top and bottom ends of the canister. The remaining 10 shell elements model the MPC canister structure away from the shell ends in the region where stress gradients are expected to be of less importance. The baseplate is modeled by 20 axisymmetric quadrilateral elements. Deformation compatibility at the connections is enforced at the top by the single weld element, and deformation and rotation compatibility at the bottom by additional shell elements between nodes 106-107 and 107-108.

The geometry of the model is listed below (terms are defined in Figure 3.4.12):

H_t = 9.5" (the minimum thickness lid is assumed)

R_L = 0.5 x 67.25" (Bill of Materials for Top Lid)

L_{MPC} = 190.5" (Drawing 1996, Sheet 1)

t_s = 0.5"

t_{BP} = 0.5 x 68.375"

β= $2\sqrt{R_s t_s} \approx 12$" (the "bending boundary layer")

Stress analysis results are obtained for two cases as follows:

a. internal pressure = 100 psi

b. internal pressure = 100 psi plus applied temperatures

For this configuration, dead weight of the top lid acts to reduce the stresses due to pressure. For example, the equivalent pressure simulating the effect of the weight of the top lid is an external pressure of 3 psi, which reduces the pressure difference across the top lid to 97 psi. The dead weight of the top lid is neglected to provide additional conservatism in the results. The dead weight of the baseplate, however, adds approximately 0.73 psi to the effective internal pressure acting on the base. The effect of dead weight is still insignificant compared to the 100 psi design pressure, and is therefore neglected. The thermal loading in the confinement vessel is obtained by developing a parabolic temperature profile to the entire length of the MPC canister and to the top lid and baseplate. The temperature data provided at locations A-I in Figure 3.4.11 and 3.4.12 are sufficient to establish the profiles. Through-thickness temperatures are assumed linearly interpolated between top and bottom surfaces of the top lid and baseplate.

Finally, in the analysis, all material properties and expansion coefficients are considered to be temperature-dependent in the model.

Results for stress intensity are reported for the case of internal pressure alone and for the combined loading of pressure plus temperature (Load Case E1.c in Table 3.1.4). Tables 3.4.7 and 3.4.8 report results at the inside and outside surfaces of the top lid and baseplate at the centerline and at the extreme radius. Canister results are reported in the "bending boundary layer" and at a location near mid-length of the MPC canister. In the tables, the calculated value is the value from the finite element analysis, the categories are P_m = primary membrane; $P_L + P_b$ = local membrane plus primary bending; and $P_L + P_b + Q$ = primary plus secondary stress intensity. The allowable strength value is obtained from the appropriate table in Section 3.1 for Level A conditions, and the safety factor SF is defined as the allowable strength divided by the calculated value. Allowable strengths for Alloy X are taken at 300 degrees F at the bottom of the MPC and 500 degrees F at the top of the MPC. These temperatures reflect actual operating conditions per Table 4.4.19. The results given in Tables 3.4.7 and 3.4.8 demonstrate the ruggedness of the MPC as a confinement boundary.

The results in Table 3.4.7 and 3.4.8 also show that the baseplate and the shell connection to the baseplate are the most highly stressed regions under the action of internal pressure. To confirm the finite element results, we perform an alternate closed form solution using classical plate and shell

theory equations that are listed in or developed from the reference (Timoshenko and Woinowsky-Krieger, Theory of Plate and Shells, McGraw Hill, Third Edition).

Assuming that the thick baseplate receives little support against rotation from the thin shell, the bending stress at the centerline is evaluated by considering a simply supported plate of radius a and thickness h, subjected to lateral pressure p. The maximum bending stress is given by

$$\sigma = \frac{3(3+\nu)}{8} p \left(\frac{a}{h}\right)^2$$

where:

a = .5 x 68.375"

h = 2.5"

ν = 0.3 (Poisson's Ratio)

p = 100 psi

Calculating the stress in the plate gives σ = 23,142 psi.

Now consider the thin MPC shell (t = 0.5") and first assume that the baseplate provides a clamped support to the shell. Under this condition, the bending stress in the thin shell at the connection to the plate is given as

$$\sigma_{Bp} = 3p\frac{a}{t}\frac{(1-\nu/2)}{\sqrt{3}(1-\nu^2)^{1/2}} = 10{,}553 \text{ psi}$$

In addition to this stress, there is a component of stress in the shell due to the baseplate rotation that causes the shell to rotate. The joint rotation is essentially driven by the behavior of the baseplate as a simply supported plate; the shell offers little resistance because of the disparity in thickness and will essentially follow the rotation of the thick plate.

Using formulas from thin shell theory, the additional axial bending stress in the shell due to this rotation θ can be written in the form

$$\sigma_{B\theta} = 12\ \beta\ D_s \frac{\theta}{t^2}$$

where

$$\theta = pa^3/8D(1+\nu) * \left(1/1+\alpha\right)$$

and

$$D = \frac{Eh^3}{12(1-\nu^2)} \qquad E = \text{plate Young's Modulus}$$

$$\alpha = \frac{2\beta a t^3}{h^3(1+\nu)}$$

$$D_s = \frac{Et^3}{12(1-\nu^2)}$$

$$\beta^2 = \sqrt{3(1-\nu^2)}/at$$

Substituting the numerical values gives

$$\sigma_{B\theta} = 40{,}563 \text{ psi}$$

We note that the approximate solution is independent of the value chosen for Young's Modulus as long as the material properties for the plate and shell are the same.

Combining the two contributions to the shell bending stress gives the total extreme fiber stress in the longitudinal direction as 51,116 psi.

The baseplate stress value, 23,142 psi, compares well with the finite element result 20,528 psi (Table 3.4.7). The shell joint stress, 51,116 psi, is greater than the finite element result (43,986 psi in Table 3.4.7). This is due to the local effects of the shell-to-baseplate connection offset. That is, the connection between shell and baseplate in the finite element model is at the surface of the baseplate, not at the middle surface of the baseplate. This offset will cause an additional bending moment that will reduce the rotation of the plate and hence, reduce the stress in the shell due to the rotation of the baseplate.

In summary, the approximate closed form solution confirms the accuracy of the finite element analysis in the baseplate region.

From Table 2.2.1, the off-normal design internal pressure is110 psi, or ten percent greater than the normal design pressure. Whereas Level A service limits are used to establish allowables for the normal design pressure, Level B service limits are used for off-normal loads; and since Subsection NB of the ASME Code permits an identical 10% increase in allowable stress intensity values for primary stress intensities generated by Level B Service Loadings, it stands to reason that the safety factors reported in Tables 3.4.7 and 3.4.8 bound the case of off-normal design internal pressure.

Under the accident pressure, the MPC baseplate experiences bending. Table NB-3217-1 permits the bending stress at the outer periphery of the baseplate and in the shell wall at the connection to be considered as a secondary bending stress if the primary bending stress at the center of the baseplate can be shown to meet the stress limits without recourse to the restraint provided by the MPC shell. To this end, the bending stress at the center of the baseplate is computed in a conservative manner assuming the baseplate is simply supported at the periphery. The bending stress for a simply supported circular plate is

$$\sigma = (9/8)p\left(r/t\right)^2$$

At the accident pressure, conservatively set at twice the normal operating pressure, the maximum stress is:

Bending stress at center of baseplate = 46,284 psi

Since this occurrence is treated as a Level D event, the stress intensity is compared with the limit from Table 3.1.14 and the safety factor computed as, "SF", where

SF = 69,300 psi/(46,284+200) psi = 1.49

3.4.4.3.1.3 Elastic Stability and Yielding of the MPC Basket under Compression Loads (Load Case F3 in Table 3.1.3)

This load case corresponds to the scenario wherein the loaded MPC is postulated to drop causing a compression state in the fuel basket panels.

a. Elastic Stability

Following the provisions of Appendix F of the ASME Code [3.4.3] for stability analysis of Subsection NG structures, (F-1331.5(a)(1)), a comprehensive buckling analysis is performed using ANSYS. For this analysis, ANSYS's large deformation capabilities are used. This feature allows

ANSYS to account for large nodal rotations in the fuel basket, which are characteristic of column buckling. The interaction between compressive and lateral loading, caused by the deformation, is exactly included. Subsequent to the large deformation analysis, the basket panel that is most susceptible to buckling failure is identified by a review of the results. The lateral displacement of a node located at the mid-span of the panel is measured for the range of impact decelerations. The buckling or collapse load is defined as the impact deceleration for which a slight increase in its magnitude results in a disproportionate increase in the lateral displacement.

The stability requirement for the MPC fuel basket under lateral loading is satisfied if two-thirds of the collapse deceleration load is greater than the design basis horizontal acceleration (Table 3.1.2). This analysis was performed for the HI-STAR 100 submittal (Docket Number 72-1008) under a 60g deceleration loading. Within the HI-STAR 100 FSAR (Docket Number 72-1008), Figures 3.4.27 through 3.4.32 are plots of lateral displacement versus impact deceleration for the MPC-24, MPC-32, and MPC-68. It should be noted that the displacements (in the HI-STAR 100 FSAR) in Figures 3.4.27 through 3.4.31 are expressed in $1x10^{-1}$ inch and Figure 3.4.32 is expressed in $1x10^{-2}$ inch. The plots in the HI-STAR 100 FSAR clearly show that the large deflection collapse load of the MPC fuel basket is greater than 1.5 times the design basis deceleration for all baskets in all orientations. The results for the MPC-24E are similar. Thus, the requirements of Appendix F are met for lateral deceleration loading under Subsection NG stress limits for faulted conditions.

An alternative solution for the stability of the fuel basket panel is obtained using the methodology espoused in NUREG/CR-6322 [3.4.13]. In particular, we consider the fuel basket panels as wide plates in accordance with Section 5 of NUREG/CR-6322. We use eq.(19) in that section with the "K" factor set to the value appropriate to a clamped panel. Material properties are selected corresponding to a metal temperature of 500 degrees F which bounds computed metal temperatures at the periphery of the basket. In general, the basket periphery sees the largest loading in an impact scenario. The critical buckling stress is:

$$\sigma_{cr} = \left(\pi / K \right)^2 \frac{E}{12(1-\nu^2)} \left(\frac{h}{a} \right)^2$$

where h is the panel thickness, a is the unsupported panel length, E is the Young's Modulus of Alloy X at 500 degrees F, ν is Poisson's Ratio, and K=0.65 (per Figure 6 of NUREG/CR-6322).

The MPC-24 has a small h/a ratio; the results of the finite element stress analyses under design basis deceleration load show that this basket is subject to the highest compressive load in the panel. Therefore, the critical buckling load is computed using the geometry of the MPC-24. The following table shows the results from the finite element stress analysis and from the stability calculation.

Panel Buckling Results From NUREG/CR-6322			
Item	**Finite Element Stress (ksi)**	**Critical Buckling Stress (ksi)**	**Factor of Safety**
Stress	13.717	49.22	3.588

For a stainless steel member under an accident condition load, the recommended safety factor is 2.12. We see that the calculated safety factor exceeds this value; therefore, we have independently confirmed the stability predictions of the large deflection analysis based on classical plate stability analysis by employing a simplified method.

Stability of the basket panels, under longitudinal deceleration loading, is demonstrated in the following manner. Under 60g deceleration in Docket Number 72-1008, the axial compressive stress in the baskets were computed for the MPC-24, 68, and 32, as:

MPC-24	3,458 psi
MPC-68	3,739 psi
MPC-32	4,001 psi

For the 45g design basis decelerations for HI-STORM 100, the basket axial stresses are reduced by 25%.

The above values represent the amplified weight, including the nonstructural sheathing and the *neutron absorber material*~~Boral~~, divided by the bearing area resisting axial movement of the basket. To demonstrate that elastic instability is not a concern, the buckling stress for an MPC-24 flat panel is computed.

For elastic stability, Reference [3.4.8] provides the formula for critical axial stress as

$$\sigma_{cr} = \frac{4\pi^2 E}{12(1-\nu^2)}\left(\frac{T}{W}\right)^2$$

where T is the panel thickness and W is the width of the panel, E is the Young's Modulus at the metal temperature and ν is the metal Poisson's Ratio. The following table summarizes the calculation for the critical buckling stress using the formula given above:

Elastic Stability Result for a Flat Panel	
Reference Temperature	725 degrees F
T (MPC-24)	5/16 inch
W	10.777 inch
E	24,600,000 psi
Critical Axial Stress	74,781 psi

It is noted the critical axial stress is an order of magnitude greater than the computed basket axial stress reported in the foregoing and demonstrates that elastic stability under longitudinal deceleration load is not a concern for any of the fuel basket configurations.

b. Yielding

The safety factor against yielding of the basket under longitudinal compressive stress from a design basis inertial loading is given, using the results for the MPC-32, by

SF = 17,100/4,001 = 4.274

Therefore, plastic deformation of the fuel basket under design basis deceleration is not credible.

3.4.4.3.1.4 MPC Baseplate Analysis (Load Case E2)

A bounding analysis is performed in the HI-STAR 100 FSAR (Docket Number 72-1008, Appendix 3.I) to evaluate the stresses in the MPC baseplate during the handling of a loaded MPC. The stresses in the MPC baseplate calculated in that appendix are compared to Level A stress limits and remain unchanged whether the overpack is HI-STAR 100, HI-STORM 100, or HI-TRAC. Therefore, no new analysis is needed. We have reported results for this region in Subsection 3.4.3 where an evaluation has been performed for stresses under three times the supported load.

3.4.4.3.1.5 Analysis of the MPC Top Closure (Load Case E2)

The FSAR for the HI-STAR 100 System (Docket Number 72-1008, Appendix 3.E) contains stress analysis of the MPC top closure during lifting. Loadings in that analysis are also valid for the HI-STORM 100 System.

3.4.4.3.1.6 Structural Analysis of the Fuel Support Spacers (Load Case E3.a)

Upper and lower fuel support spacers are utilized to position the active fuel region of the spent nuclear fuel within the poisoned region of the fuel basket. It is necessary to ensure that the spacers will continue to maintain their structural integrity after an accident event. Ensuring structural integrity implies that the spacer will not buckle under the maximum compressive load, and that the maximum compressive stress will not exceed the compressive strength of the spacer material (Alloy X). Detailed calculations in Docket Number 72-1008, Appendix 3.J, demonstrate that large structural margins in the fuel spacers are available for the entire range of spacer lengths which may be used in HI-STORM 100 applications (for the various acceptable fuel types). The calculations for the HI-STORM 100 45g load are bounded by those for the HI-STAR 100 60g load.

3.4.4.3.1.7 External Pressure (Load Case E1.b, Table 3.1.4)

Design external pressure is applied to the MPC model. The outer surface of the MPC shell is subject to external pressure. The magnitude of the external pressure applied to the model is taken

from Table 2.2.1. Analysis of the MPC under the external pressure is provided in the HI-STAR 100 FSAR Docket Number 72-1008 (Appendix 3.H) and therefore, is not repeated here.

3.4.4.3.1.8 *Miscellaneous MPC Structural Evaluations*

Calculations are performed to determine the minimum fuel basket weld size, the capacity of the sheathing welds, the stresses in the MPC cover plates, and the stresses in the fuel basket angle supports. The following paragraphs briefly describe each of these evaluations.

The fillet welds in the fuel basket honeycomb are made by an autogenous operation that has been shown to produce highly consistent and porosity free weld lines. However, Subsection NG of the ASME Code permits only 40% quality credit on double fillet welds which can be only visually examined (Table NG-3352-1). Subsection NG, however, fails to provide a specific stress limit on such fillet welds. In the absence of a Code mandated limit, Holtec International's standard design procedure requires that the weld section possess as much load resistance capability as the parent metal section. Since the loading on the honeycomb panels is essentially that of section bending, it is possible to develop a closed form expression for the required weld throat t corresponding to panel thickness h.

The sheathing is welded to the fuel basket cell walls to protect and position the neutron absorber material. Force equilibrium relationships are used to demonstrate that the sheathing weld is adequate to support a 45g deceleration load applied vertically and horizontally to the sheathing and the confined neutron absorber material. The analysis assumes that the weld is continuous and then modifies the results to reflect the amplification due to intermittent welding.

The MPC cover plates are welded to the MPC lid during loading operations. The cover plates are part of the confinement boundary for the MPC. No credit is taken for the pressure retaining abilities of the quick disconnect couplings for the MPC vent and drain. Therefore, the MPC cover plates must meet ASME Code, Section III, Subsection NB limits for normal, off-normal, and accident conditions. Conservatively, the accident condition pressure loading is applied, and it is demonstrated that the Level A limits for Subsection NB are met.

The fuel basket internal to the MPC canister is supported by a combination of angle fuel basket supports and flat plate or solid bar fuel basket supports. These fuel basket supports are subject to significant load only when a lateral acceleration is applied to the fuel basket and the contained fuel. The quasi-static finite element analyses of the MPC's, under lateral inertia loading, focused on the structural details of the fuel basket and the MPC shell. Basket supports were modeled in less detail which served only to properly model the load transfer path between fuel basket and canister. Safety factors reported for the fuel basket supports from the finite element analyses, are overly conservative, and do not reflect available capacity of the fuel basket angle support. A strength of materials analysis of the fuel basket angle supports is performed to

complement the finite element results. The weld stresses are computed at the support-to-shell interface, and membrane and bending stresses in the basket support angle plate itself. Using this strength of materials approach, we demonstrate that the safety factors for the fuel basket angle supports are larger than indicated by the finite element analysis.

The results of these evaluations are summarized in the tables below.

Minimum Weld Sizes for Fuel Baskets			
Basket Type	***Panel Thickness (h), in***	***t/h Ratio***	***Minimum Weld Size (t), in***
MPC-24	*5/16*	*0.57*	*0.178*
MPC-68	*1/4*	*0.516*	*0.129*
MPC-32	*9/32*	*0.57*	*0.160*
MPC-24E	*5/16*	*0.455*	*0.142*

Miscellaneous Stress Results for MPC			
Item	***Stress (ksi)***	***Allowable Stress (ksi)***	***Safety Factor***
Shear Stress in Sheathing Weld	*2.968*	*27.93*	*9.41*
Bending Stress in MPC Cover Plate	*17.60*	*24.425*	*1.39*
Shear Stress in MPC Cover Plate Weld	*3.145*	*18.99*	*6.04*
Shear Stress in Fuel Basket Support Weld	*4.711*	*9.408*	*2.00*
Combined Stress in Fuel Basket Support Plates	*32.393*	*59.1*	*1.82*

3.4.4.3.2 HI-STORM 100 Storage Overpack Stress Calculations

The structural functions of the storage overpack are stated in Section 3.1. The analyses presented here demonstrate the ability of components of the HI-STORM 100 storage overpack to perform their structural functions in the storage mode. Load Cases considered are given in Table 3.1.5. The nomenclature used to identify the load cases (Load Case Identifier) considered is also given in Table 3.1.5.

The purpose of the analyses is to provide the necessary assurance that there will be no unacceptable release of radioactive material, unacceptable radiation levels, or impairment of ready retrievability of the MPC from the storage overpack. Results obtained using the HI-STORM 100 configuration are identical to or bound results for the HI-STORM 100S configuration.

3.4.4.3.2.1 HI-STORM 100 Compression Under the Static Load of a Fully Loaded HI-TRAC Positioned on the Top of HI-STORM 100 (Load Case 01 in Table 3.1.5)

During the loading of HI-STORM 100, a HI-TRAC transfer cask with a fully loaded MPC may be placed on the top of a HI-STORM 100 storage overpack. During this operation, the HI-TRAC may be held by a single-failure-proof lifting device so a handling accident is not credible. The HI-STORM 100 storage overpack must, however, possess the compression capacity to support the additional dead load. The following analysis provides the necessary structural integrity demonstration; results for the HI-STORM 100 overpack are equal to or bound those for the HI-STORM 100S.

Define the following quantities for analysis purposes:

W_{HT} = Weight of HI- TRAC (loaded) = 243,000 lb (Table 3.2.2)

The dimensions of the compression components of HI-STORM 100 are as follows:

outer diameter of outer shell =	$D_o = 132.5"$
thickness of outer shell =	$t_o = 0.75"$
outer diameter of inner shell =	$D_i = 76"$
thickness of inner shell =	$t_i = 1.25"$
thickness of radial ribs =	$t_r = 0.75"$

The metal area of the outer metal shell is

$$A_o = \frac{\pi}{4}(D_o^2 - (D_o - 2t_o)^2) = \frac{\pi}{4}(132.5^2 - 131^2)$$
$$= 310.43\,in^2$$

The metal area of the radial ribs is

$$A_r = 4t_r(D_o - 2t_o - D_i)/2 = \frac{3}{2}(131 - 76) = 82.5\,in^2$$

The metal area of the inner shell is

$$A_i = \frac{\pi}{4}(D_i^2 - (D_i - 2t_i)^2) = \frac{\pi}{4}(76^2 - 73.5^2)$$
$$= 293.54\ in^2$$

There are four radial ribs that extend full length and can carry load. The concrete radial shield can also support compression load. The area of concrete available to support compressive loading is

$$A_{concrete} = \frac{\pi}{4}((D_o - 2t_o)^2 - (D_i)^2) - A_r$$
$$= \frac{\pi}{4}(131^2 - 76^2) - 82.5\ in^2$$
$$= (8{,}994 - 82.5)\ in^2 = 8{,}859.5\ in^2$$

The areas computed above are calculated at a section below the air outlet vents. To correct the above areas for the presence of the air outlet vents (HI-STORM 100 only since HI-STORM 100S has the air outlet vents located in the lid), we note that Bill-of-Materials 1575 in Chapter 1 gives the size of the horizontal plate of the air outlet vents as:

Peripheral width = w = 16.5"
Radial depth = d = 27.5" (over concrete in radial shield)

Using these values, the following final areas are obtained:

$A_o = A_o(\text{no vent}) - 4t_o w = 260.93$ sq. inch

$A_i = A_i(\text{no vent}) - 4t_i w = 211.04$ sq. inch

$A_{concrete} = A_{concrete}(\text{no vent}) - 4dw = 7044.2$ sq. inch

The loading case is a Level A load condition. The load is apportioned to the steel and to the concrete in accordance with the values of EA for the two materials (E(steel) = 28,000,000 psi and E(concrete)=3,605,000 psi).

$$EA(steel) = 28x10^6\ psi\ x\ (260.93 + 211.04 + 82.5)in^2$$
$$= 15525.2\ lb\ x10^6\ lbs.$$

$$EA(concrete) = 3.605 \times 10^6 \times (7044.2)\ in^2$$
$$= 25{,}394.3 \times 10^6\ lb.$$

Therefore, the total HI-TRAC load will be apportioned as follows:

F_{STEEL} = (15525.2/40,919.5) x 243,000 = 92,196.2 lb.

$F_{CONCRETE}$ = (25,394.3/40,919.5) x 243,000 = 150,803.8 lb.

Therefore, if the load is apportioned as above, with all load-carrying components in the path acting, the compressive stress in the steel is

$$\sigma_{STEEL} = \frac{F_{STEEL}}{A_o + A_i + A_r} = 134.3\ psi$$

If we conservatively neglect the compression load bearing capacity of concrete, then

$$\sigma_{STEEL} = \frac{243{,}000}{554.5} = 438\ psi$$

If we include the concrete, then the maximum compressive stress in the concrete is:

$$\sigma_{CONCRETE} = \frac{F_{CONCRETE}}{A_{CONCRETE}} = 21.4\ psi$$

It is clear that HI-STORM 100 storage overpack can support the dead load of a fully loaded 125 Ton HI-TRAC placed on top for MPC transfer into or out of the HI-STORM 100 storage overpack cavity. The calculated stresses at a cross-section through the air outlet ducts are small and give rise to large factors of safety. The metal cross-section at the base of the HI-STORM storage overpack will have a slightly larger metal area (because the width of the air-inlet ducts is smaller) but will be subject to additional dead load from the weight of the supported metal components of the HI-STORM storage overpack plus the loaded HI-TRAC weight. At the base of the storage overpack, the additional stress in the outer shell and the radial plates is due solely to the weight of the component. The additional stress in these components is computed as:

$\Delta\sigma$ = (150 lb./cu.ft.) x 18.71 ft./144 sq.in./sq.ft. = 19.5 psi

This stress will be further increased by a small amount because of the material cut away by the air-inlet ducts; however, the additional stress still remains small. The inner shell, however, is subject to additional loading from the top lid of the storage overpack and from the radial shield. From the Structural Calculation Package (HI-981928)(see Subsection 3.6.4 for the reference), and from Table 3.2.1, the following weights are obtained (using the higher 100S lid weight):

HI-STORM 100S Top Lid weight < 25,500 lb.
HI-STORM 100 Inner Shell weight < 19,000 lb.
HI-STORM 100 Shield Shell weight < 11,000 lb.

Using the calculated inner shell area at the top of the storage overpack for conservatism, gives the metal area of the inner shell as:

$A_i = A_i(\text{no vent}) - 4t_iw$ = 211.04 sq. inch

Therefore, the additional stress from the HI-STORM 100S storage overpack components, at the base of the overpack, is:

$\Delta\sigma$ = 263 psi

and a maximum compressive stress in the inner shell predicted as:

Maximum stress = 438 psi + 263 psi = 701 psi

The safety factor at the base of the storage overpack inner shell (minimum section) is

SF = 17,500psi/701psi = 24.96

The preceding analysis is bounding for the 100 Ton HI-TRAC transfer cask because of the lower HI-TRAC weight.

The preceding analysis is valid for both the HI-STORM 100 and the HI-STORM 100S since the bounding lid weight has been used.

3.4.4.3.2.2 HI-STORM 100 Lid Integrity Evaluation (Load Case 02.c, Table 3.1.5)

A non-mechanistic tip over of the HI-STORM 100 results in high decelerations at the top of the storage overpack. The storage overpack lid diameter is less than the storage overpack outer diameter. This ensures that the storage overpack lid does not directly strike the ground but requires analysis to demonstrate that the lid remains intact and does not separate from the body of the storage overpack. Figure 3.4.19 shows the scenario.

Calculations are performed to determine the response ~~Appendix 3.K presents details~~ of the HI-STORM 100 storage overpack lid ~~stress response~~ to the tip-over deceleration loading directed in the plane of the lid. The deceleration level for the non-mechanistic tip-over bounds all other decelerations, directed in the plane of the lid, experienced under other accident conditions such as flood or earthquake as can be demonstrated by evaluating the loads resulting from these natural phenomena events.

~~Appendix 3.L presents details of a calculation that demonstrates that the four studs hold the storage overpack lid in place, relative to the HI-STORM 100 body, for a postulated HI-STORM 100 tip-over event.~~ It is shown that the weight of the HI-STORM 100 lid, amplified by the design basis deceleration, can be supported by the shear capacity available in the four studs. The detailed calculations ~~in Appendix 3.L~~ demonstrate that if only a single stud is loaded initially during a tipover (because of tolerances), the stud hole will enlarge rather than the stud fail in shear. Therefore, it is assured that all four bolts will resist the tipover load regardless of the initial position of the HI-STORM 100 lid.

Similar calculations have been performed for the HI-STORM 100S lid and stud configuration. Because of the lid configuration, a longer stud length is required. To preclude bending of the studs due to lid movement, relative to the body of the HI-STORM 100S, clearance holes are provided to insure that the studs only take tension A shear ring provides the entire resistance against amplified in-plane load and ensures that the lid maintains its position, relative to the overpack. .

The following tables summarize the limiting results obtained from the detailed analyses ~~in Appendices 3.K, 3.L~~ for the HI-STORM 100, and from the similar detailed analysis for the HI-STORM 100S.

HI-STORM 100 Top Lid Integrity			
Item	**Value (ksi)**	**Allowable (ksi)**	**Safety Factor**
Lid Shell-Lid Top Plate Weld Shear Stress	6.529	29.4	4.503
Lid Shell-Lid Top Plate Combined Stress	8.84	29.4	3.326
Attachment Bolt Shear Stress	34.3	60.9	1.776
Attachment Bolt Combined Shear and Tension Interaction at interface with Anchor Block	-------	------	1.27
Inner and Outer Shell Weld to Base	15.12	29.4	1.945
Shield Block Shell-to-Lid Weld Shear Stress	5.507	29.4	5.339
Shield Block Shell Stress	5.652	29.4	5.201
Attachment Bolt Tensile Stress	33.541	107.13	3.194
Shear Ring-to Overpack Shell Weld Stress	28.63	42.0	1.467
Shear Ring Bearing Stress	16.68	63.0	3.78
Lid Shell Ring-to-Shear Ring Weld Stress	17.99	42.0	2.335

3.4.4.3.2.3 Vertical Drop of HI-STORM 100 Storage ~~O~~overpack (Load Case 02.a of Table 3.1.5)

A loaded HI-STORM 100, with the top lid in place, drops vertically and impacts the ISFSI. Figure 3.4.20 illustrates the drop scenario. The regions of the structure that require detailed examination are the storage overpack top lid, the inlet vent horizontal plate, the pedestal shield and shield shell, the inlet vent vertical plate, and all welds in the load path. *These components are examined for* ~~Appendix 3.M examines~~ the Level D event of a HI-STORM 100 drop developing the design basis deceleration.

The table provided below summarizes the results of the analyses ~~detailed in Appendix 3.M~~ for the weight and configuration of the HI-STORM 100. The results for the HI-STORM 100S are bounded by the results given below. Any calculation pertaining to the pedestal is bounding since the pedestal dimensions and corresponding weights are less in the HI-STORM 100S.

HI-STORM 100 Load Case 02.a Evaluation			
Item	**Value (ksi)**	**Allowable (ksi)**	**Safety Factor**
Lid Bottom Plate Bending Stress Intensity	27.69	59.65	2.15†
Weld- lid bottom plate-to-lid shell	21.62	29.4	1.36
Lid Shell – Membrane Stress Intensity	1.856	39.75	21.42
Lid Top (2" thick) Plate Bending Stress Intensity	11.27	59.65	5.294*
Inner Shell –Membrane Stress Intensity	11.33	39.75	3.508
Outer Shell –Membrane Stress Intensity	3.401	39.75	11.686
Inlet Vent Horizontal Plate Bending Stress Intensity	35.25	59.65	1.692
Inlet Vent Vertical Plate Membrane Stress Intensity	9.998	39.75	3.976
Pedestal Shield – Compression	1.249	1.535	1.229
Pedestal Shell – Circumferential Stress	14.28	33.15	2.321
Weld – outer shell-to-baseplate	3.854	29.4	7.629
Weld – inner shell-to-baseplate	7.321	29.4	4.016
Weld-Pedestal shell-to-baseplate	1.138	29.4	25.828

† Note that ~~Appendix 3.X shows that~~ the dynamic load factor for the lid top plate is negligible and for the lid bottom plate is 1.06. This dynamic load factor has been incorporated in the above table.

* For the HI-STORM 100S, this safety factor is conservatively evaluated ~~in Appendix 3.M~~ to be 1.658 because of increased load on the upper of the two lid plates.

~~Appendix 3.AK contains a~~An assessment of the potential for instability of the compressed inner and outer shells under the compressive loading during the drop event *has also been performed.* The methodology is from ASME Code Case N-284 (Metal Containment Shell Buckling Design Methods, Division I, Class MC (8/80)). This Code Case has been previously accepted by the NRC as an acceptable method for evaluation of stability in vessels. The results obtained are conservative in that

the loading in the shells is assumed to be uniformly distributed over the entire length of the shells. In reality, the component due to the amplified weight of the shell varies from zero at the top of the shell to the maximum value at the base of the shell. It is concluded ~~in Appendix 3.AK~~ that large factors of safety exist so that elastic or plastic instability of the inner and outer shells does not provide a limiting condition. The results for the HI-STORM 100 bound similar results for the HI-STORM 100S since the total weight of the "S" configuration is substantially decreased (see Subsection 3.2).

The results ~~from Appendix 3.M and 3.AK~~ do not show any gross regions of stress above the material yield point that would imply the potential for gross deformation of the storage overpack subsequent to the handling accident. MPC stability has been evaluated in the HI-STAR 100 FSAR for a drop event with 60g deceleration and shown to satisfy the Code Case N-284 criteria. Therefore, ready retrievability of the MPC is maintained as well as the continued performance of the HI-STORM 100 storage overpack as the primary shielding device.

3.4.4.3.3 HI-TRAC Transfer Cask Stress Calculations

The structural functions of the transfer cask are stated in Section 3.1. The analyses presented here demonstrate the ability of components of the HI-TRAC transfer cask to perform their structural functions in the transfer mode. Load Cases considered are given in Table 3.1.5.

The purpose of the analyses is to provide the necessary assurance that there will be no unacceptable release of radioactive material, unacceptable radiation levels, or impairment of ready retrievability.

3.4.4.3.3.1 Analysis of Pocket Trunnions (Load Case 01 of Table 3,1.5)

HI-TRAC has pocket trunnions attached to the outer shell and to the water jacket. During the rotation of HI-TRAC from horizontal to vertical or vice versa (see Figure 3.4.18), these trunnions serve to define the axis of rotation. The HI-TRAC is also supported by the lifting trunnions during this operation. Two load conditions are considered: Level A when all four trunnions support load during the rotation; and, Level B when the hoist cable is assumed slack so that the entire load is supported by the rotation trunnions. A dynamic amplification of 15% is assumed in both cases appropriate to a low-speed operation. ~~Appendices 3.AA and 3.AI (for the 125 Ton and 100 Ton units, respectively) present the analysis of the pocket trunnion.~~ Figure 3.4.23 shows a free body of the trunnion and shows how the applied force and moment are assumed to be resisted by the weld group that connects the trunnion to the outer shell. Drawings 1880 (sheet 10) and 2145 (sheet 10) show the configuration. An optional construction for the 100 Ton HI-TRAC permits the pocket trunnion base to be split to reduce the "envelope" of the HI-TRAC. For that construction, bolts and dowel pins are used to insure that the force and moment applied to the pocket trunnions are transferred properly to the body of the transfer cask. *The analysis* ~~Appendix 3.AI~~ also evaluates the bolts and dowel pins and demonstrates that safety factors greater than 1.0 exist for bolt loads, dowel bearing and tear-out, and dowel shear. Allowable strengths and loads are computed using applicable sections of ASME Section III, Subsection NF.

The table below summarizes the results *for the 125 Ton and 100 Ton units* ~~from the two appendices~~:

Pocket Trunnion Weld Evaluation Summary			
Item	**Value (ksi)**	**Allowable (ksi)†**	**Safety Factor**
125 Ton Pocket Trunnion-Outer Shell Weld Group Stress	5.331	23.275	4.366
125 Ton Pocket Trunnion–Water Jacket Weld Group Stress	4.383	23.275	5.31
100 Ton Pocket Trunnion-Outer Shell Weld Group Stress	4.346	23.275	5.355
100 Ton Pocket Trunnion–Water Jacket Weld Group Stress	3.766	23.275	6.181
100 Ton Pocket Trunnion–Bolt Tension at Optional Split	45.23	50.07	1.107
100 Ton Pocket Trunnion–Bearing Stress on Base Surfaces at Dowel	6.497	32.7	5.033
100 Ton Pocket Trunnion–Tear-out Stress on Base Surfaces at Dowel	2.978	26.09	8.763
100 Ton Pocket Trunnion–Shear Stress on Dowel Cross Section at Optional Split	29.04	37.93	1.306

† Allowable stress is reported for the Level B loading, which results in the minimum safety factor.

To provide additional information on the local stress state adjacent to the rotation trunnion, ~~Appendix 3.AA also includes~~ a new finite element analysis *is undertaken to provide* ~~providing~~ details on the state of stress in the metal structure surrounding the rotation trunnions for the 125 Ton HI-TRAC. The finite element analysis has been based on a model that includes major structural contributors from the water jacket enclosure shell panels, radial channels, end plates, outer and inner shell, and bottom flange. In the finite element analysis, the vertical trunnion load has been oriented in the direction of the HI-TRAC 125 longitudinal axis. The structural model has been confined to the region of the HI-TRAC adjacent to the rotation trunnion block; the extent of the model in the longitudinal direction has been determined by calculating the length of the "bending boundary layer" associated with a classical shell analysis. This *is* ~~was~~ considered to

be a sufficient length to capture maximum shell stresses arising from the Level B (off-normal) rotation trunnion loading. ~~Appendix 3.AA contains the results of the finite element simulations with complete graphical output showing the longitudinal and circumferential stress distribution in the inner and outer shells and in the radial channels.~~ The local nature of the stress around the trunnion block is clearly demonstrated by the *finite element* ~~graphical~~ results.

Consistent with the requirements of ASME Section III, Subsection NF, for Class 3 components, safety factors for primary membrane stress have been computed. Primary stresses are located away from the immediate vicinity of the trunnion; although the NF Code sets no limits on primary plus secondary stresses that arise from the gross structural discontinuity immediately adjacent to the trunnion, these stresses are listed for information. The results~~, assembled from the results in Appendix 3.AA,~~ are summarized in the table below for the Level B load distribution for the 125-ton HI-TRAC.

ITEM – 125 Ton HI-TRAC	CALCULATED VALUE	ALLOWABLE VALUE
Longitudinal Stress - (ksi) (Primary Stress –Inner Shell)	-0.956	23.275
Tangential Stress (ksi) (Primary Stress - Inner Shell)	-1.501	23.275
Longitudinal Stress (ksi) (Primary Stress – Outer Shell)	-0.830	23.275
Tangential Stress (ksi) (Primary Stress - Outer Shell)	-0.436	23.275
Longitudinal Stress - (ksi) (Primary Stress – Radial Channels)	2.305	23.275
Tangential Stress (ksi) (Primary Stress - Radial Channels)	-0.631	23.275
Longitudinal Stress - (ksi) (Primary plus Secondary Stress -Inner Shell)	1.734	No Limit (34.9)*
Tangential Stress (ksi) (Primary plus Secondary Stress - Inner Shell)	-1.501	NL
Longitudinal Stress (ksi) (Primary plus Secondary Stress - Outer Shell)	2.484	NL
Tangential Stress (ksi) (Primary plus Secondary Stress - Outer Shell)	-2.973	NL
Longitudinal Stress - (ksi) (Primary plus Secondary Stress - Radial Channels)	-13.87	NL
Tangential Stress (ksi) (Primary plus Secondary Stress - Radial Channels)	-2.303	NL

* The NF Code sets no limits (NL) for primary plus secondary stress (see Table 3.1.17). Nevertheless, to demonstrate the robust design with its large margins of safety, we list here, for information only, the allowable value for Primary Membrane plus Primary Bending Stress appropriate to temperatures up to 650 degrees F.

The only stress of any significance is the longitudinal stress in the radial channels. This stress

occurs immediately adjacent to the trunnion block/radial channel interface and by its localized nature is identifiable as a stress arising at the gross structural discontinuity (secondary stress).

The finite element analysis has also been performed for the 100 Ton HI-TRAC transfer cask~~; results are reported in Appendix 3.AI~~. The following table summarizes the results:

ITEM – 100 Ton HI-TRAC	CALCULATED VALUE	ALLOWABLE VALUE
Longitudinal Stress - (ksi) (Primary Stress –Inner Shell)	-0.756	23.275
Tangential Stress (ksi) (Primary Stress - Inner Shell)	-2.157	23.275
Longitudinal Stress (ksi) (Primary Stress – Outer Shell)	-0.726	23.275
Tangential Stress (ksi) (Primary Stress - Outer Shell)	-0.428	23.275
Longitudinal Stress - (ksi) (Primary Stress – Radial Channels)	2.411	23.275
Tangential Stress (ksi) (Primary Stress - Radial Channels)	-0.5305	23.275
Longitudinal Stress - (ksi) (Primary plus Secondary Stress -Inner Shell)	2.379	NL
Tangential Stress (ksi) (Primary plus Secondary Stress - Inner Shell)	-2.157	NL
Longitudinal Stress (ksi) (Primary plus Secondary Stress - Outer Shell)	3.150	NL
Tangential Stress (ksi) (Primary plus Secondary Stress - Outer Shell)	-3.641	NL
Longitudinal Stress - (ksi) (Primary plus Secondary Stress - Radial Channels)	-15.51	NL
Tangential Stress (ksi) (Primary plus Secondary Stress - Radial Channels)	-2.294	NL

The finite element analyses of the metal structure adjacent to the trunnion block did not include the state of stress arising from the water jacket internal pressure. These stresses ~~are computed in Appendix 3.AG and~~ are conservatively computed based on a two-dimensional strip model that neglects the lower annular plate. The water jacket bending stresses ~~calculated in Appendix 3.AG~~ are summarized below:

~~Appendix 3.AG~~ Result for Tangential Bending Stress in Water Jacket Outer Panel from Water Pressure (including hydrostatic and inertia effects)	Calculated Value (ksi)
125 Ton HI-TRAC	18.41
100 Ton HI-TRAC	22.47

To establish a minimum safety factor for the outer panels of the water jacket for the Level A condition, we must add primary membrane circumferential stress from the trunnion load analysis ~~(Appendices 3.AA and 3.AI with reduction factor from Level B to Level A load)~~ to primary circumferential bending stress from the water jacket bending stress ~~(Appendix 3.AG)~~. Then, the safety factors may be computed by comparison to the allowable limit for primary membrane plus primary bending stress. The following results are obtained:

Results for Load Case 01 in Water Jacket (Load Case 01) – Level A Load			
Circumferential Stress in Water Jacket Outer Enclosure	**CALCULATED VALUE (ksi)**	**ALLOWABLE VALUE (ksi)**	**SAFETY FACTOR (allowable value/calculated value)**
125 Ton HI-TRAC	18.797	26.25	1.397
100 Ton HI-TRAC	22.781	26.25	1.152

To arrive at minimum safety factors for primary membrane plus bending stress in the outer panel of the water jacket for the Level B condition, we amplify the finite element results *from the trunnion load analysis*~~in accordance with Appendices 3.AA and 3.AI~~, add the appropriate stress from *the two-dimensional water jacket calculation*~~Appendix 3.AG~~, and compare the results to the increased Level B allowable. The following results are obtained:

Results for Load Case 01 in Water Jacket (Load Case 01) – Level B Load			
Circumferential Stress in Water Jacket Outer Enclosure	**CALCULATED VALUE (ksi)**	**ALLOWABLE VALUE (ksi)**	**SAFETY FACTOR (allowable value/calculated value)**
125 Ton HI-TRAC	19.041	35.0	1.84
100 Ton HI-TRAC	23.00	35.0	1.52

All safety factors are greater than 1.0; the Level A load condition governs.

3.4.4.3.3.2 Lead Slump in 125 Ton HI-TRAC - Horizontal Drop Event (Case 02.b in Table 3.1.5)

During a side drop of the 125 Ton HI-TRAC transfer cask, the lead shielding must be shown not to slump and cause significant amounts of shielding to be lost in the top area of the lead annulus. Slumping of the lead is not considered credible in the HI-TRAC transfer cask because of:

a. the shape of the interacting surfaces
b. the ovalization of the shell walls under impact
c. the high coefficient of friction between lead and steel
d. The inertia force from the MPC inside the HI-TRAC will compress the inner shell at the impact location and locally "pinch" the annulus that contains the lead; this opposes the tendency for the lead to slump and open up the annulus at the impact location.

Direct contact of the outer shell of the HI-TRAC with the ISFSI pad is not credible since there is a water jacket that surrounds the outer shell. The water jacket metal shell will experience most of the direct impact. Nevertheless, to conservatively analyze the lead slump scenario, it is assumed that there is no water jacket, the impact occurs far from either end of the HI-TRAC so as to ignore any strengthening of the structure due to end effects, the impact occurs directly on the outer shell of the HI-TRAC, and the contact force between HI-TRAC and the MPC is ignored. All of these assumptions are conservative in that their imposition magnifies any tendency for the lead to slump.

To confirm that lead slump is not credible, a finite element analysis of the lead slump problem, incorporating the conservatisms listed above, during a postulated 125 Ton HI-TRAC horizontal drop (see Figure 3.4.22) is carried out. ~~Details of the analysis (finite element model and plotted results) are presented in Appendix 3.F.~~ The 125 Ton HI-TRAC cask body modeled consists only of an inner steel shell, an outer steel shell, and a thick lead annulus shield contained between the inner and outer shell. A unit length of HI-TRAC is modeled and the contact at the lead/steel interface is modeled as a compression-only interface. Interface frictional forces are conservatively neglected. As the 125 Ton HI-TRAC has a greater lead thickness, analysis of the 125 Ton HI-TRAC is considered to bound the 100 Ton HI-TRAC.

The analysis is performed in two parts:

First, to maximize the potential for lead/steel separation, the shells are ignored and the gap elements grounded. This has the same effect as assuming the shells to be rigid and maximizes the potential and magnitude of any separation at the lead/steel interface (and subsequent slump). This also maximizes the contact forces at the portion of the interface that continues to have compression forces developed. The lead annulus is subjected to a 45g deceleration and the deformation, stress field, and interface force solution developed. This solution establishes a conservative result for the movement of the lead relative to the metal shells.

In the second part of the analysis, the lead is removed and replaced by the conservative (high) interface forces from the first part of the analysis. These interface forces, together with the 45g deceleration-induced inertia forces from the shell self weight are used to obtain a solution for the stress and deformation field in the inner and outer metal shells.

The results of the analysis ~~described in Appendix 3.F,~~ are as follows:

a. The maximum predicted lead slump at a location 180 degrees from the impact point is 0.1". This gap decreases gradually to 0.0" after approximately 25 degrees from the vertical axis. ~~It is shown in Appendix 3.F that t~~*T*he decrease in the diameter of the inner shell of the transfer cask (in the direction of the deceleration) is approximately 0.00054". This demonstrates that ovalization of the HI-TRAC shells does not occur. Therefore, the lead shielding deformation is confined to a local region with negligible deformation of the confining shells.

b. The stress intensity distribution in the shells demonstrates that high stresses are concentrated, as anticipated, only near the assumed point of impact with the ISFSI pad. The value of the maximum stress intensity (51,000 psi) remains below the allowable stress intensity for primary membrane plus primary bending for a Level D event (58,700 psi). Thus, the steel shells continue to perform their function and contain the lead. The stress distribution, obtained using the conservatively large interface forces, demonstrates that permanent deformation could occur only in a localized region near the impact point. Since the "real" problem precludes direct impact with the outer shell, the predicted local yielding is simply a result of the conservatisms imposed in the model.

It is concluded that a finite element analysis of the lead slump under a 45g deceleration in a side drop clearly indicates that there is no appreciable change in configuration of the lead shielding and no overstress of the metal shell structure. Therefore, retrievability of the MPC is not compromised and the HI-TRAC transfer cask continues to provide shielding.

3.4.4.3.3.3 HI-TRAC Transfer Lid Stress Analysis During HI-TRAC Drop Accident (Load Case 02.b in Table 3.1.5)

~~Appendix 3.AD presents t~~*T*he *stress in the* 125 Ton HI-TRAC transfer lid *is analyzed* ~~stress analysis~~ when the lid is subject to the deceleration loads of a side drop. Figure 3.4.22 is a sketch of the scenario. *The analysis shows* ~~It is shown in Appendix 3.AD~~ that the cask body, under a deceleration of 45g's, will not separate from the transfer lid during the postulated side drop. This event is considered a Level D event in the ASME parlance.

The bolts that act as doorstops to prevent opening of the doors are also checked ~~in this appendix~~ for their load capacity. It is required that sufficient shear capacity exists to prevent both doors from opening and exposing the MPC.

The only difference between the 100 Ton and 125 Ton HI-TRAC transfer lid doors is that the 100 Ton has less lead and has no middle steel plate. ~~Appendix 3.AJ presents analyses~~*A* similar *analysis of* ~~to Appendix 3.AD for~~ the 100 Ton HI-TRAC ~~and~~ shows that all safety factors are greater than 1.0. The table given below summarizes the *results for both units*~~work in Appendices 3.AD and 3.AJ~~:

Transfer Lid Attachment Integrity Under Side Drop			
Item – Shear Capacity	**Value (kip) or (ksi)**	**Capacity (kip) or (ksi)**	**Safety Factor= Capacity/Value**
125 Ton Attachment (kip)	1,272.0	1,770.0	1.392
125 Ton Door Lock Bolts (ksi)	20.24	48.3	2.387
100 Ton Attachment (kip)	1,129.0	1,729.0	1.532
100 Ton Door Lock Bolts (ksi)	13.81	48.3	3.497

All safety factors are greater than 1.0 and are based on actual interface loads~~.~~. ~~The actual interface load for both transfer casks is computed in Appendix 3.AN.~~ For the 125-Ton and 100-Ton HI-TRACs, the actual interface load (primary impact at transfer lid) computed from the handling accident analysis is bounded by the values given below:

BOUNDING INTERFACE LOADS COMPUTED FROM HANDLING ACCIDENT ANALYSES	
Item	**Bounding Value ~~from Appendix 3.AN~~ (kip)**
125-Ton HI-TRAC	1,300
100-Ton HI-TRAC	1,150

3.4.4.3.3.4 Stress Analysis of the HI-TRAC Water Jacket (Load Case 03 in Table 3.1.5)

The water jacket is assumed subject to internal pressure from pressurized water and gravity water head. Calculations *are performed* to determine the water jacket stress under internal pressure plus hydrostatic load ~~are performed in Appendix 3.AG~~. Results are obtained for the water jacket configuration and the connecting welds for both HI-TRAC transfer casks. The table below summarizes the results of the analysis ~~performed in Appendix 3.AG~~.

Water Jacket Stress Evaluation			
Item	**Value (ksi)**	**Allowable (ksi)**	**Safety Factor**
125 Ton HI-TRAC Water Jacket Enclosure Shell Panel Bending Stress	18.41	26.25	1.426
100 Ton HI-TRAC Water Jacket Enclosure Shell Panel Bending Stress	22.47	26.25	1.168
125 Ton HI-TRAC Bottom Flange Bending Stress	18.3	26.25	1.434
100 Ton HI-TRAC Water Jacket Bottom Flange Bending Stress	16.92	26.25	1.551
125 Ton HI-TRAC Weld Stress -Enclosure Panel Single Fillet Weld	2.22	21.0	9.454
100 Ton HI-TRAC Weld Stress – Enclosure Panel Single Fillet Weld	1.841	21.0	11.408
125 Ton HI-TRAC Weld Stress – Bottom Flange-to Outer Shell Double Fillet Weld	14.79	21.0	1.42
125 Ton HI-TRAC - Enclosure Panel Direct Stress	1.571	17.5	11.142
100 Ton HI-TRAC - Enclosure Panel Direct Stress	1.736	17.5	10.84

3.4.4.3.3.5 HI-TRAC Top Lid Separation (Load Case 02.b in Table 3.1.5)

~~Appendix 3.AH examines t~~The potential of top lid separation under a 45g deceleration side drop event *requires examination*. It is concluded *by analysis* that the connection provides acceptable protection against top lid separation. It is also shown that the bolts and the lid contain the MPC within the HI-TRAC cavity during and after a drop event. The results from the 125 Ton HI-TRAC bound the corresponding results from the 100 Ton HI-TRAC because the top lid bolts are identical in the two units and the 125 Ton HI-TRAC top lid weighs more. The table below provides the results of the analysis.

HI-TRAC Top Lid Separation Analysis			
Item	**Value**	**Capacity**	**Safety Factor= Capacity/Value**
Attachment Shear Force (lb.)	123,750	958,651	7.747
Tensile Force in Stud (lb.)	132,000	1,118,436	8.473
Bending Stress in Lid (ksi)	35.56	58.7	1.651
Shear Load per unit Circumferential Length in Lid (lb./in)	533.548	29,400	55.103

3.4.4.4 Comparison with Allowable Stresses

Consistent with the formatting guidelines of Reg. Guide 3.61, calculated stresses and stress intensities from the finite element and other analyses are compared with the allowable stresses and stress intensities defined in Subsection 3.1.2.2 per the applicable sections of [3.4.2] and [3.4.4] for defined normal and off-normal events and [3.4.3] for accident events (Appendix F).

3.4.4.4.1 MPC

Table 3.4.6 provides summary data extracted from the numerical analysis results for the fuel basket, enclosure vessel, and fuel basket supports based on the design basis deceleration. The results presented in Table 3.4.6 do not include any dynamic amplification due to internal elasticity of the structure (i.e., local inertia effects). ~~Appendix 3.X~~ *Calculations* suggests that a uniform conservative dynamic amplifier would be 1.08 independent of the duration of impact. If we recognize that the tip-over event for HI-STORM 100 is a long duration event, then a dynamic amplifier of 1.04 is appropriate. The summary data provided in Table 3.4.3 and 3.4.4 gives the lowest safety factor computed for the fuel basket and for the MPC, respectively. Modification of the fuel basket safety factor for dynamic amplification leaves considerable margin.

Factors of safety greater than 1 indicate that calculated results are less than the allowable strengths.

A perusal of the results in Tables 3.4.3 and 3.4.4 under different load combinations for the fuel basket and the enclosure vessel reveals that all factors of safety are above 1.0 even if we use the most conservative value for dynamic amplification factor. The relatively modest factor of safety in the fuel basket under side drop events (Load Case F3.b and F3.c) in Table 3.4.3 warrants further explanation since a very conservative finite element model of the structure has been utilized in the analysis.

The wall thickness of the storage cells, which is by far the most significant variable in a fuel basket's structural strength, is significantly greater in the MPCs than in comparable fuel baskets licensed in the past. For example, the cell wall thickness in the TN-32 basket (Docket No. 72-1021, M-56), is 0.1 inch and that in the NAC-STC basket (Docket No. 71-7235) is 0.048 inch. In contrast, the cell wall thickness in the MPC-68 is 0.25 inch. In spite of their relatively high flexural rigidities, computed margins in the fuel baskets are rather modest. This is because of some assumptions in the analysis that lead to an overstatement of the state of stress in the fuel basket. For example:

i. The section properties of longitudinal fillet welds that attach contiguous cell walls to each other are completely neglected in the finite element model (Figure 3.4.7). The fillet welds strengthen the cell wall section modulus at the very locations where maximum stresses develop.

ii. The radial gaps at the fuel basket-MPC shell and at the MPC shell-storage overpack interface are explicitly modeled. As the applied loading is incrementally increased, the MPC shell and fuel basket deform until a "rigid" backing surface of the storage overpack is contacted, making further unlimited deformation under lateral loading impossible. Therefore, some portion of the fuel basket and enclosure vessel (EV) stress has the characteristics of secondary stresses (which by definition, are self-limited by deformation in the structure to achieve compatibility). For conservativeness in the incremental analysis, we make no distinction between deformation controlled (secondary) stress and load controlled (primary) stress in the stress categorization of the MPC-24, 32, and 68 fuel baskets. We treat all stresses, regardless of their origin, as primary stresses. Such a conservative interpretation of the Code has a direct (adverse) effect on the computed safety factors. As noted earlier, the results for the MPC-24E are properly based only on primary stresses to illustrate the conservatism in the reporting of results for the MPC-24, 32, and 68 baskets.

iii. A uniform pressure simulates the SNF inertia loading on the cell panels, which is a most conservative approach for incorporating the SNF/cell wall structure interaction.

The above assumptions act to depress the computed values of factors of safety in the fuel basket finite element analysis and render conservative results.

The reported factors of safety do not include the effect of dynamic load amplifiers. ~~As noted in Appendices 3.A and 3.X, t~~The duration of impact and the predominant natural frequency of the basket panels under drop events result in the dynamic load factors that do not exceed 1.08. Therefore, since all reported factors of safety are greater than the DLF, the MPC is structurally adequate for its intended functions.

Tables 3.4.7 and 3.4.8 report stress intensities and safety factors for the confinement boundary subject to internal pressure alone and internal pressure plus the normal operating condition temperature with the most severe thermal gradient. The final values for safety factors in the various

locations of the confinement boundary provide assurance that the MPC enclosure vessel is a robust pressure vessel.

3.4.4.4.2 Storage Overpack and HI-TRAC

The result from analyses of the storage overpack and the HI-TRAC transfer cask is shown in Table 3.4.5. The location of each result is indicated in the table. Safety factors for lifting operations where three times the lifted load is applied are reported in Section 3.4.3.

The table shows that all allowable stresses are much greater than their associated calculated stresses and that safety factors are above the limit of 1.0.

3.4.4.5 Elastic Stability Considerations

3.4.4.5.1 MPC Elastic Stability

Stability calculations for the MPC have been carried out in the HI-STAR 100 FSAR, Docket Number 72-1008, Appendix 3.H. The calculations in that submittal bound calculations for the MPC in HI-STORM 100 since all loadings are identical except for the peak deceleration under accident events, which has been reduced from 60g's to 45g's.

3.4.4.5.2 HI-STORM 100 Storage Overpack Elastic Stability

HI-STORM 100 (and 100S) storage overpack shell buckling is not a credible scenario since the two steel shells plus the entire radial shielding act to resist vertical compressive loading. Subsection 3.4.4.3.2.3 develops values for compressive stress in the steel shells of the storage overpack. Because of the low value for compressive stress coupled with the fact that the concrete shielding backs the steel shells, we can conclude that instability is unlikely. Note that the entire weight of the storage overpack can also be supported by the concrete shielding acting in compression. Therefore, in the unlikely event that a stability limit in the steel was approached, the load would simply shift to the massive concrete shielding. Notwithstanding the above comments, stability analyses of the storage overpack have been performed for bounding cases of longitudinal compressive stress with nominal circumferential compressive stress and for bounding circumferential compressive stress with nominal axial compressive stress. This latter case is for a bounding all-around external pressure on the HI-STORM 100 outer shell. The latter case is listed as Load Case 05 in Table 3.1.5 and is performed to demonstrate that explosions or other environmental events that could lead to an all-around external pressure on the outer shell do not cause a buckling instability. ASME Code Case N-284, a methodology accepted by the NRC, has been used for this analysis. ~~Appendix 3.AK reports results of all stability analyses performed in support of this FSAR. In that appendix, t~~The storage overpack shells are examined individually assuming that the four radial plates provide circumferential support against a buckling deformation mode. The analysis of the storage overpack outer shell for a bounding external pressure of

p_{ext} = 30 psi

that, together with a nominal compressive axial load that bounds the dead weight load at the base of the outer shell, gives a safety factor against an instability of ~~(see Load Case 3 in Appendix 3.AK)~~:

Safety Factor = (1/0.466) x 1.34 = 2.88

The factor 1.34 is included in the above result since the analysis methodology of Code Case N-284 builds in this factor for a stability analysis for an accident condition.

The external pressure for the overpack stability considered here significantly bounds the short-time 10 psi differential pressure (between outer shell and internal annulus) specified in Table 2.2.1.

The same postulated external pressure condition can also act on the HI-TRAC during movement from the plant to the ISFSI pad. In this case, the lead shielding acts as a backing for the outer shell of the HI-TRAC transfer cask just as the concrete does for the storage overpack. The water jacket metal structure provides considerable additional structural support to the extent that it is reasonable to state that instability under external pressure is not credible. If it is assumed that the all-around water jacket support is equivalent to the four locations of radial support provided in the storage overpack, then it is clear that the instability result for the storage overpack bounds the results for the HI-TRAC transfer cask. This occurs because the R/t ratio (mean radius-to-wall thickness) of the HI-TRAC outer shell is less than the corresponding ratio for the HI-STORM storage overpack. Therefore, no HI-TRAC analysis is performed ~~in Appendix 3.AK~~.

3.4.5 Cold

A discussion of the resistance to failure due to brittle fracture is provided in Subsection 3.1.2.3.

The value of the ambient temperature has two principal effects on the HI-STORM 100 System, namely:

i. The steady-state temperature of all material points in the cask system will go up or down by the amount of change in the ambient temperature.

ii. As the ambient temperature drops, the absolute temperature of the contained helium will drop accordingly, producing a proportional reduction in the internal pressure in accordance with the Ideal Gas Law.

In other words, the temperature gradients in the system under steady-state conditions will remain the same regardless of the value of the ambient temperature. The internal pressure, on the other hand, will decline with the lowering of the ambient temperature. Since the stresses under normal storage condition arise principally from pressure and thermal gradients, it follows that the stress field in the MPC under –40 degree F ambient would be smaller than the "heat" condition of storage, treated in

the preceding subsection. Additionally, the allowable stress limits tend to increase as the component temperatures decrease.

Therefore, the stress margins computed in Section 3.4.4 can be conservatively assumed to apply to the "cold" condition as well.

Finally, it can be readily shown that the HI-STORM 100 System is engineered to withstand "cold" temperatures (-40 degrees F), as set forth in the Technical Specification, without impairment of its storage function.

Unlike the MPC, the HI-STORM 100 storage overpack is an open structure; it contains no pressure. Its stress field is unaffected by the ambient temperature, unless low temperatures produce brittle fracture due to the small stresses which develop from self-weight of the structure and from the minute difference in the thermal expansion coefficients in the constituent parts of the equipment (steel and concrete). To prevent brittle fracture, all steel material in HI-STORM 100 is qualified by impact testing as set forth in the ASME Code (Table 3.1.18).

The structural material used in the MPC (Alloy X) is recognized to be completely immune from brittle fracture in the ASME Codes.

As no liquids are included in the HI-STORM 100 storage overpack design, loads due to expansion of freezing liquids are not considered. The HI-TRAC transfer cask utilizes demineralized water in the water jacket. However, the specified lowest service temperature for the HI-TRAC is 0 degrees F and a 25% ethylene glycol solution is required for the temperatures from 0 degrees F to 32 degrees F. Therefore, loads due to expansion of freezing liquids are not considered.

There is one condition, however, that does require examination to insure ready retrievability of the fuel. Under a postulated loading of an MPC from a HI-TRAC transfer cask into a cold HI-STORM 100 storage overpack, it must be demonstrated that sufficient clearances are available to preclude interference when the "hot" MPC is inserted into a "cold" storage overpack. To this end, an analysis for free thermal expansions under cold conditions of storage has been performed ~~in Appendix 3.AF~~. The storage overpack is assumed to have been uniformly cooled to 0 degrees F from its normal assembly temperature (assumed as 70 degrees F in all analyses). The MPC is assumed to have the temperature distribution associated with being contained within a HI-TRAC transfer cask. For additional conservatism in the analysis, the MPC temperatures for the "hot condition of storage" (100 degrees F ambient) in a HI-TRAC are used to maximize the radial and axial growth of the loaded MPC. ~~These MPC temperatures are available in Appendix 3.I.~~ The results from the evaluation of free thermal expansion described above ~~and carried out in detail in Appendix 3.AF~~ for this "cold condition of transfer" are summarized in the table below:

THERMOELASTIC DISPLACEMENTS IN THE HOT MPC AND COLD HI-STORM STORAGE OVERPACK UNDER COLD TEMPERATURE TRANSFER CONDITION				
HOT CANISTER – COLD HI-STORM				
	Radial Direction (in.)		**Axial Direction (in.)**	
Unit	**Initial Clearance**	**Final Clearance**	**Initial Clearance**	**Final Clearance**
MPC (worst case)	0.5	0.364	1.0	0.24

The final radial clearance (greater than 0.25" radial) is sufficient to preclude jamming of the MPC upon insertion into a cold HI-STORM 100 storage overpack.

3.4.6 HI-STORM 100 Kinematic Stability under Flood Condition (Load Case A in Table 3.1.1)

The flood condition subjects the HI-STORM 100 System to external pressure, together with a horizontal load due to water velocity. Because the HI-STORM 100 storage overpack is equipped with ventilation openings, the hydrostatic pressure from flood submergence acts only on the MPC. As stated in subsection 3.1.2.1.1.3, the design external pressure for the MPC bounds the hydrostatic pressure from flood submergence. Subsection 3.4.4.5.2 has reported a positive safety factor against instability from external pressure in excess of that expected from a complete submergence in a flood. The analysis performed below is also valid for the HI-STORM 100S.

The water velocity associated with flood produces a horizontal drag force, which may act to cause sliding or tip-over. In accordance with the provisions of ANSI/ANS 57.9, the acceptable upper bound flood velocity, V, must provide a minimum factor of safety of 1.1 against overturning and sliding. For HI-STORM 100, we set the upper bound flood velocity design basis at 15 feet/sec. Subsequent calculations conservatively assume that the flow velocity is uniform over the height of the storage overpack.

The overturning horizontal force, F, due to hydraulic drag, is given by the classical formula:

$$F = Cd\ A\ V^*$$

where:

V^* is the velocity head = $\frac{\rho V^2}{2g}$; (ρ is water weight density, and g is acceleration due to gravity).

A: projected area of the HI-STORM 100 cylinder perpendicular to the fluid velocity vector.

Cd: drag coefficient

The value of Cd for flow past a cylinder at Reynolds number above 5E+05 is given as 0.5 in the literature (viz. Hoerner, Fluid Dynamics, 1965).

The drag force tending to cause HI-STORM 100's sliding is opposed by the friction force, which is given by

$$F_f = \mu K W$$

where:

μ = limiting value of the friction coefficient at the HI-STORM 100/ISFSI pad interface (conservatively taken as 0.25, although literature citations give higher values).

K = buoyancy coefficient (documented in HI-981928, Structural Calculation Package for HI-STORM 100 (see citation in Subsection 3.6.4).

W: Minimum weight of HI-STORM 100 with an empty MPC.

Sliding Factor of Safety

The factor of safety against sliding, b_1, is given by

$$\beta_1 = \frac{F_f}{F} = \frac{\mu KW}{Cd\, A\, V^*}$$

It is apparent from the above equation, β, will be minimized if a lower bound weight of HI-STORM 100 is used in the above equation.

As stated previously, μ= 0.25, Cd = 0.5.

V^* corresponding to 15 ft./sec. water velocity is 218.01 lb per sq. ft.

A = length x diameter of HI-STORM 100 = 132.5" x 231.25"/144 sq. in./sq.ft. = 212.78 sq. ft.

K = buoyancy factor = 0.64 (per calculations in HI-981928)

W = 303,000 lbs. (Table 3.2.1 with empty MPC-68)

Substituting in the above formula for β, we have

$\beta_1 = 2.09 > 1.1$ (required)

The HI-STORM 100S has a lower weight and if coupled with an empty MPC-32 reduces the value of "W" to 286,798 lb. The safety factor against sliding is reduced to 1.979 for this configuration.

Overturning Factor of Safety

For determining the margin of safety against overturning b_2, the cask is assumed to pivot about a fixed point located at the outer edge of the contact circle at the interface between HI-STORM 100 and the ISFSI. The overturning moment due to a force F_T applied at height H^* is balanced by a restoring moment from the reaction to the cask buoyant force KW acting at radius D/2.

$$F_T H^* = KW \frac{D}{2}$$

$$F_T = \frac{K W D}{2 H^*}$$

W is the minimum weight of the storage overpack with an empty MPC.

We have,

W = 303,000 lb. (Table 3.2.1)

H^* = 118.6" (maximum height of mass center per Table 3.2.3)

D = 132.5" (Holtec Drawing 1495)

K = 0.64 (calculated in HI-981928)

F_T = 108,396 lb.

F_T is the horizontal drag force at incipient tip-over.

F = Cd A V^* = 23,194 lbs. (drag force at 15 feet/sec)

The safety factor against overturning, β_2, is given as:

$$\beta_2 = \frac{F_T}{F} = 4.67 > 1.1 \text{ (required)}$$

Use of the minimum weight HI-STORM 100S in the above calculation results in minimal change to the result since the weight reduction also results in a lowering of the center of gravity, and F_T is not significantly changed.

In the next subsection, results are presented to show that the load F (equivalent to an inertial deceleration of F/360,000 lb = 0.0644 g's applied to the loaded storage overpack) does not lead to large global circumferential stress or ovalization of the storage overpack that could prevent ready retrievability of the MPC. It is shown in Subsection 3.4.7 that a horizontal load equivalent to 0.47g's does not lead to circumferential stress levels and ovalization of the HI-STORM storage overpack to prevent ready retrievability of the MPC. The load used for that calculation clearly bounds the side load induced by flood.

3.4.7 Seismic Event and Explosion - HI-STORM 100

3.4.7.1 Seismic Event (Load Case C in Table 3.1.1)

The HI-STORM 100 System plus its contents may be assumed to be subject to a seismic event consisting of three orthogonal statistically independent acceleration time-histories. For the purpose of performing a conservative analysis to determine the maximum ZPA that will not cause incipient tipping, the HI-STORM 100 System is considered as a rigid body subject to a net horizontal quasi-static inertia force and a vertical quasi-static inertia force. This is consistent with the approach used in previously licensed dockets. The vertical seismic load is conservatively assumed to act in the most unfavorable direction (upwards) at the same instant. The vertical seismic load is assumed to be equal to or less than the net horizontal load with ε being the ratio of vertical component to one of the horizontal components. For use in calculations, define D_{BASE} as the contact patch diameter, and H_{CG} as the height of the centroid of an empty HI-STORM 100 System (no fuel). Conservatively, assume

D_{BASE} = 132.5" (Drawing 1495, Sheet 1 specifies 133.875" including overhang for welding)

Tables 3.2.1 and 3.2.3 give HI-STORM 100 weight data and center-of-gravity heights.

The weights and center-of-gravity heights are reproduced here for calculation of the composite center-of-gravity height of the storage overpack together with an empty MPC.

Weight (pounds)	C.G. Height (Inches); H
Overpack - W_o = 265,866	116.8
MPC-24 - W_{24} = 39,667	108.9 + 24 = 132.9†
MPC-68 - W_{68} = 39,641	109.9 + 24 = 133.9
MPC-32 –W_{32} = 34,375	109.3 + 24 = 133.3
MPC-24E – W_{24E} = 42,069	107.9 + 24 = 131.9

† From Table 3.2.3, it is noted that MPC C.G. heights are measured from the base of the MPC. Therefore, the thickness of the overpack baseplate and the concrete MPC pedestal must be added (Drawing 1495, Sheet 2) to determine the height above ground.

The height of the composite centroid, H_{CG}, is determined from the equation

$$H_{cg} = \frac{W_o \times 116.8 + W_{MPC} \times H}{W_o + W_{MPC}}$$

Performing the calculations for all of the MPCs gives the following results:

	H_{cg} (inches)
MPC-24 with storage overpack	118.89
MPC-68 with storage overpack	119.02
MPC-32 with storage overpack	118.69
MPC-24E with storage overpack	118.86

A conservative overturning stability limit is achieved by using the largest value of H_{CG} (call it H) from the above. Because the HI-STORM 100 System is a radially symmetric structure, the two horizontal seismic accelerations can be combined vectorially and applied as an overturning force at the C.G. of the cask. The net overturning static moment is

$$WG_H H$$

where W is the total system weight and G_H is the resultant zero period acceleration seismic loading (vectorial sum of two orthogonal seismic loads) so that WG_H is the inertia load due to the resultant horizontal acceleration. The overturning moment is balanced by a vertical reaction force, acting at the outermost contact patch radial location $r = D_{BASE}/2$. The resistive moment is minimized when the vertical zero period acceleration G_V tends to reduce the apparent weight of the cask. At that instant, the moment that resists "incipient tipping" is:

$$W (1- G_V) r$$

Performing a static moment balance and eliminating W results in the following inequality to ensure a "no-overturning condition:

$$G_H + \frac{r}{H} G_V \leq \frac{r}{H}$$

Using the values of r and H for the HI-STORM 100 (r = 66.25", H = 119.02"), representative combinations of G_H and G_V that satisfy the limiting equality relation are computed and tabulated below:

Acceptable Net Horizontal G-Level (HI-STORM100), G_H	Acceptable Vertical G-Level, G_V
0.468	0.16
0.445	0.20
0.417	0.25
0.358	0.357

We repeat the above computations using the weight and c.g. location of the HI-STORM 100S. Because of the lowered center of gravity positions, the maximum net horizontal "G" levels are slightly increased.

Performing the calculations for all of the MPCs gives the following results:

	H_{cg} (inches)
MPC-24 with storage overpack	113.55
MPC-68 with storage overpack	113.69
MPC-32 with storage overpack	113.34
MPC-24E with storage overpack	113.53

Using the values of r and H for the HI-STORM 100S (r = 66.25", H = 113.69"), representative combinations of G_H and G_V that satisfy the limiting equality relation are computed and tabulated below:

Acceptable Net Horizontal G-Level (HI-STORM 100S), G_H	Acceptable Vertical G-Level, G_V
0.489	0.16
0.466	0.20
0.437	0.25
0.368	0.368

Primary Stresses in the HI-STORM 100 Structure Under Net Lateral Load Over 180 degrees of the Periphery

Under a lateral loading, the storage overpack will experience axial primary membrane stress in the inner and outer shells as it resists bending as a "beam-like" structure. Under the same kind of lateral loading over one-half of the periphery of the cylinder, the shells will tend to ovalize under the loading and develop circumferential stress. Calculations for stresses in both the axial and circumferential direction are required to demonstrate satisfaction of the Level D structural integrity requirements and to provide confidence that the MPC will be readily removable after a seismic event, if necessary. An assessment of the stress state in the structure under the seismic induced load will be shown to bound the results for any other condition that induces a peripheral load around part

of the HI-STORM 100 storage overpack perimeter. The specific analyses are performed using the geometry and loading for the HI-STORM 100; the results obtained for stress levels and the safety assessment are also applicable to an assessment of the HI-STORM 100S.

A simplified calculation to assess the flexural bending stress in the HI-STORM 100 structure under the limiting seismic event (at which tipping is incipient) is presented in the following:

From the acceptable acceleration table presented above, maximum horizontal acceleration is bounded by 0.47g. The corresponding lateral seismic load, F, is given by

$$F = 0.47\ W$$

This load will be maximized if the upper bound HI-STORM 100 weight (W = 360,000 lbs. (Table 3.2.1)) is used. Accordingly,

$$F = (0.47)\ (360{,}000) = 169{,}200 \text{ lbs.}$$

No dynamic amplification is assumed as the overpack, considered as a beam, has a natural frequency well into the rigid range.

The moment, M, at the base of the HI-STORM 100 due to this lateral force is given by

$$M = \frac{F H}{2}$$

where H = height of HI-STORM 100 (taken conservatively as 235 inches). Note that the loading has now been approximated as a uniform load acting over the full height of the cask.

The flexural stress, σ, is given by the ratio of the moment M to the section modulus of the steel shell structure, z, which is computed to be 12,640 $in.^3$ (Structural Calculation Package HI-981928).

Therefore,

$$\sigma = \frac{(169{,}200)\ (235)}{(12{,}640)\ (2)} = 1{,}573 \text{ psi}$$

We note that the strength of concrete has been neglected in the above calculation.

The maximum axial stress in the storage overpack shell will occur on the "compressive" side where the flexural bending stress algebraically sums with the direct compression stress σ_d from vertical compression.

From the representative acceleration table the vertical seismic accelerations corresponding to the net 0.47g horizontal acceleration is below 0.16g.

Therefore, using the maximum storage overpack weight (bounded by 270,000 lbs. from data in Table 3.2.1)

$$\sigma_d = \frac{(270{,}000)\,(1.16)}{554.47} = 565 \text{ psi}$$

where 554.47 sq. inch is the metal area (cross section) of the steel structure in the HI-STORM 100 storage overpack as computed in Subsection 3.4.4.3.2.1. The total axial stress, therefore, is

$$\sigma_T = 1{,}573 + 565 = 2{,}138 \text{ psi}$$

Per Table 3.1.12, the allowable *membrane* stress intensity for a Level D event is 39,750 psi at 350 degrees F.

The Factor of Safety, β, is, therefore

$$\beta = \frac{39{,}750}{2{,}138} = 18.59$$

Examination of the *stability calculations for the overpack outer shell under a 45-g vertical end drop* ~~results for the stability load case 2 (which considers bounding loads) in Appendix 3.AK~~ demonstrates that no instability will result from this compressive load induced by a seismic or other environmental load leading to bending of the storage overpack as a beam.

The previous calculation has focused on the axial stress in the members developed assuming that the storage overpack does not overturn but resists the lateral load by remaining in contact with the ground and bending like a beam. Since the lateral loading is only over a portion of the periphery, there is also the potential for this load to develop circumferential stress in the inner and outer shells to resist ovalization of the shells. To demonstrate continued retrievability of the MPC after a seismic event, it must be shown that either the stresses remain in the elastic range or that any permanent deformation that develops due to plasticity does not intrude into the MPC envelope after the event is ended. In the following subsection, *classical formulas* ~~a classical result from Appendix 3.B~~ for the deformation of rings under specified surface loadings *are* ~~is~~ used to provide a conservative solution for the circumferential stresses. Specifically, *the* ~~Appendix 3.B contains a complete~~ solution for a point-supported ring subject to a gravitational induced load, *as depicted in the sketch below, is implemented* ~~around the periphery of the ring~~. This solution provides a conservative estimate of the

circumferential stress and the deformation of the ring that will develop under the actual applied seismic load. ~~Specifically, the following classical ring problem, shown in the sketch below, is applied to obtain the circumferential stress and deformation field under the postulated seismic event:~~

Ring supported at base and loaded by its own weight, w, given per unit circumferential length.

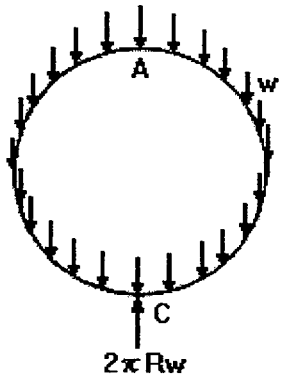

The solution ~~in Appendix 3.B~~ considers the geometry and load appropriate to a unit length of the inner and outer shells of the HI-STORM 100 storage overpack with a total weight equal to the overpack bounding weight (no MPC) subject to a 45g deceleration inertial loading. The numerical results *for the 45g tipover event* ~~in Appendix 3.B~~ can be directly applied here by multiplying by the factor "X", where "X" reflects the differences in the decelerations and the weights used for the *tipover event* ~~case considered in Appendix 3.B~~ and for the seismic load case here in this subsection.

X = (0.47g/45g) x (360,000lb./270,000lb.) = 0.0139

Using this factor on the *tipover* solution ~~in Appendix 3.B, (Attachment B-1, Case 15.16)~~ gives the following bounding results for maximum stresses (without regard for sign and location of the stress) and deformations:

Maximum circumferential stress due to bending moment = (29,310 psi x X) = 407 psi

Maximum circumferential stress due to mean tangential force = (18,900 lb./2 sq.inch) x X = 131.4 psi

Change in diameter in the direction of the load = -0.11" x X = -0.0015"

Change in diameter perpendicular to the direction of the load = +0.06" x X = 0.0008"

From the above results, it is clear that no permanent ovalization of the storage overpack occurs during the seismic event and that circumferential stresses will remain elastic and are bounded by the stresses computed based on considering the storage overpack as a simple beam. Therefore, the safety factors based on maximum values of axial stress are appropriate. The magnitudes of the diameter changes that are suggested by the ring solution clearly demonstrate that ready retrievability of the MPC is maintained after the seismic event.

Because of the low values for the calculated axial stress, the conclusions of the previous section are also valid for the HI-STORM 100S.

Potential for Concrete Cracking

It can be readily shown that the concrete shielding material contained within the HI-STORM 100 structure will not crack due to the flexuring action of HI-STORM 100 during a bounding seismic event that leads to a maximum axial stress in the storage overpack. For this purpose, the maximum axial strain in the steel shell is computed by dividing the tensile stress developed by the seismic G forces (for the HI-STORM 100, for example) by the Young's Modulus of steel.

$$\zeta = \frac{1{,}321}{28\text{E}+06} = 47.\text{E-}06$$

where the Young's Modulus of steel is taken from Table 3.3.2 at 350 degrees F.

The acceptable concrete strain in tension is estimated from information in ACI-318.1 for plain concrete. The ratio of allowable tensile stress to concrete Young' Modulus is computed as

Allowable ConcreteStrain = $(5 \times (0.75) \times (f)^{1/2})/(57{,}000(f)^{1/2}) = 65.8\text{E-}06$

In the above expression, f is the concrete compressive strength.

Therefore, we conclude that considerable margins against tensile cracking of concrete under the bounding seismic event exist.

Sliding Analysis

An assessment of sliding of the HI-STORM 100 System on the ISFSI pad during a postulated limiting seismic event is performed using a one-dimensional "slider block on friction supported surface" dynamic model. The results for the shorter HI-STORM 100S are comparable. The HI-STORM 100 is simulated as a rigid block of mass *m* placed on a surface which is subject to a sinusoidal acceleration of amplitude *a*. The coefficient of friction of the block is assumed to be reduced by a factor α to recognize the contribution of vertical acceleration in the most adverse manner (vertical acceleration acts to reduce the downward force on the friction interface). The equation of motion for such a "slider block" is given by:

$$m\ddot{x} = R + m\,a \sin \omega t$$

where:

$\ddot{x}$: relative acceleration of the slider block (double dot denotes second derivative of displacement x in time)

a: amplitude of the sinusoidal acceleration input

ω: frequency of the seismic input motion (radians/sec)

t: time coordinate

R is the resistive Coulomb friction force that can reach a maximum value of μ(mg) (μ= coefficient of friction) and which always acts in the direction of opposite to $\dot{x}(t)$.

Solution of the above equation can be obtained by standard numerical integration for specified values of m, a, w and a. The following input values are used.

a = 0.47g

α = 0.84 = 1 - vertical acceleration (vertical acceleration is 0.16g for net horizontal acceleration equal to 0.47 from the acceleration table provided in the foregoing)

m = 360,000 lbs/g

μ = 0.25

For establishing the appropriate value of ω, reference is made to the USAEC publication TID-7024, "Nuclear Reactor and Earthquakes", page 35, 1963, which states that the significant energy of all seismic events in the U.S. essentially lies in the range of 0.4 to 10 Hz. Taking the mid-point value

$\omega = (6.28)\,(0.5)\,(0.4+10) = 32.7$ rad/sec.

The numerical solution of the above equation yields the maximum excursion of the slider block x_{max} as 0.12 inches, which is negligible compared to the spacing between casks.

Calculations performed at lower values of ω show an increase in x_{max} with reducing ω. At 1 Hz, for example, $x_{max} = 3.2$ inches. It is apparent from the above that there is a large margin of safety against inter-module collision within the HI-STORM 100 arrays at an ISFSI, where the minimum installed spacing is over 2 feet (Table 1.4.1).

The above dynamic analysis indicates that the HI-STORM 100 System undergoes minimal lateral vibration under a seismic input with net horizontal ZPA g-values as high as 0.47 even under a

bounding (from below) low interface surface friction coefficient of 0.25. Data reported in the literature (ACI-349R (97), Commentary on Appendix B) indicates that values of the coefficient of friction, μ, as high as 0.7 are obtained at steel/concrete interfaces.

To ensure against unreasonably low coefficients of friction, the ISFSI pad design may require a "broom finish" at the user's discretion. The bottom surface of the HI-STORM 100 is manufactured from plate stock (i.e. non-machine finish). A coefficient of friction value of 0.53 is considered to be a conservative numerical value for the purpose of ascertaining the potential for incipient sliding of the HI-STORM 100 System. The coefficient of friction is required to be verified by test (see Table 2.2.9).

The relationship between the vertical ZPA, G_V, (conservatively assumed to act opposite to the normal gravitational acceleration), and the resultant horizontal ZPA G_H to insure against incipient sliding is given from static equilibrium considerations as:

$$G_H + \mu G_V \leq \mu$$

Using a conservative value of μ equal to 0.53, the above relationship provides governing ZPA limits for a HI-STORM 100 (or 100S) System arrayed in a freestanding configuration. The table below gives representative combinations that meet the above limit.

G_H (in g's)	G_V (in g's)
0.445	0.16
0.424	0.20
0.397	0.25
0.350	0.34

If the values for the DBE event at an ISFSI site satisfy the above inequality relationship for incipient sliding with coefficient of friction equal to 0.53, then the non-sliding criterion set forth in NUREG-1536 is assumed to be satisfied a priori. However, if the ZPA values violate the inequality by a small amount, then it is permissible to satisfy the non-sliding criterion by implementing measures to roughen the HI-STORM 100/ISFSI pad interface to elevate the value of μ to be used in the inequality relation. To demonstrate that the value of μ for the ISFSI pad meets the required value implied by the above inequality, a series of Coulomb friction (under the QA program described in Chapter 13) shall be performed as follows:

Pour a concrete block with horizontal dimensions no less than 2' x 2' and a block thickness no less than 0.5'. Finish the top surface of the block in the same manner as the ISFSI pad surface will be prepared.

Prepare a 6" x 6" x 2" SA516 Grade 70 plate specimen (approximate weight = 20.25 lb.) to simulate the bottom plate of the HI-STORM 100 overpack. Using a calibrated friction gage attached to the steel plate, perform a minimum of twenty (20) pull tests to measure the static coefficient of friction at the interface between the concrete block and the steel plate. The pull

tests shall be performed on at least ten (10) different locations on the block using varying orientations for the pull direction.

The coefficient of friction to be used in the above sliding inequality relationship will be set as the average of the results from the twenty tests.

The satisfaction of the "no-sliding" criterion set down in the foregoing shall be carried out along with the "no-overturning" qualification (using the static moment balance method in the manner described at the beginning of this subsection) and documented as part of the ISFSI facility's CFR72.212 evaluation.

3.4.7.2 Explosion (Load Case 05 in Table 3.1.5)

In the preceding subsection, it has been demonstrated that incipient tipping of the storage overpack will not occur under a side load equal to 0.47 times the weight of the cask. For a fully loaded cask, this side load is equal to

F = 169,200 lb.

If it is assumed that this side load is uniformly distributed over the height of the cask and that the cask centroid is approximately at the half-height of the overpack, then an equivalent pressure, P, acting over 180 degrees of storage overpack periphery, can be defined as follows:

P x (DH) = F

Where D = overpack outside diameter, and H = height of storage overpack

For D = 132.5" and H = 235", the equivalent pressure is

P = 169,200 lb/(132.5" x 235") = 5.43 psi

Therefore, establishing 5 psi as the design basis steady state pressure differential (Table 2.2.1) across the overpack diameter ensures that incipient tipping will not occur.

Since the actual explosion produces a transient wave, the use of a static incipient tip calculation is very conservative. To evaluate the margin against tip-over from a short-time pressure pulse, a Working Model analysis of the two-dimensional dynamic motion of the HI-STORM subject to a given initial angular velocity is carried out. Figures 3.4.25 and 3.4.26 provide details of the model and the solution for a HI-STORM 100 System (simulated as a rigid body) having a weight and inertia property appropriate to a minimum weight cask. The results show that an initial angular velocity of 0.626 radians/second does not lead to a tipover of the storage overpack. The results bound those obtained for the HI-STORM 100S since the overall cask height is reduced.

The initial angular velocity can be related to a square wave pressure pulse of magnitude P and time duration T by the following formula:

$I\omega = (P \times D \times H) \times (0.5 \times H) \times T$

The above formula relates the change in angular motion resulting from an impulsive moment about the base of the overpack. D is the diameter of the outer shell, H is the height of the storage overpack, and I is the mass moment of inertia of the storage overpack about the mass center (assumed to be at half-height). For D=132.5", H=235", P=10 psi, T=1 second, and I=64,277,000 lb.inch sec^2 ~~(calculated in Appendix 3.C)~~, the resulting initial angular velocity is:

$\omega = 0.569$ radians/second

Therefore, an appropriate short time pressure limit is 10 psi with pulse duration less than or equal to 1 second. Table 2.2.1 sets this as the short-time external pressure differential.

The analysis in Subsection 3.4.7.1 evaluates ovalization of the shell by considering the seismically applied load as a line loading along the height of the overpack that is balanced by inertial body forces in the metal ring. The same solutions ~~in Appendix 3.B~~ can be used to examine the circumferential stress state that would be induced to resist an external pressure that developed around one-half of the periphery. Such a pressure distribution may be induced by a pressure wave crossing the cask from a nearby explosion. It is shown here~~, by reference to solutions in Appendix 3.B,~~ that a uniform pressure load over one-half of the overpack outer shell gives rise to an elastic stress state and deformation state that is bounded by a large margin by the results just presented for the seismic event in Subsection 3.4.7.1.

The case of an external pressure load from an explosion pressure wave (Load Case 05 in Table 3.1.5) is examined by combining the solutions *for two different load cases* ~~of Case1 and Case 3 in Appendix 3.B~~. The combined case that results is a balance of pressure load over one-half the perimeter and inertial body forces. The sketch below describes this:

Case 1 + Case 3

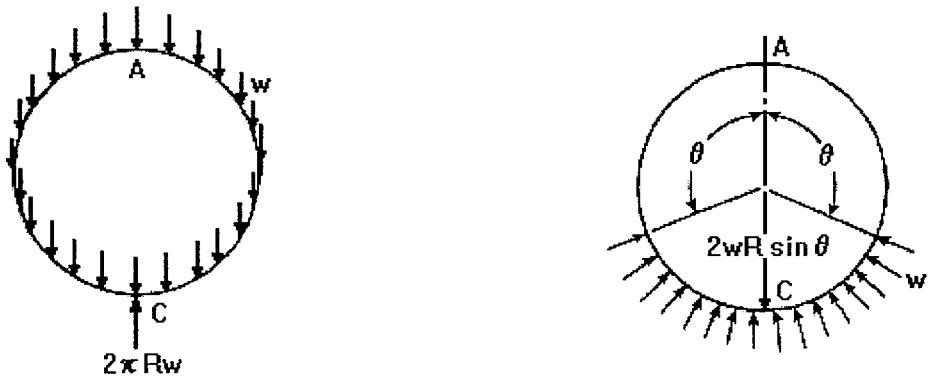

~~In Appendix 3.B, b~~*B*oth cases are considered under identical total loads (with the angle in case 3 set to 90 degrees). Therefore, adding the results from the two cases results in the desired combined case; namely, the balance of a peripheral external pressure with internal all around loading simulating an inertia load (since the reactions are identical in magnitude and opposite in direction, there is a complete cancellation of the concentrated loads).

Examination of the results ~~in Appendix 3.B~~ shows that the algebraic sum of the two ~~sets of~~ solutions give*s* results that are smaller in magnitude than the case 1 solution for a line loading balanced by inertially induced body forces. The applied loading used to develop the solution *for* ~~in Appendix 3.B,~~ case 1~~,~~ is 56,180 lb. per inch of storage overpack axial length. This load is equivalent to an external pressure P = 424 psi applied over one-half of the outer perimeter of the shell as is shown below:

P x D = 56,180 lb./inch D = 132.5"

P = 424 psi

Since this is higher by a large margin than any postulated external pressure load, circumferential stresses induced by the differential pressure specified in Table 2.2.1 are insignificant. Specifically, by adding the results from the two solutions (ring load case 1 for a point support reaction to a body force + ring load case 3 for a point support reaction to a lateral pressure over one-half of the perimeter) ~~considered in Appendix 3.B~~, it is determined that the circumferential bending stress from case 1 ~~in that appendix~~ is reduced by the factor "R" to obtain the corresponding stress from the combined case. R is computed as the ratio of moment magnitudes from the combined case to the results of case 1 alone.

R = (maximum bending moment from case 1 + case 3)/(maximum bending moment from case 1)
= 0.75/6.197 = 0.12

~~(results for individual cases are in Appendix 3.B)~~

Examination of the graphs from the moment distribution from the two solutions ~~in Appendix 3.B~~ shows that the individual terms always subtract and nearly cancel each other at every location.

Therefore, it is concluded that the maximum circumferential stress that develops under a pressure of 424 psi applied over one-half of the perimeter, and conservatively assumed balanced by inertia loading, is

Stress = 29,310 psi x 0.12 = 3517 psi

The stress due to a differential pressure of 10 psi (Table 2.2.1) is only 2.36% of the above value and needs no further evaluation for stress limits or deformation to demonstrate retrievability of the MPC.

3.4.7.3 Anchored HI-STORM Systems Under High-Seismic DBE (Load Case C in Table 3.1.1)

The anchored HI-STORM System (Figures 1.1.4 and 1.1.5) is assumed to be subjected to quasi-static inertial seismic loads corresponding to the ZPA design basis limits given in Table 2.2.8. The results from this quasi-static analysis are used to evaluate structural margins for the preloaded anchor studs and the sector lugs. In the quasi-static evaluation, the effect of the "rattling" of the MPC inside of the overpack is accounted for by the imposition of a dynamic load factor of 2.0 on the incremental stresses that arise during the seismic event. In addition to the quasi-static analysis, confirmatory 3-D dynamic analyses are performed using base acceleration excitation histories developed from two sets of response spectra. Figure 3.4.30 shows the two sets of response spectra that are assumed to be imposed at the top of the ISFSI pad. One set of response spectra is the Regulatory Guide 1.60 spectra for 5% damping with zero period acceleration conservatively amplified to 1.5 in each direction. This spectra set has been used as the input spectra at many nuclear plants in the U.S. (although generally, the ZPA was much below 1.0). Three statistically independent acceleration time histories (two horizontal labeled as "H1", "H2") and one vertical (labeled as "VT") have been developed. A twenty-second duration event was considered. Figures 3.4.31 to 3.4-33 show the time histories. The second set of response spectra used for time history analysis has similar levels of zero period acceleration but has higher peak spectral acceleration values in the low frequency range (2-3 Hz). This spectra set is the design basis set for a Pacific coast U.S. plant. Figures 3.4.34 to 3.4-36 (labeled as "FN", "FP" for the two horizontal acceleration histories and "FV" for the vertical acceleration time history), show the corresponding time histories simulating a long duration seismic event (170 seconds).

The objectives of the quasi-static and dynamic seismic analyses are the following:

i. Quantify the structural safety factor in the anchor studs and in the sector lugs that constitute the fastening system for the loaded HI-STORM 100A overpack. The structural safety factor is defined as the ratio of the permitted stress (stress intensity) per Subsection "NF" of the ASME Code to the maximum stress (stress intensity) developed in the loaded component.

ii. Compute the safety factor against fatigue failure of the anchor studs from a single seismic event.

iii. Quantify the interface loads applicable to the ISFSI pad to enable the ISFSI owner to design the ISFSI pad under the provisions of ACI-349 (85). The bounding interface loads computed for the maximum intensity seismic event (ZPA) and for extreme environmental loads may be used in pad design instead of the site-specific loads calculated for the loadings applicable to the particular ISFSI.

The above design objectives are satisfied by performing analyses of a loaded HI-STORM 100A System using a conservative set of input data and a conservative dynamic model. Calculations using the quasi-static model assume that the net horizontal inertia loads and the vertical inertia load

correspond to the weight of the loaded cask times the appropriate ZPA. The results from the analyses are set down as the interface loads, and may be used in the ISFSI pad design work effort by the ISFSI owner. The information on the seismic analysis is presented in five paragraphs as follows:

Input data for analysis
Quasi-static model and results
Dynamic model and modeling assumptions.
Results of dynamic analysis
Summary of interface loads

a. Input Data for Analysis:

Key input data for the seismic analysis of a loaded HI-STORM 100A System is summarized in Table 3.4.10. As can be seen from Table 3.4.10, the input data used in the analysis is selected to bound the actual data, wherever possible, so as to maximize the seismic response. For example, a bounding weight of the loaded MPC and HI-STORM 100A overpack is used because an increase in the weight of the system directly translates into an increased inertial loading on the structure.

For quasi-static analysis, bounding ZPA values of 1.5 in all three directions are used with the vertical event directed upward to maximize the stud tension. The resulting ZPA's are then further amplified by the dynamic load factor (DLF=2.0) to reflect "rattling" of the MPC within the overpack. Input data for anchor stud lengths are representative. We consider long and short studs in order to evaluate the effect of stud spring rate.

For the confirmatory dynamic analyses, the time history base excitations are shown in Figures 3.4.31 through 3.4.36 and the propensity for "rattling" is included in the model.

b. Quasi-Static Model and Results

We consider the HI-STORM100A baseplate as a rigid plate resting on the ISFSI pad with the twenty-eight studs initially preloaded so as to impart a compressive load at the baseplate pad interface that is balanced by a tensile load in the studs prior to the seismic event occurring. The discrete studs are replaced by a thin ring located at the stud circle radius for analysis purposes. The thickness of the thin ring is set so that the ring area is equal to the total stress area of the twenty-eight studs. Figure 3.4.37 shows a view of a segment of the baseplate with the outline of the ring. The ISFSI pad is represented by a linear spring and a rotational spring with spring constants determined from the exact solution for a rigid circular punch pressed into a elastic half-space. We assume that subsequent to pre-tensioning the studs, the seismic event occurs, represented by a net horizontal load DH and a net vertical load DV. In the analysis, the input loads DH and DV are:

$$G_H = (1.5^2 \times 2)^{1/2} \times DLF = 4.242 \; ; \quad G_V = 1.5 \times DLF = 3.0$$

$$DH = G_H \times 360{,}000 \text{ lb.} \; ; \quad DV = -G_V \times 360{,}000 \text{ lb}$$

DH is the magnitude of the vector sum of the two horizontal ZPA accelerations multiplied by the bounding HI-STORM 100A weight. Similarly, DV is an upward directed load due to the vertical ZPA acceleration. The upward direction is chosen in order to maximize the stud tension as the assemblage of studs and foundation resists overturning from the moment induced by DH applied at the centroid of the cask. Figure 3.4.38 shows the free-body diagram associated with the seismic event. Essentially, we consider an analysis of a pre-compressed interface and determine the interface joint behavior under the imposition of an external loading (note that this kind of analysis is well established in the pressure vessel and piping area where it is usually associated with establishing the effectiveness of a gasketed joint). An analysis is performed to determine the maximum stud tension that results if the requirement of no separation between baseplate and pad is imposed under the imposed loading. The following result is obtained from static equilibrium, for a preload stress of 60 ksi, when the "no separation condition" is imposed:

$$\frac{2a/3h_{cg}\left(F_{preload}/W+1\right)\left(1+\alpha_1\right)}{G_H-2a/3h_{cg}\left(G_V(1+\alpha_1)/(1+\alpha)\right)}=1.016$$

In the above equation,

$F_{preload}$ = (Total stress area of twenty-eight, 2" diameter studs) x 60 ksi = 4,200,000 lb.

W = Bounding weight of loaded HI-STORM 100A = 360,000 lb.

a = 73.25 inches,

h_{cg} = 118.5 inches

The coefficients α and α_1 relate the stiffness of the totality of studs to the stiffness of the foundation under direct loading and under rotation. The result given above is for the representative case of stud free length "L", equal to

L= 42 inches, which gives α and α_1 equal to 0.089 and 0.060, respectively.

A simplified confirmatory analysis of the above problem can be performed by considering the limiting case of a rigid baseplate and a rigid ISFSI pad. In the limit of a rigid ISFSI pad (foundation), the coefficients α and α_1 go to zero. A related solution for the case of a rigid baseplate and a rigid foundation can be obtained when the criteria is not incipient separation, but rather, a more "liberal" incipient rotation about a point on the edge of the baseplate. That solution is given in "Mechanical Design of Heat Exchangers and Pressure Vessel Components", by Singh and Soler (Arcturus Publishers, 1984). The result is (for 60 ksi prestress in each stud):

$$\frac{a/h_{cg}\left(F_{preload}/W+1\right)}{G_H-a/h_{cg}\left(G_V\right)}=1.284$$

Although not a requirement of any design code imposed herein, the right hand side of the previous relationships can be viewed as the safety factor against incipient separation (or rotation about an edge) at the radius "a". Note that since we have assumed a bounding event, there is an additional margin of 1.5 in results since the Reg. Guide 1.60 event has not been applied with a ZPA in excess of 1.0.

For the real seismic event associated with a western U.S. plant having a slightly lower horizontal ZPA and a reduced vertical ZPA (see Figure 3.4.30). Using the same DLF =2.0 to account for "rattling" of the confined MPC:

$$G_H = 4.1 \quad ; \quad G_V = 2.6,$$

the aforementioned safety factors are:

SF (incipient separation) = 1.076
SF (incipient edging) = 1.372

The increment of baseplate displacement and rotation, up to incipient separation, is computed from the equilibrium and compatibility equations associated with the free body in Figure 3.4.38 and the change in stud tension computed. The following formula gives the stud tensile stress in terms of the initial preload and the incremental change from the application of the horizontal and vertical seismic load.

$$\sigma_{stud} = \sigma_{preload} + \alpha \frac{W}{NA_{stress}} \left(\frac{-G_V}{1+\alpha} + \left(\frac{3h_{cg}}{2a} \right) \left(\frac{c}{a} \right) \left(\frac{G_H}{1+\alpha_1} \right) \right)$$

In the above formula,

N = number of studs = 28 (maximum number based on HI-STORM dimensions). For lower seismic inputs, this might be reduced (in groups of 4 to retain symmetry).

A_{stress} = tensile stress area of a 2" diameter stud

2c = stud circle diameter

The results demonstrate that there is a relatively small change in stud stress from the initial pre-tension condition with the ISFSI pad foundation resisting the major portion of the overturning moment. For the geometry considered (maximum stud free length and nominal prestress), the maximum tensile stress in the stud increases by 9.1%. The following table summarizes the results from the quasi-static analysis using minimum ultimate strength for the stud to compute the safety factors. Note that under the seismic load, the direct stress in the stud is limited to 70% of the stud ultimate strength (per Appendix F of the ASME Code Section III). The allowable pad compressive

stress is determined from the ACI Code assuming confined concrete and the minimum concrete compressive strength from Table 2.0.4. Because of the large compressive load at the interface from the pre-tensioning operation, the large frictional resistance inhibits sliding of the cask. Consequently, there will be no significant shear stress in the studs. Safety factors for sliding are obtained by comparing the ratio of horizontal load to vertical load with the coefficient of friction between steel and concrete (0.53). Values in parenthesis represent results obtained using ZPA values associated with the real seismic event for the western U.S. plant instead of the bounding Reg. Guide 1.60 event.

SUMMARY OF RESULTS FOR STUDS AND INTERFACE FROM QUASI-STATIC SEISMIC EVALUATION WITH DLF = 2.0, Stud Prestress = 60 ksi			
Item	**Calculated Value**	**Allowable Value**	**Safety Factor = (Allowable Value/Calculated Value)**
Stud Stress(ksi) (42" stud free length)	65.48 (65.18)	87.5	1.336 (1.343)
Maximum Pad Pressure (ksi)(42" stud free length)	3.126 (3.039)	4.76	1.52 (1.57)
Stud Stress (ksi)(16" stud free length)	73.04 (72.34)	87.5	1.20 (1.21)
Maximum Pad Pressure(ksi) (16" stud free length)	2.977 (2.898)	4.76	1.60 (1.64)
Overpack Sliding	0.439 (0.407)	0.53	1.21 (1.31

The effect of using a minimum stud free length in the embedment design is to increase the values of the coefficients α and α_1 because the stud stiffness increases. The increase in stud stiffness, relative to the foundation stiffness results in an increase in incremental load on the studs. This is a natural and expected characteristic of preloaded configurations. It is noted that the stud safety factors are based on minimum ultimate strength and can be increased, without altering the calculated results, by changing the stud material.

The quasi-static analysis methodology has also been employed to evaluate the effects of variation in the initial prestress on the studs. The following tables reproduce the results above for the cases of lower bound stud prestress (55 ksi) and upper bound stud prestress (65 ksi) on the studs. Only the results using the values associated with the Reg. Guide 1.60 bounding event are reported.

SUMMARY OF RESULTS FOR STUDS AND INTERFACE FROM QUASI- STATIC SEISMIC EVALUATION WITH DLF = 2.0, Stud Prestress = 55 ksi			
Item	**Calculated Value**	**Allowable Value**	**Safety Factor = (Allowable Value/Calculated Value)**
Stud Stress(ksi) (42" stud free length)	60.48	87.5	1.45
Maximum Pad Pressure (ksi)(42" stud free length)	3.012	4.76	1.58
Stud Stress (ksi)(16" stud free length)	68.07	87.5	1.29
Maximum Pad Pressure(ksi) (16" stud free length)	2.862	4.76	1.663

Overpack Sliding	0.488	0.53	1.09
SUMMARY OF RESULTS FOR STUDS AND INTERFACE FROM QUASI- STATIC SEISMIC EVALUATION WITH DLF = 2.0, Stud Prestress = 65 ksi			
Item	**Calculated Value**	**Allowable Value**	**Safety Factor = (Allowable Value/Calculated Value)**
Stud Stress(ksi) (42" stud free length)	70.48	87.5	1.24
Maximum Pad Pressure (ksi)(42" stud free length)	3.24	4.76	1.47
Stud Stress (ksi)(16" stud free length)	78.07	87.5	1.12
Maximum Pad Pressure(ksi) (16" stud free length)	3.091	4.76	1.54
Overpack Sliding	0.399	0.53	1.33

The results above confirm the expectations that an increase in preload increases the safety factor against sliding. The calculated coefficient of friction in the above tables is computed as the ratio of applied horizontal load divided by available vertical load. For all combinations examined, ample margin against incipient separation at the interface exists.

Based on the results from the quasi-static analysis, an assessment of the safety factors in the sector lugs is obtained by performing a finite element analysis of a repeated element of one of the sector lugs. Figure 3.4.39 shows the modeled section and the finite element mesh. The stud load is conservatively applied as a uniform downward pressure applied over a 5"x5" section of the extended baseplate simulating the washer between two gussets. This is conservative as the rigidity of the washer is neglected. The opposing pressure loading from the interface pressure is applied as a pressure over the entire extended baseplate flat plate surface. Only one half the thickness of each gusset plate is included in the model. Two cases are considered: (1) the pre-loaded state (a Normal Condition of Storage-Level A stress limits apply); and, (2), the seismic load condition at the location of the maximum tensile load in a stud (an Accident Condition of Storage – Level D stress intensity limits apply). Figures 3.4.40 and 3.4.41 present the stress results for the following representative input conditions:

Level A analysis - Preload stress/bolt = 60 ksi

Level D analysis - Maximum Bolt stress(includes seismic increment) = 65.5 ksi

In the Level A analysis, the resisting local foundation pressure exactly balances the preload. For the Level D analysis, the opposing local foundation pressure = 190 psi (average over the area between gussets. This represents the reduced pressure under the highest loaded stud under the induced rotation of the storage system.

The most limiting weld stress is obtained by evaluating the available load capacity of the fillet weld attaching the extended baseplate annulus region to the gussets (approximately 25 inches of weld per segment) using a limit strength equal to 42% of the ultimate strength of the base material.

The following table summarizes the limiting safety factors for the sector lugs. Allowable values for primary bending stress and stress intensity are from Tables 3.1.10 and 3.1.12 for SA-516 Grade 70 @ 300 degrees F.

SUMMARY OF RESULTS FOR SECTOR LUGS FROM QUASI-STATIC SEISMIC EVALUATION			
Item	**Calculated Value**	**Allowable Value**	**Safety Factor = (Allowable Value/Calculated Value)**
Maximum Primary Membrane + Bending Stress Away From Loaded Region and Discontinuity (ksi) – Case 1 - Preload	15.62	26.3	1.68
Maximum Primary Membrane + Bending Stress Intensity Away From Loaded Region and Discontinuity (ksi) – Case 2 - Preload + Seismic	36.67	60.6	1.65
Maximum Weld Shear Load (kips)	150.8	194.9	1.29

c. Dynamic Model and Modeling Assumptions:

The dynamic model of the HI-STORM 100A System consists of the following major components.

i. The HI-STORM 100 overpack is modeled as a six degree-of-freedom (rigid body) component.

ii. The loaded MPC is also modeled as a six degree-of-freedom (rigid body) component that is free to rattle inside the overpack shell. Gaps between the two bodies reflect the nominal dimensions from the drawings.

iii. The contact between the MPC and the overpack is characterized by a coefficient of restitution and a coefficient of friction. For the dynamic analysis, the coefficient of restitution is set to 0.0, reflecting the large areas of nearly flat surface that come into contact and have minimal relative rebound. The coefficient of friction is set to 0.5 between all potentially contacting surfaces of the MPC/overpack interface.

iv. The anchor studs, preloaded to axial stress σ_i (Table 3.4.10), induce a contact stress between the overpack base and the ISFSI pad. The loaded cask-pad interface can support a certain amount of overturning moment before an uplift (loss of circularity of the contact patch) occurs. The anchor studs are modeled as individual linear springs connecting the periphery of the extended baseplate to the ISFSI pad section. The resistance of the foundation is modeled by a vertical linear spring and three rotational springs connected between the cask baseplate center point and the surface

of the flat plate modeling the driven ISFSI pad. The ISFSI pad is driven with the three components of acceleration time history applied simultaneously.

The HI-STORM 100A dynamic model described above is implemented on the public domain computer code WORKING MODEL (also known as VisualNastran) (See Subsection 3.6.2 for a description of the algorithm).

Figures 3.4.42 and 3.4.43 show the rigid body components of the dynamic model before and after assembly. The linear springs are not shown. Mass and inertia properties of the rigid bodies are consistent with the bounding property values in Table 3.4.10.

c. Results of Dynamic Analysis

Figures 3.4.44 –3.4.47 show results of the dynamic analysis using the Reg. Guide 1.60 seismic time histories as input accelerations to the ISFSI pad. Figure 3.4.44 shows variation in the vertical foundation compressive force. Figure 3.4.45 shows the corresponding load variation over time for the stud having the largest instantaneous tensile load. An initial preload of approximately 150,000 lb is applied to each stud (corresponding to 60,160 psi stud tensile stress). This induces an initial compression load at the interface approximately equal to 571,000 lb. (including the dead weight of the loaded HI-STORM). Figures 3.4.44 and 3.4.45 clearly demonstrate that the foundation resists the majority of the oscillatory and impactive loading as would be expected of a preloaded configuration. Figure 3.4.46 shows the impulse (between the MPC and HI-STORM 100A) as a function of time. It is clear that the "spikes" in both the foundation reaction and the stud load over the total time of the event are related to the impacts of the rattling MPC. The results provide a graphic demonstration that the rattling of the MPC inside the overpack must be accounted for in any quasi-static representation of the event. The quasi-static results presented herein for the anchored system, using a DLF = 2.0, are in excellent agreement with the dynamic simulation results.

We note that the dynamic simulation, which uses an impulse-momentum relationship to simulate the rattling contact, leads to results having a number of sharp peaks. Given that the stress intensity limits in the Code assume static analyses, filtering of the dynamic results is certainly appropriate prior to comparing with any static allowable strength. We conservatively do not perform any filtering of the results prior to comparison with the quasi-static analysis; we note only that any filtering of the dynamic results to eliminate high-frequency effects resulting from the impulse-momentum contact model would increase the safety factors. Finally, Figure 3.4.47 shows the ratio of the net interface horizontal force (needed to maintain equilibrium) to the instantaneous compression force at the ISFSI pad interface with the base of the HI-STORM 100A. This ratio, calculated at each instant of time from the dynamic analysis results using the Reg. Guide 1.60 event, represents an instantaneous coefficient of friction that is required to ensure no interface relative movement. Figure 3.4.47 demonstrates that the required coefficient of friction is below the available value 0.53. Thus, the dynamic analysis confirms that the foundation interface compression, induced by the preloading action, is sufficient to maintain a positive margin against sliding without recourse to any resistance from the studs.

The results of the dynamic analysis using acceleration time histories from the Reg. Guide 1.60 response spectra (grounded at 1.5 g's) confirm the ability of the quasi-static solution, coupled with a dynamic load factor, to correctly establish structural safety factors for the anchored cask. The dynamic analysis confirms that stud stress excursions from the preload value are minimal despite the large overturning moments that need to be balanced.

A second dynamic simulation has been performed using the seismic time histories appropriate to a pacific coast U.S. nuclear plant (Figures 3.4.34-3.4.36). The ZPA of these time histories are slightly less than the Reg. Guide 1.60 time histories but the period of relatively strong motion extends over a longer time duration. The results from this second simulation exhibit similar behavior as those results presented above and provide a second confirmation of the validity of the safety factors

predicted by the quasi-static analysis. Reverence [3.4.14] (see Subsection 3.8) provides archival information and backup calculations for the results summarized here.

Stress cycle counting using Figure 3.4.45 suggests 5 significant stress cycles per second provides a bounding number for fatigue analysis. A fatigue reduction factor of 4 is appropriate for the studs (per ASME Code rules). Therefore, a conservative analysis of fatigue for the stud is based on an alternating stress range of:

S(alt) = .5 x (22,300 psi) x 4 = 44,600 psi for 5 cycles per second. The value for the stress range is obtained as the difference between the largest tensile stress excursions from the mean value as indicated in the figure.

To estimate fatigue life, we use a fatigue curve from the ASME Code for high strength steel bolting materials (Figure I.9.4 in Appendix I, ASME Code Section III Appendices). For an amplified alternating stress intensity range of 44,600 psi, Figure I.9.4 predicts cyclic life of 3,000 cycles. Therefore, the safety factor for failure of a stud by fatigue during one Reg. Guide 1.60 seismic event is conservatively evaluated as:

SF(stud fatigue) = 3,000/100 = 30.

For the long duration event, even if we make the conservative assumption of a nine-fold increase in full range stress cycles, the safety factor against fatigue failure of an anchor stud from a single seismic event is 3.33. Recognizing that the fatigue curve itself is developed from test data with a safety factor of 20 on life and 4 on stress, the results herein demonstrate that fatigue failure of the anchor stud, from a single seismic event, is not credible.

d. Summary of Interface Loads for ISFSI Pad Design

Bounding interface loads are set down for use by the ISFSI pad designer and are based on the validated quasi-static analysis and a dynamic load factor of 2.0:

BOUNDING INTERFACE LOADS FOR ISFSI PAD STRUCTURAL/SEISMIC DESIGN	
D (Cask Weight)	360 kips
D (Anchor Preload @ 65 ksi)	4,550 kips
E (Vertical Load)	1,080 kips
E (Net Horizontal Surface ShearLoad)	1,527.35 kips
E (Overturning Moment)	15,083 kip-ft.

3.4.8 Tornado Wind and Missile Impact (Load Case B in Table 3.1.1 and Load Case 04 in Table 3.1.5)

During a tornado event, the HI-STORM 100 System is assumed to be subjected to a constant wind force. It is also subject to impacts by postulated missiles. The maximum wind speed is specified in Table 2.2.4 and the three missiles, designated as large, intermediate, and small, are described in Table 2.2.5.

In contrast to a freestanding HI-STORM 100 System, the anchored overpack is capable of withstanding much greater lateral pressures and impulsive loads from large missiles. The quasi-static analysis result, presented in the previous subsection, can be used to determine a maximum permitted base overturning moment that will provide at least the same stud safety factors. This is accomplished by setting $G_V = 0.0$, DLF =1 and finding an appropriate G_H that gives equal or better stud safety factors. The resulting value of G^*_H establishes the limit overturning moment for combined tornado missile plus wind., M_L. (G^*_H x Weight x h_{cg}) is conservatively set as the maximum permissible moment at the base of the cask due to combined action of lateral wind and tornado missile loading. Thus, if the lateral force from a tornado missile impact is F at height h and that from steady tornado wind action is a resultant force W acting at cask mid-height (0.5H), and the two loads are acting synergistically to overturn the cask, then their magnitudes must satisfy the inequality

$$0.5WH + Fh \leq M_L$$

where the limit moment is established to ensure that the safety factors for seismic load remain bounding.

M_L = 18,667 kip-ft.

Tornado missile impact factors should be factored into "F" prior to determining the validity of the above inequality for any specific site.

In the case of a free-standing system, the post impact response of the HI-STORM 100 System is required to assess stability. Both the HI-STORM 100 storage overpack, and the HI-TRAC transfer cask are assessed for missile penetration.

~~Appendix 3.C contains~~ *The* results for the post-impact response of the HI-STORM 100 storage overpack ~~where it is~~ demonstrate~~d there~~ that the combination of tornado missile plus either steady

tornado wind or instantaneous tornado pressure drop causes a rotation of the HI-STORM 100 to a maximum angle of inclination less than 3 degrees from vertical. This is much less than the angle required to overturn the cask. ~~The appropriate value for the drag coefficient used in the computation of the lateral force on the storage overpack from tornado wind is justified in Appendix 3.C.~~ The results for the HI-STORM 100 are bounding since the HI-STORM 100S is shorter and its center of gravity is closer to ground.

~~Appendix 3.C computes t~~*T*he maximum force (not including the initial pulse due to missile impact) acting on the projected area of the storage overpack *is computed* to be:

F = 91,920 lbs.

The instantaneous impulsive force due to the missile strike is not computed here; its effect is felt as an initial angular velocity imparted to the storage overpack at time equal to zero. The net resultant force due to the simultaneous pressure drop is not an all-around distributed loading that has a net resultant, but rather is more likely to be distributed only over 180 degrees (or less) of the storage overpack periphery. The circumferential stress and deformation field will be of the same order of magnitude as that induced by a seismic loading. Since the magnitude of the force due to F is less than the magnitude of the net seismically induced force considered in Subsection 3.4.7, the storage overpack global stress analysis performed in Subsection 3.4.7 remains governing. In the next subsection, results are provided for the circumferential stress and ovalization of the portion of the storage overpack due to the bounding estimate for the impact force of the intermediate missile.

3.4.8.1 HI-STORM 100 Storage Overpack

~~Appendix 3.C~~ *This subsection* considers the post impact behavior of the HI-STORM 100 System after impact from tornado missiles. During an impact, the system consisting of missile plus storage overpack and MPC satisfies conservation of linear and angular momentum. The large missile impact is assumed to be inelastic. This assumption conservatively transfers all of the momentum from the missile to the system. The intermediate missile and the small missile are assumed to be unyielding and hence the entire initial kinetic energy is assumed to be absorbed by motion of the cask and local yielding and denting of the storage overpack surface. It is shown that cask stability is maintained under the postulated wind and large missile loads. The conclusion is also valid for the HI-STORM 100S since the lowered total height and the center of gravity location inherently provides additional stability margin.

The penetration potential of the missile strikes (Load Case 04 in Table 3.1.5) is examined *first* ~~in Appendix 3.G. It is shown in Appendix 3.G~~ *The detailed calculations show* that there will be no penetration through the concrete surrounding the inner shell of the storage overpack or penetration of the top closure plate. Therefore, there will be no impairment to the confinement boundary due to missile strikes during a tornado. Since the inner shell is not compromised by the missile strike, there will be no permanent deformation of the inner shell. Therefore, ready retrievability is assured after the missile strike. The following *paragraphs* ~~results~~ summarize the *analysis* work ~~in Appendix 3.G~~.

a. The small missile will dent any surface it impacts, but no significant puncture force is generated. The 1" missile can enter the air ducts, but geometry prevents a direct impact with the MPC.

b. The following table summarizes the denting and penetration analysis performed for the intermediate missile ~~in Appendix 3.G~~. Denting is used to connote a local deformation mode encompassing material beyond the impacting missile envelope, while penetration is used to connote a plug type failure mechanism involving only the target material immediately under the impacting missile.

Location	Denting (in.)	Thru-Thickness Penetration
Storage overpack outer Shell	5.67	Yes (>0.75 in.)
Radial Concrete	7.65	No (<27.25 in.)
Storage overpack Top Lid	0.4	No (<4 in.)

The primary stresses that arise due to an intermediate missile strike on the side of the storage overpack and in the center of the storage overpack top lid are ~~also~~ determined *next* ~~in Appendix 3.G~~. The analysis of the storage lid for the HI-STORM 100 bounds that for the HI-STORM 100S; because of the additional energy absorbing material (concrete) in the direct path of a potential missile strike on the top lid of the HI-STORM 100S lid, the energy absorbing requirements of the circular plate structure are much reduced. ~~It is demonstrated there~~ *The analysis demonstrates* that Level D stress limits are not exceeded in either the overpack outer shell or the top lid. The safety factor in the storage overpack, considered as a cantilever beam under tip load, is computed, as is the safety factor in the top lids, considered as two centrally loaded plates. The applied load, in each case, is the missile impact load. A summary of the results for axial stress in the storage overpack~~, as obtained from Appendix 3.G,~~ is given in the table below:

HI-STORM 100 MISSILE IMPACT - Global Axial Stress Results			
Item	**Value (ksi)**	**Allowable (ksi)**	**Safety Factor**
Outer Shell – Side Strike	15.01	39.75	2.648
Top Lid - (End Strike)	44.14	*58.7*~~59.65~~	1.33~~51~~

To demonstrate ready retrievability of the MPC, we must show that the storage overpack suffers no permanent deformation of the inner shell that would prevent removal of the MPC after the missile strike. To demonstrate ready retrievability (for both HI-STORM 100 and for HI-STORM 100S) a conservative evaluation of the circumferential stress and deformation state due to the missile strike on the outer shell *is* ~~was~~ performed. ~~Appendix 3.G calculates a~~ *A* conservative estimate for the 8" diameter missile impact force, "Pi", on the side of the storage overpack *is calculated* as:

Pi = 881,900 lb.

This force is conservative in that the target overpack is assumed rigid; any elasticity serves to reduce the peak magnitude of the force and increase the duration of the impact. The use of the upper bound value is the primary reason for the high axial stresses resulting from this force. To demonstrate continued ability to retrieve the MPC subsequent to the strike, circumferential stress and deformation that occurs locally in the ring section near the location of the missile strike are investigated.

~~Results in Appendix 3.B are presented under different ring loadings.~~*Subsection 3.4.7 presents stress and displacement results* for a composite ring of unit width consisting of the inner and outer shells of the storage overpack. The solution~~s in Appendix 3.B~~ assume*s* that the net loading is 56,184 lb. applied on the 1" wide ring (equivalent to a 45G deceleration applied uniformly along the height on a storage overpack weight of 270,000 lb.). Thi*s*~~e~~ solution ~~for case1 in Appendix 3.B~~ can be applied directly to evaluate the circumferential stress and deformation caused by a tornado missile strike on the outer shell. Using the results *for the 45g tipover event* ~~in Appendix 3.B~~, an attenuation factor to adjust the results ~~from case 1 in Appendix 3.B~~ is developed that reflects the difference in load magnitude and the width of the ring that is effective in resisting the missile strike force. The strike force Pi is resisted by a combination of inertia force and shear resistance from the portion of the storage overpack above and below the location of the strike. The ring theory solution to determine the circumferential stress and deformation conservatively assumes that inertia alone, acting on an effective length of ring, balances the applied point load Pi. The effective width of ring that balances the impact load is conservatively set as the diameter of the impacting missile (8") plus the effect of the "bending boundary layer" length. This boundary layer length is conservatively set as a multiple of twice the square root of the product of mean radius times the average thickness of two shells making up the cylindrical body of the storage overpack. ~~From Appendix 3.B, t~~*T*he mean radius of the composite cylinder and the average thickness of the inner and outer shells~~,~~ are

R_{mean} = 48"

T =.5 x (.75"+1.25") = 1"

The bending boundary layer "β" in a shell is generally accepted to be given as $(2(R_{mean}T)^{1/2})$ = 13.85" for this configuration. That is, the effect of a concentrated load is resisted mainly in a length along the shell equal to the bending boundary layer. For a strike away from the ends of the shell, a boundary layer length above and below the strike location would be effective (i.e., double the boundary layer length). However, to conservatively account for resistance above and below the location of the strike, this calculated result is only increased by 1.5 in the following analysis (rather than 2). Therefore, the effective width of ring is assumed as:

13.85" x 1.5 + 8" = 28.78"

The solution for *the 45g tipover event* ~~case 1 in Appendix 3.B~~ (performed for a unit ring width and a load of 56,184 lb.) is directly applicable if we multiply all stress and displacement results by the

factor "Y" where

Y = (1"/28.78") x (881,900 lb./56,184 lb.) = 0.545

Using this factor ~~on the solution in Appendix 3.B, (Attachment B-1, Case 15.16)~~ gives the following bounding results for maximum circumferential stresses (without regard for sign and location of the stress) and deformations due to the postulated tornado missile strike on the side of the storage overpack outer shell:

Maximum circumferential stress due to bending moment = (29,310 psi x Y) = 15,974 psi

Maximum circumferential stress due to mean tangential force = (18,900 lb./2 sq.inch) x Y = 10,301 psi

Change in diameter in the direction of the load = -0.11" x Y = -0.06"

Change in diameter perpendicular to the direction of the load = +0.06" x Y = 0.033"

Based on the above calculation, the safety factor on maximum stress for this condition is

SF = 39,750psi/15,974psi = 2.49

The allowable stress for the above calculation is the Level D membrane stress intensity limit from Table 3.1.12. This is a conservative result since the stress intensity is localized and need not be compared to primary membrane stress intensity. Even with the overestimate of impact strike force used in the calculations here ~~and in Appendix 3.G~~, the stresses remain elastic and the calculated diameter changes are small and do not prevent ready retrievability of the MPC. Note that because the stresses remain in the elastic range, there will be no post-strike permanent deformation of the inner shell.

3.4.8.2 HI-TRAC Transfer Cask

3.4.8.2.1 Intermediate Missile Strike

HI-TRAC is always held by the handling system while in a vertical orientation completely outside of the fuel building (see Chapter 2 and Chapter 8). Therefore, considerations of instability due to a tornado missile strike are not applicable. However, the structural implications of a missile strike require consideration.

The penetration potential of the 8" missile strike on HI-TRAC (Load Case 04 in Table 3.1.5) is examined *at two locations* ~~in Appendix 3.H. Two locations are examined~~:

1. the lead backed outer shell of HI-TRAC.
2. the flat transfer lid consisting of multiple steel plates with a layer of lead backing.

In each case, it is shown that there is no penetration consequence that would lead to a radiological release. The following *paragraphs* ~~results~~ summarize the analys*es* *results* ~~in Appendix 3.H~~.

a. The small missile will dent any surface it impacts, but no significant puncture force is generated.

b. The following table summarizes the denting and penetration analysis performed for the intermediate missile ~~in Appendix 3.H~~. Denting connotes a local deformation mode encompassing material beyond the impacting missile envelope, while penetration connotes a plug type failure mechanism involving only the target material immediately under the impacting missile. Where there is through-thickness penetration, *the* ~~it is shown in Appendix 3.H that~~ lead and *the* inner plate absorb any residual energy remaining after penetration of the outer plate in the 100 Ton HI-TRAC transfer lid. ~~Both HI-TRAC transfer casks are evaluated in Appendix 3.H.~~ The table summarizes the bounding results *for both transfer casks*.

Location	Denting (in.)	Thru-Thickness Penetration
Outer Shell - lead backed	0.498	No (<1.0 in.)
Outer Transfer Lid Door	0.516	No (<0.75 in.) (125 Ton unit) Yes (>0.5 in.) (100 Ton unit)

While the transfer cask is being transported in a horizontal orientation, the MPC lid is exposed. We conservatively assume no protective plate in place during this transport operation and evaluate the capacity of the lid peripheral groove weld to resist the impact load. The *calculated* result ~~of calculations in Appendix 3.H~~, conservatively based on a reduced 5/8" weld, is as follows:

HI-TRAC MISSILE IMPACT - Capacity Results			
Item	**Value (lb)**	**Capacity (lb)**	**Safety Factor = Capacity/Value**
Top Lid Weld	2,262,000	2,789,000	1.23

The final calculation in this subsection is an evaluation of the circumferential stress and deformation consequences of the horizontal missile strike on the periphery of the HI-TRAC shell. It is assumed that the HI-TRAC is simply supported at its ends (while in transit) and is subject to a direct impact from the 8" diameter missile. To compute stresses, an estimate of the peak impact force is required. The effect of the water jacket to aid in the dissipation of the impact force is conservatively neglected. The only portion of the HI-TRAC cylindrical body that is assumed to resist the impact load is the two metal shells. The lead is assumed only to act as a separator to maintain the spacing between the shells. The previous results from the lead slump analysis demonstrate that this conservative

assumption on the behavior of the lead is valid. The peak value of the impact force is a function of the stiffness of the target. The target stiffness in this postulated event has the following contributions to the stiffness of the structure.

a. a global stiffness based on a beam deformation mode, and
b. a local stiffness based on a shell deformation mode

~~Appendix 3.Z contains information on the two transfer casks that permit the calculation of a global spring constant (i.e. the inverse of the global deflection of the cask body as a beam under a unit concentrated load).~~ The~~is~~ *global* spring constant *(i.e., the inverse of the global deflection of the cask body as a beam under a unit concentrated load)*~~, however,~~ is a function of location of the strike along the length of the cask. The spring constant value varies from a minimum for a strike at the half-height to a maximum value for a strike near the supports (the trunnions). Since the peak impact force is larger for larger stiffness, it is conservative to maximize the spring constant value. Therefore, in the calculation, we neglect this spring constant for the computation of peak impact force and focus only on the spring constant arising from the local deformation as a shell, in the immediate vicinity of the strike. To this end, the spring constant is estimated by considering the three-dimensional effects of the shell solution to be replaced by the two-dimensional action of a wide ring. The width of the ring is equal to the "bending boundary layer" length on either side of the strike location plus the diameter of the striking missile. Following the analysis methodology already utilized subsection 3.4.8.1, the following information is obtained ~~from Appendix 3.AM~~:

The mean radius of the composite cylinder and the average thickness of the inner and outer shells, are (use the 100 Ton HI-TRAC data since it provides an upper bound on stress and deformation):

R_{mean} = 36.893

T =.5 x (.75"+1.00") = 0.875"

The bending boundary layer "β" in a shell is generally accepted to be given as $(2(R_{mean}T)^{1/2})$. To account for resistance above and below the location of the strike, this calculated result is conservatively increased by multiplying by 1.5. Therefore, the effective width of ring is:

11.22" x 1.5 + 8" = 24.84"

~~Appendix 3.AM contains a ring analysis of~~ *The missile impact is modeled as* a point load, *acting on the ring,* of magnitude equal to Pi = 20,570 lb. The use of a point load in the analysis is conservative in that it overemphasizes the local stress. The actual strike area is an 8" diameter circle (or larger, if the effect of the water jacket were included).

The force is assumed resisted by inertia forces in the ring section. From the results ~~in Appendix 3.AM~~, a spring constant can be defined as the applied load divided by the change in diameter of the ring section in the direction of the applied load. ~~Using the configuration and results in Appendix 3.AM~~*Based on this approach*, the following local spring constant is obtained:

$K = Pi/D1_H = Pi/0.019" = 1{,}083{,}000$ lb./inch

To determine the peak impact force, a dynamic analysis of a two-body system has been performed using the "Working Model" dynamic simulation code. A two mass-spring damper system is considered with the defined spring constant representing the ring deformation effect. Figure 3.4.24 shows the results from the dynamic analysis of the impact using the computer code "Working Model". The small square mass represents the missile, while the larger mass represents the portion of the HI-TRAC "ring" assumed to participate in the local impact. The missile weight is 275.5 lb. and the participating HI-TRAC weight is set to the weight of the equivalent ring used to determine the spring constant.

The peak impact force that results in each of the two springs used to simulate the local elasticity of the HI-TRAC (ring) is:

F(spring) = 124,400 lb.

Since there are two springs in the model, the total impact force is:

P(impact) = 248,800 lb.

To estimate circumferential behavior of the ring under the impact, the *previous* solution ~~in Appendix 3.AM~~ (using a load of 20,570 lb.) is used and amplified by the factor "Z", where:

Z = 248,800 lb./20,570 lb. = 12.095

~~From Appendix 3.AM~~*Consequently*, the maximum circumferential stress due to the ring moment, away from the impact location, is:

3,037psi x (69,260 in-lb/180,900 in-lb) x Z = 14,230 psi

At the same location, the mean stress adds an additional component (~~Appendix 3.AM gives the mean tangential force in the ring;~~ the ring area is computed based on the effective width of the ring).

(5,143 lb./43.47 sq.in) x Z = 1431 psi

Therefore, the safety factor on circumferential stress causing ovalization of an effective ring section that is assumed to resist the impact is:

SF(ring stress) = 39,750 psi/(1431psi + 14,230psi) = 2.54

The allowable stress for this safety factor calculation is obtained from Table 3.1.12 for primary

membrane stress intensity for a Level D event at 350 degrees F material temperature. Noting that the actual circumferential stress in the ring remains in the elastic range, it is concluded that the MPC remains readily retrievable after the impact since there is no permanent ovalization of the cavity after the event. As noted previously, the presence of the water jacket adds an additional structural barrier that has been conservatively neglected in this analysis.

3.4.8.2.2 Large Missile Strike

The effects of a large tornado missile strike on the side (water jacket outer enclosure) of a loaded HI-TRAC has been simulated using a transient finite element model of the transfer cask and loaded MPC. The transient finite element code LSDYNA3D has been used (approved by the NRC for use in impact analysis (see Appendix 3.A, reference [3.A.4] for the benchmarking of this computer code)). An evaluation of MPC retrievability and global stress state (away from the impact area) are of primary interest. The finite element model includes the loaded MPC, the HI-TRAC inner and outer shells, the HI-TRAC water jacket, the lead shielding, and the appropriate HI-TRAC lids. The water in the water jacket has been neglected for conservatism in the results. The large tornado missile has been simulated by an impact force-time pulse applied on an area representing the frontal area of an 1800-kg. vehicle. The force-time data used has been previously approved by the USNRC (Bechtel Topical Report BC-TOP-9A, "Design of Structures for Missile Impact", Revision 2, 9/1974). The frontal impact area used in the finite element analysis is that area recommended in NUREG-0800, SRP 3.5.1.4, Revision 2, 1981.

~~Appendix 3.AN describes the finite element model, the input data used, and provides graphical results necessary to the evaluation of retrievability and state of stress.~~ A summary of the results ~~from Appendix 3.AN~~ is presented below for both transfer casks. The allowable value listed for the stress intensity for this Level D event comes from Table 3.1.17.

SUMMARY OF RESULTS FROM LARGE TORNADO MISSILE IMPACT ANALYSIS		
ITEM – HI-TRAC 100	**CALCULATED VALUE**	**ALLOWABLE VALUE**
Maximum Stress Intensity in Water Jacket (ksi)	28.331	58.7
Maximum Stress Intensity in Inner Shell (ksi)	11.467	58.7
Maximum Plastic Strain in Water Jacket	0.0000932	-
Maximum Plastic Strain in Inner Shell	0.0	-

The results from the dynamic analysis have been summarized below

ITEM – HI-TRAC 125	CALCULATED VALUE	ALLOWABLE VALUE
Maximum Stress Intensity in Water Jacket (ksi)	19.073	58.7
Maximum Stress Intensity in Inner Shell (ksi)	6.023	58.7
Maximum Plastic Strain in Water Jacket	0.0	-
Maximum Plastic Strain in Inner Shell	0.0	-

The above results demonstrate that:

1. The retrievability of the MPC in the wake of a large tornado missile strike is not adversely affected since the inner shell does not experience any plastic deformation.

2. The maximum primary stress intensity, away from the impact interface on the HI-TRAC water jacket, is below the applicable ASME Code Level D allowable limit for NF, Class 3 structures.

3.4.9 HI-TRAC Drop Events (Load Case 02.b in Table 3.1.5)

During transit, the HI-TRAC transfer cask may be carried horizontally with the transfer lid in place. Analyses have been performed to demonstrate that under a postulated carry height; the design basis 45g deceleration is not exceeded. The analyses have been performed using two different simulation models. A simplified model of the drop event is performed using the computer simulation code "Working Model 2D". The analysis using "Working Model 2D" assumed the HI-TRAC and the contained MPC acted as a single rigid body. A second model of the drop event uses DYNA3D, considers the multi-body analysis of HI-TRAC and the contained MPC as individual bodies, and is finite element based. In what follows, we outline the problem and the results obtained using each solution methodology.

3.4.9.1 Working Model 2D Analysis of Drop Event

The analysis model conservatively neglects all energy absorption by any component of HI-TRAC; all kinetic energy is transferred to the ground through the spring-dampers that simulate the foundation (ground). If the HI-TRAC suffers a handling accident causing a side drop to the ground, impact will only occur at the top and bottom ends of the vessel. The so-called "hard points" are the top end lifting trunnions, the bottom end rotation trunnions, and the projecting ends of the transfer lid. Noting that the projecting hard points are of different dimensions and will impact the target at different times because of the HI-TRAC geometry, any simulation model must allow for this possibility.

A dynamic analysis of a horizontal drop, with the lowest point on the HI-TRAC assumed 50" above the surface of the target (larger than the design basis limit of 42"), is considered ~~in Appendix 3.Z~~ for the 125 Ton HI-TRAC and for the 100 Ton HI-TRAC. Figure 3.4.22 shows the transfer cask orientation. The HI-TRAC is considered as a rigid body (~~Appendix 3.Z contains~~ calculations ~~that~~ demonstrate that the lowest beam mode frequency is well above 33 Hz so that no dynamic amplification need be included). The effects of the ISFSI pad and the underlying soil are included using a simple spring-damper model based on a static classical Theory of Elasticity solution. The "worst" orientation of a horizontally carried HI-TRAC with the transfer cask impacting an elastic surface is considered. The HI-TRAC is assumed to initially impact the target with the impact force occurring over the rectangular surface of the transfer lid (11.875" x 81"). "Worst" is defined here as meaning an impact at a location having the maximum value of an elastic spring constant simulating the resistance of the target interface. ~~Appendix 3.AL provides the calculation of the elastic spring-damper that simulates the contact spring.~~ The geometry and material properties ~~used in Appendix 3.AL~~ reflect the USNRC accepted reference pad and soil (Table 2.2.9 - the pad thickness used is 36" and the Young's Modulus of the elastic soil is the upper limit value E=28,000 psi). The use of an elastic representation of the target surface is conservative as it minimizes the energy absorption capacity of the target and maximizes the deceleration loads developed during the impact. ~~Also considered in Appendix 3.AL is a calculation of t~~The spring constant *is also calculated* based on an assumption that impact at the lower end of HI-TRAC first occurs at the pocket trunnion. The results ~~in Appendix 3.AL~~ demonstrate that this spring constant is lower and therefore would lead to a lower impact force. Therefore, the dynamic analysis of the handling accident is performed assuming initial impact with the flat rectangular short end of the transfer lid. Subsequent to the initial impact, the HI-TRAC rotates in accordance with the dynamic equations of equilibrium and a secondary impact at the top of the transfer cask occurs. The impact is at the edge of the water jacket.

The following table summarizes the results from the dynamic analyses (using the Working Model 2D computer code~~) documented in Appendix 3.Z~~:

HI-TRAC Handling Analysis – Working Model Analysis of Horizontal Drop			
Item	**Value**	**Allowable**	**Safety Factor**
125 Ton HI-TRAC–Primary Impact Deceleration (g's)	32.66	45	1.38
125 Ton HI-TRAC – Secondary Impact Deceleration (g's)	26.73	45	1.68
100 Ton HI-TRAC – Primary Impact Deceleration (g's)	33.18	45	1.36
100 Ton HI-TRAC – Secondary Impact Deceleration (g's)	27.04	45	1.66
Axial Membrane Stress Due to 125-Ton HI-TRAC Bending as a Beam - Level D Drop (psi)	19.06	39.75	2.085
Axial Membrane Stress Due to 100-Ton HI-TRAC Bending as a Beam - Level D Drop (psi)	15.77	39.75	2.52

In the table above, the decelerations are measured at points corresponding to the base and top of the fuel assemblies contained inside the MPC. The dynamic drop analysis reported above, using the

Working Model 2D rigid body-spring model proved that decelerations are below the design basis value and that global stresses were within allowable limits.

3.4.9.2 DYNA3D Analysis of Drop Event

An independent evaluation of the drop event to delineate the effect of target non-linearity and the flexibility of the transfer cask has been performed using DYNA3D. ~~Appendix 3.AN provides details of the HI-TRAC drop model, the data input, and extensive graphical results.~~ Both HI-TRAC transfer casks are modeled as part of the cask-pad-soil interaction finite element model set forth in NUREG/CR-6608 and validated by an NRC reviewed and approved Holtec topical report (see reference [3.A.4] in Appendix 3.A). The model uses the identical MPC and target pad/soil models employed in the accident analyses of the HI-STORM 100 overpack. The HI-TRAC inner and outer shells, the contained lead, the transfer lid, the water jacket metal structure, and the top lids are included in the model. The water jacket is assumed empty for conservatism.

Two side drop orientations are considered (see Figures 3.4.27 and 3.4.28). The first drop assumes that the plane of the lifting and rotation trunnions is horizontal with primary impact on the short side of the transfer lid. This maximizes the angle of slapdown, and represents a credible drop configuration where the HI-TRAC cask is dropped while being carried horizontally. The second drop orientation assumes primary impact on the rotation trunnion and maximizes the potential for the lifting trunnion to participate in the secondary impact. This is a non-credible event that assumes complete separation from the transfer vehicle and a ninety-degree rotation prior to impact. Nevertheless, it is the only configuration where the trunnions could be involved in both primary and secondary impacts.

For each simulation performed, the lowest point on the HI-TRAC cask (either the transfer lid edge or the rotation trunnion) is set at 42" above the target interface. Decelerations are measured at the top lid, the cask centroidal position, and the transfer lid. Normal forces were measured at the primary impact interface, at the secondary impact interface, and at the top lid/MPC interface. Decelerations are filtered at 350 Hz. The following key results summarize the analyses ~~documented in the new Appendix 3.AN~~:

ITEM	HI-TRAC 125		HI-TRAC 100		ALLOWABLE
Initial Orientation of Trunnions	**Horizontal**	**Vertical**	**Horizontal**	**Vertical**	
Max. Top Lid Vertical Deceleration – Secondary Impact (g's)	25.5	32	36.5	45†	45
Centroid Vertical Deceleration – at Time of Secondary Impact (g's)	9.0	13.0	10.0	17.5	45
Max. Transfer Lid Vertical Deceleration – Primary Impact (g's)	30.8	23.5	35.0	31.75	45
Maximum Normal Force at Primary Impact Site (kips)	1,950.	1,700	1,700	1,700	-
Maximum Normal Force at Secondary Impact Site (kips)	1,300.	1,850.	1,500.	1,450.	-
Maximum MPC/Top Lid Interface Force (kips)	132.	-	39.	-	-
Maximum Diametral Change of Inner Shell (inch)	0.228	0.113	Not Computed	0.067	0.3725
Maximum Von Mises Stress (ksi)	37.577	38.367	40.690	40.444	58.7*

† The deceleration at the top of the basket is estimated at 41 g's

* Allowable Level D Stress Intensity for Primary Plus Secondary Stress Intensity

The results ~~presented in Appendix 3.AN and~~ summarized above demonstrate that both HI-TRAC transfer casks are sufficiently robust to perform their function during and after the postulated handling accidents. We also note that the results, using the Working Model single rigid body dynamic model (see Subsection 3.4.9.1), are in reasonable agreement with the results predicted by the DYNA3D multi-body finite element dynamic model although performed for a different drop height with deceleration measurements at different locations on the HI-TRAC.

The results reported above for maximum interface force at the top lid/MPC interface are used as input to *a separate* ~~the~~ analysis, *which* ~~in Appendix 3.AH to~~ demonstrates that the top lid contains the MPC during and after a handling accident. The results reported above for the maximum normal force at the primary impact site (the transfer lid) have been used to calculate the maximum interface force at the bottom flange/transfer lid interface. This result is needed to insure that the interface ~~input~~ forces used ~~in Appendices 3.AD and 3.AJ~~ to evaluate transfer lid separation are indeed bounding. To obtain the interface force between the HI-TRAC transfer lid and the HI-TRAC bottom flange, it is sufficient to take a free-body of the transfer lid and write the dynamic force equilibrium equation for the lid. Figure 3.4.29 shows the free body with appropriate notation. The equation of equilibrium is:

$$M_{TL} a_{TL} = F_I - G_I$$

where

M_{TL} = the mass of the transfer lid

a_{TL} = the time varying acceleration of the centroid of the transfer lid

F_I = the time varying contact force at the interface with the target

G_I = the time varying interface force at the bottom flange/transfer lid interface

Solving for the interface force gives the result

$$G_I = F_I - M_{TL} a_{TL}$$

Using the appropriate transfer lid mass and acceleration, together with the target interface force at the limiting time instant, provides values for the interface force. The table below provides the results of this calculation for both HI-TRAC transfer casks.

Item	Calculated from Equilibrium (kips)
125 Ton HI-TRAC – Trunnions Horizontal	1,183.
125 Ton HI-TRAC – Trunnions Vertical	1,272.
100 Ton HI-TRAC – Trunnions Horizontal	1,129.
100 Ton HI-TRAC – Trunnions Vertical	1,070.

3.4.10 HI-STORM 100 Non-Mechanistic Tip-over and Vertical Drop Event (Load Cases 02.a and 02.c in Table 3.1.5)

Pursuant to the provision in NUREG-1536, a non-mechanistic tip-over of a loaded HI-STORM 100 System on to the ISFSI pad is considered in this report. Analyses are also performed to determine the maximum deceleration sustained by a vertical free fall of a loaded HI-STORM 100 System from an 11" height onto the ISFSI pad. The objective of the analyses is to demonstrate that the plastic deformation in the fuel basket is sufficiently limited to permit the stored SNF to be retrieved by normal means, does not have a adverse effect on criticality safety, and that there is no significant loss of radiation shielding in the system.

Ready retrievability of the fuel is presumed to be ensured: if global stress levels in the MPC structure meet Level D stress limits during the postulated drop events; if any plastic deformations are localized; and if no significant permanent ovalization of the overpack into the MPC envelope space, remains after the event.

Subsequent to the accident events, the storage overpack must be shown to contain the shielding so that unacceptable radiation levels do not result from the accident.

Appendix 3.A provides a description of the dynamic finite element analyses undertaken to establish the decelerations resulting from the postulated event. A non-mechanistic tip-over is considered together with an end drop of a loaded HI-STORM 100 System. A dynamic finite element analysis of each event is performed using a commercial finite element code well suited for such dynamic analyses with interface impact and non-linear material behavior. This code and methodology have been fully benchmarked against Lawrence Livermore Laboratories test data and correlation [3.4.12].

The table below provides the values of computed peak decelerations at the top of the fuel basket for the vertical drop and the non-mechanistic tipover scenarios. It is seen that the peak deceleration is below 45 g's.

Filtered Results for Drop and Tip-Over Scenarios for HI-STORM

Drop Event	Max. Deceleration at the Top of the Basket (g's)	
	Set A(36" Thick Pad)	Set B(28" Thick Pad)
End Drop for 11 inches	43.98	41.53
Non-Mechanistic Tip-over	42.85	39.91

The tipover analysis performed in Appendix 3.A is based on the HI-STORM 100 geometry and a bounding weight. The fact that the HI-STORM 100S is shorter and has a lower center of gravity suggests that the impact kinetic energy is reduced so that the target would absorb the energy with a lower maximum deceleration. However, since the actual weight of a HI-STORM 100S is less than that of a HI-STORM 100, the predicted maximum rigid body deceleration would tend to increase slightly. Since there are two competing mechanisms at work, it is not a foregone conclusion that the maximum rigid body deceleration level is, in fact, reduced if a HI-STORM 100S suffers a non-mechanistic tipover onto the identical target as the HI-STORM 100. In what follows, we present a summary of the analysis undertaken to demonstrate conclusively that the result for maximum deceleration level in the HI-STORM 100 tipover event does bound the corresponding value for the

HI-STORM 100S, and, therefore, we need only perform a detailed dynamic finite element analysis for the HI-STORM 100.

Appendix 3.A presents a result for the angular velocity of the cylindrical body representing a HI-STORM 100 just prior to impact with the defined target. The result is expressed in Subsection 3.A.6 in terms of the cask geometry, and the ratio of the mass divided by the mass moment of inertia about the corner point that serves as the rotation origin. Since the mass moment of inertia is also linearly related to the mass, the angular velocity at the instant just prior to target contact is independent of the cask mass. Subsequent to target impact, we investigate post-impact response by considering the cask

as a cylinder rotating into a target that provides a resistance force that varies linearly with distance from the rotation point. We measure "time" as starting at the instant of impact, and develop a one-degree-of freedom equation for the post-impact response (for the rotation angle into the target) as:

$$\ddot{\theta} + \omega^2\theta = 0$$

where

$$\omega^2 = \frac{kL^3}{3I_A}$$

The initial conditions at time=0 are: the initial angle is zero and the initial angular velocity is equal to the rigid body angular velocity acquired by the tipover from the center-of-gravity over corner position. In the above relation, L is the length of the overpack, I is the mass moment of inertia defined in Appendix 3.A, and k is a "spring constant" associated with the target resistance. If we solve for the maximum angular acceleration subsequent to time =0, we obtain the result in terms of the initial angular velocity as:

$$\ddot{\theta}_{max} = \omega\dot{\theta}_0$$

If we form the maximum linear acceleration at the top of the four-inch thick lid of the overpack, we can finally relate the decelerations of the HI-STORM 100 and the HI-STORM 100S solely in terms of their geometry properties and their mass ratio. The value of "k", the target spring rate is the same for both overpacks so it does not appear in the relationship between the two decelerations. After substituting the appropriate geometry and calculated masses, we determine that the ratio of maximum rigid body decelerations at the top surface of the four-inch thick top lid plates is:

$$A_{\text{HI-STORM 100S}}/A_{\text{HI-STORM 100}} = 0.946$$

Therefore, as postulated, there is no need to perform a separate DYNA3D analysis for the HI-STORM 100S hypothetical tipover.

~~Appendix 3.B contains a~~ *A* simple elastic strength of materials calculation *is performed* to demonstrate that the cylindrical storage overpack will not permanently deform to the extent that the MPC cannot be removed by normal means after a tip-over event. ~~It is demonstrated in that appendix~~ *The results demonstrate* that the maximum diametrical closure of the cylindrical cavity is less than the initial clearance between the overpack MPC support channels and the MPC canister. Primary circumferential membrane stresses in the MPC shell remain in the elastic range during a tip-over (see Table 3.4.6 summary safety factors); therefore, no permanent global ovalization of the MPC shell occurs as a result of the drop.

To demonstrate that the shielding material will continue to perform its function after a tip-over

accident, the stress and strain levels in the metal components of the storage overpack are examined at the end of the tip-over event. The results obtained in Appendix 3.A for impact decelerations conservatively assumed a rigid storage overpack model to concentrate nearly all energy loss in the target. However, to assess the state of stress and strain in the storage overpack after an accident causing a tip-over, the tip-over analysis was also performed using a non-rigid storage overpack model using overpack material properties listed in Appendix 3.A. Figure 3.4.13 shows the calculated von Mises stress in the top lid and outer shell at 0.08 seconds after the initiation of impact. Figure 3.4.14 shows the residual plastic strains in the same components. Figures 3.4.15 and 3.4.16 provide similar results for the inner shell, the radial plates, and the support channels. The results show that while some plastic straining occurs, accompanied by stress levels above the yield stress of the material, there is no tearing in the metal structure which confines the radiation shielding (concrete). Therefore, there is no gross failure of the metal shells enclosing the concrete. The shielding concrete will remain inside the confines of the storage overpack and maintain its performance after the tipover event.

3.4.11 Storage Overpack and HI-TRAC Transfer Cask Service Life

The term of the 10CFR72, Subpart L C of C, granted by the NRC is 20 years; therefore, the License Life (please see glossary) of all components is 20 years. Nonetheless, the HI-STORM 100 and 100S Storage overpacks and the HI-TRAC transfer cask are engineered for 40 years of design life, while satisfying the conservative design requirements defined in Chapter 2, including the regulatory requirements of 10CFR72. In addition, the storage overpack and HI-TRAC are designed, fabricated, and inspected under the comprehensive Quality Assurance Program discussed in Chapter 13 and in accordance with the applicable requirements of the ACI and ASME Codes. This assures high design margins, high quality fabrication, and verification of compliance through rigorous inspection and testing, as describe in Chapter 9 and the design drawings in Section 1.5. Technical Specifications defined in Chapter 12 assure that the integrity of the cask and the contained MPC are maintained throughout the components' design life. The design life of a component, as defined in the Glossary, is the minimum duration for which the equipment or system is engineered to perform its intended function if operated and maintained in accordance with the FSAR. The design life is essentially the lower bound value of the service life, which is the expected functioning life of the component or system. Therefore, component longevity should be: licensed life < design life < service life. (The licensed life, enunciated by the USNRC, is the most pessimistic estimate of a component's life span.) For purposes of further discussion, we principally focus on the service life of the HI-STORM 100 System components that, as stated earlier, is the reasonable expectation of equipment's functioning life span.

The service life of the storage overpack and HI-TRAC transfer cask is further discussed in the following sections.

3.4.11.1 Storage Overpack

The principal design considerations that bear on the adequacy of the storage overpack for the service life are addressed as follows:

Exposure to Environmental Effects

In the following text, all references to HI-STORM 100 also apply to HI-STORM 100S. All exposed surfaces of HI-STORM 100 are made from ferritic steels that are readily painted. Concrete, which serves strictly as a shielding material, is completely encased in steel. Therefore, the potential of environmental vagaries such as spalling of concrete, are ruled out for HI-STORM 100. Under normal storage conditions, the bulk temperature of the HI-STORM 100 storage overpack will, because of its large thermal inertia, change very gradually with time. Therefore, material degradation from rapid thermal ramping conditions is not credible for the HI-STORM 100 storage overpack. Similarly, corrosion of structural steel embedded in the concrete structures due to salinity in the environment at coastal sites is not a concern for HI-STORM 100 because HI-STORM 100 does not rely on rebars (indeed, it contains no rebars). As discussed in Appendix 1.D, the aggregates, cement and water used in the storage cask concrete are carefully controlled to provide high durability and resistance to temperature effects. The configuration of the storage overpack assures resistance to freeze-thaw degradation. In addition, the storage overpack is specifically designed for a full range of enveloping design basis natural phenomena that could occur over the 40-year design life of the storage overpack as defined in Subsection 2.2.3 and evaluated in Chapter 11.

Material Degradation

The relatively low neutron flux to which the storage overpack is subjected cannot produce measurable degradation of the cask's material properties and impair its intended safety function. Exposed carbon steel components are coated to prevent corrosion. The controlled environment of the ISFSI storage pad mitigates damage due to direct exposure to corrosive chemicals that may be present in other industrial applications.

Maintenance and Inspection Provisions

The requirements for periodic inspection and maintenance of the storage overpack throughout the 40-year design life are defined in Chapter 9. These requirements include provisions for routine inspection of the storage overpack exterior and periodic visual verification that the ventilation flow paths of the storage overpack are free and clear of debris. ISFSIs located in areas subject to atmospheric conditions that may degrade the storage cask or canister should be evaluated by the licensee on a site-specific basis to determine the frequency for such inspections to assure long-term performance. In addition, the HI-STORM 100 System is designed for easy retrieval of the MPC from the storage overpack should it become necessary to perform more detailed inspections and repairs on the storage overpack.

The above findings are consistent with those of the NRC's Waste Confidence Decision Review [3.4.11], which concluded that dry storage systems designed, fabricated, inspected, and operate in accordance with such requirements are adequate for a 100-year service life while satisfying the requirements of 10CFR72.

3.4.11.2 Transfer Cask

The principal design considerations that bear on the adequacy of the HI-TRAC Transfer Cask for the service life are addressed as follows:

Exposure to Environmental Effects

All transfer cask materials that come in contact with the spent fuel pool are coated to facilitate decontamination. The HI-TRAC is designed for repeated normal condition handling operations with high factors of safety, particularly for the lifting trunnions, to assure structural integrity. The resulting cyclic loading produces stresses that are well below the endurance limit of the trunnion material, and therefore, will not lead to a fatigue failure in the transfer cask. All other off-normal or postulated accident conditions are infrequent or one-time occurrences that do not contribute significantly to fatigue. In addition, the transfer cask utilizes materials that are not susceptible to brittle fracture during the lowest temperature permitted for loading, as discussed in Chapter 12.

Material Degradation

All transfer cask materials that are susceptible to corrosion are coated. The controlled environment in which the HI-TRAC is used mitigates damage due to direct exposure to corrosive chemicals that may be present in other industrial applications. The infrequent use and relatively low neutron flux to which the HI-TRAC materials are subjected do not result in radiation embrittlement or degradation of the HI-TRAC's shielding materials that could impair the HI-TRAC's intended safety function. The HI-TRAC transfer cask materials are selected for durability and wear resistance for their deployment.

Maintenance and Inspection Provisions

The requirements for periodic inspection and maintenance of the HI-TRAC transfer cask throughout the 40-year design life are defined in Chapter 9. These requirements include provisions for routine inspection of the HI-TRAC transfer cask for damage prior to each use, including an annual inspection of the lifting trunnions. Precautions are taken during lid handling operations to protect the sealing surfaces of the pool lid. The leak tightness of the liquid neutron shield is verified periodically. The water jacket pressure relief valves and other fittings used can be easily removed.

3.4.12 MPC Service Life

The term of the 10CFR72, Subpart L C of C, granted by the NRC (i.e., licensed life) is 20 years. Nonetheless, the HI-STORM 100 MPC is designed for 40 years of design life, while satisfying the conservative design requirements defined in Chapter 2, including the regulatory requirements of 10CFR72. Additional assurance of the integrity of the MPC and the contained SNF assemblies throughout the 40-year life of the MPC is provided through the following:

- Design, fabrication, and inspection in accordance with the applicable requirements of the ASME Code as described in Chapter 2 assures high design margins.

- Fabrication and inspection performed in accordance with the comprehensive Quality Assurance program discussed in Chapter 13 assures competent compliance with the fabrication requirements.

- Use of materials with known characteristics, verified through rigorous inspection and testing, as described in Chapter 9, assures component compliance with design requirements.

- Use of welding procedures in full compliance with Section III of the ASME Code ensures high-quality weld joints.

Technical Specifications, as defined in Chapter 12, have been developed and imposed on the MPC that assure that the integrity of the MPC and the contained SNF assemblies are maintained throughout the 40-year design life of the MPC.

The principal design considerations bearing on the adequacy of the MPC for the service life are summarized below.

Corrosion

All MPC materials are fabricated from corrosion-resistant austenitic stainless steel and passivated aluminum. The corrosion-resistant characteristics of such materials for dry SNF storage canister applications, as well as the protection offered by these materials against other material degradation effects, are well established in the nuclear industry. The moisture in the MPC is removed to eliminate all oxidizing liquids and gases and the MPC cavity is backfilled with dry inert helium at the time of closure to maintain an atmosphere in the MPC that provides corrosion protection for the SNF cladding throughout the dry storage period. The preservation of this non-corrosive atmosphere is assured by the inherent seal worthiness of the MPC confinement boundary integrity (there are no gasketed joints in the MPC).

Structural Fatigue

The passive non-cyclic nature of dry storage conditions does not subject the MPC to conditions that might lead to structural fatigue failure. Ambient temperature and insolation cycling during normal dry storage conditions and the resulting fluctuations in MPC thermal gradients and internal pressure is the only mechanism for fatigue. These low stress, high-cycle conditions cannot lead to a fatigue failure of the MPC that is made from stainless alloy stock (endurance limit well in excess of 20,000 psi). All other off-normal or postulated accident conditions are infrequent or one-time occurrences, which cannot produce fatigue failures. Finally, the MPC uses materials that are not susceptible to brittle fracture.

Maintenance of Helium Atmosphere

The inert helium atmosphere in the MPC provides a non-oxidizing environment for the SNF cladding to assure its integrity during long-term storage. The preservation of the helium atmosphere in the MPC is assured by the robust design of the MPC confinement boundary described in Section 7.1. Maintaining an inert environment in the MPC mitigates conditions that might otherwise lead to SNF cladding failures. The required mass quantity of helium backfilled into the canister at the time of closure, as defined in the Technical Specification contained in Subsection 12.3.3, and the associated leak tightness requirements for the canister defined in the Technical Specification contained in Chapter 12, are specifically set down to assure that an inert helium atmosphere is maintained in the canister throughout the 40-year design life.

Allowable Fuel Cladding Temperatures

The helium atmosphere in the MPC promotes heat removal and thus reduces SNF cladding temperatures during dry storage. In addition, the SNF decay heat will substantially attenuate over a 40-year dry storage period. Maintaining the fuel cladding temperatures below allowable levels during long-term dry storage mitigates the damage mechanism that might otherwise lead to SNF cladding failures. The allowable long-term SNF cladding temperatures used for thermal acceptance of the MPC design are conservatively determined, as discussed in Section 4.3.

Neutron Absorber Boron Depletion

The effectiveness of the fixed borated neutron absorbing material used in the MPC fuel basket design requires that sufficient concentrations of boron be present to assure criticality safety during worst case design basis conditions over the 40-year design life of the MPC. Information on the characteristics of the borated neutron absorbing material used in the MPC fuel basket is provided in Subsection 1.2.1.3.1. The relatively low neutron flux, which will continue to decay over time, to which this borated material is subjected, does not result in significant depletion of the material's available boron to perform its intended safety function. In addition, the boron content of the material used in the criticality safety analysis is conservatively based on the minimum specified boron areal density (rather than the nominal), which is further reduced by 25% for analysis purposes, as described in Section 6.1. Analysis discussed in Section 6.2 demonstrates that the boron depletion in the *neutron absorber material*~~Boral~~ is negligible over a 50-year duration. Thus, sufficient levels of boron are present in the fuel basket neutron absorbing material to maintain criticality safety functions over the 40-year design life of the MPC.

The above findings are consistent with those of the NRC's Waste Confidence Decision Review, which concluded that dry storage systems designed, fabricated, inspected, and operated in the manner of the requirements set down in this document are adequate for a 100-year service life, while satisfying the requirements of 10CFR72.

3.4.13 Design and Service Life

The discussion in the preceding sections seeks to provide the logical underpinnings for setting the design life of the storage overpacks, the HI-TRAC transfer cask, and the MPCs as forty years. Design life, as stated earlier, is a lower bound value for the expected performance life of a component (service life). If operated and maintained in accordance with this Final Safety Analysis Report, Holtec International expects the service life of its HI-STORM 100 and HI-STORM 100S components to substantially exceed their design life values.

Table 3.4.1
FINITE ELEMENTS IN THE MPC STRUCTURAL MODELS

MPC Type	**Model Type**		
Element Type	**Basic**	**0 Degree Drop**	**45 Degree Drop**
MPC-24	1542	1773	1772
BEAM3	1498	1498	1498
PLANE82	8	8	8
CONTAC12	36	34	34
CONTAC26	0	230	230
COMBIN14	0	3	2
MPC-32	1374	1604	1603
BEAM3	1346	1346	1346
CONTAC12	28	27	24
CONTAC26	0	229	228
COMBIN14	0	2	5
MPC-68	1842	2066	2063
BEAM3	1782	1782	1782
PLANE82	16	16	16
CONTAC12	44	43	40
CONTAC26	0	223	222
COMBIN14	0	2	3
MPC-24E	1070	1124	1122
BEAM3	1030	1030	1030
PLANE82	0	0	0
CONTAC12	40	38	38
CONTAC26	0	53	52
COMBIN14	0	3	2

TABLE 3.4.2
HI-STORM 100 SYSTEM MATERIAL COMPATIBILITY WITH OPERATING ENVIRONMENTS

Material/Component	Fuel Pool (Borated and Unborated Water)†	ISFSI Pad (Open to Environment)
Alloy X: - MPC Fuel Basket - MPC Baseplate - MPC Shell - MPC Lid - MPC Fuel Spacers	Stainless steels have been extensively used in spent fuel storage pools with both borated and unborated water with no adverse reactions or interactions with spent fuel.	The MPC internal environment will be inert (helium) atmosphere. No adverse interactions identified.
Aluminum: - Heat Conduction Elements	Aluminum and stainless steel form a galvanic couple. However, aluminum will be used in a passivated state. Upon passivation, aluminum forms a thin ceramic (Al_2O_3) barrier. Therefore, during the short time they are exposed to pool water, corrosion of aluminum is not expected.	In a non-aqueous atmosphere, galvanic corrosion is not expected.
Neutron Absorber Material~~Boral~~: ~~Neutron Absorber~~	The *neutron absorber material*~~Boral~~ will be passivated before installation in the fuel basket. Extensive in-pool experience on spent fuel racks with no adverse reactions.	No adverse potential reactions identified.

† HI-TRAC/MPC short-term operating environment during loading and unloading.

TABLE 3.4.2 (CONTINUED)
HI-STORM 100 SYSTEM MATERIAL COMPATIBILITY WITH OPERATING ENVIRONMENTS

Material/Component	Fuel Pool (Borated and Unborated Water)†	ISFSI Pad (Open to Environment)
Steels: - SA350-LF3 - SA203-E - SA516 Grade 70 - SA193 Grade B7 - SA106 (HI-TRAC)	All exposed steel surfaces (except seal areas, and pocket trunnions) will be coated with paint specifically selected for performance in the operating environments. Even without coating, no adverse reactions (other than nominal corrosion) have been identified. Lid bolts are plated and the threaded portion of the bolt anchor blocks is coated to seal the threaded area.	Internal surfaces of the HI-TRAC will be painted and maintained. Exposed external surfaces (except those listed in fuel pool column) will be painted and will be maintained with a fully painted surface. No adverse reactions identified.
Steels: - SA516 Grade 70 - SA203-E - SA350-LF3 Storage Overpack	HI-STORM 100 storage overpack is not exposed to fuel pool environment.	Internal and external surfaces will be painted (except for bolt locations that will have protective coating). External surfaces will be maintained with a fully painted surface. No adverse reaction identified.
Stainless Steels: - SA240 304 - SA193 Grade B8 - 18-8 S/S Miscellaneous Components	Stainless steels have been extensively used in spent fuel storage pools with both borated and unborated water with no adverse reactions.	Stainless steel has a long proven history of corrosion resistance when exposed to the atmosphere. These materials are used for bolts and threaded inserts. No adverse reactions with steel have been identified. No impact on performance.

† HI-TRAC/MPC short-term operating environment during loading and unloading.

TABLE 3.4.2 (CONTINUED)
HI-STORM 100 SYSTEM MATERIAL COMPATIBILITY
WITH OPERATING ENVIRONMENTS

Material/Component	Fuel Pool (Borated and Unborated Water)†	ISFSI Pad (Open to Environment)
Nickel Alloy: - SB637-NO7718 Lifting Trunnion	No adverse reactions with borated or unborated water.	Exposed to weathering effects. No adverse reactions with storage overpack closure plate. No impact on performance.
Brass/Bronze: - Pressure Relief Valve HI-TRAC	Small surface of pressure relief valve will be exposed. No significant adverse impact identified.	Exposed to external weathering. No loss of function expected.
Holtite-A: - Solid Neutron Shield	The neutron shield is fully enclosed. No adverse reaction identified. No adverse reactions with thermal expansion foam or steel.	The neutron shield is fully enclosed in the outer enclosure. No adverse reaction identified. No adverse reactions with thermal expansion foam or steel.
Silicone Foam: - Thermal Expansion Foam	Fully enclosed. No adverse reaction identified. No adverse reactions with solid neutron shield material or steel.	Foam is fully enclosed in outer enclosure. No adverse reaction identified. No adverse reactions with neutron shield or steel.

† HI-TRAC/MPC short-term operating environment during loading and unloading.

TABLE 3.4.2 (CONTINUED)
HI-STORM 100 SYSTEM MATERIAL COMPATIBILITY WITH OPERATING ENVIRONMENTS

Material/Component	Fuel Pool (Borated and Unborated Water)†	ISFSI Pad (Open to Environment)
Paint: - Carboline 890 - Thermaline 450	Carboline 890 used for all HI-STORM 100 surfaces and only HI-TRAC exterior surfaces. Acceptable performance for short-term exposure in mild borated pool water. Thermaline 450 selected for HI-TRAC internal surfaces for excellent high temperature resistance properties. Will only be exposed to demineralized water during in-pool operations as annulus is filled prior to placement in the spent fuel pool and the inflatable seal prevents fuel pool water in-leakage. No adverse interaction identified which could affect MPC/fuel assembly performance.	Good performance on surfaces. Discoloration is not a concern.
Elastomer Seals:	No adverse reactions identified.	Only used during fuel pool operations.
Lead:	Enclosed by carbon steel. Lead is not exposed to fuel pool water. Lead has no interaction with carbon steel.	Enclosed by carbon steel. Lead is not exposed to ambient environment. Lead has no interaction with carbon steel.
Concrete:	Storage overpack is not exposed to fuel pool water.	Concrete is enclosed by carbon steel and not exposed to ambient environment. Concrete has no interaction with carbon steel.

† HI-TRAC/MPC short-term operating environment during loading and unloading.

TABLE 3.4.3
FUEL BASKET RESULTS - MINIMUM SAFETY FACTORS

Load Case I.D.	Loading†	Safety Factor	Location in FSAR ~~Where the Analysis is Performed~~
F1	T, T'	No interference	*Subsection 3.4.4.2*~~3.I, 3.U, 3.W,3.AF~~
F2	D + H	2.79	3.AA of Docket 72-1008
F3			
F3.a	D + H' (end drop)	3.59	F3.a 3.4.4.3.1.3
F3.b	D + H' (side drop 0 deg.)	1.43	F3.b Table 3.4.6
F3.c	D + H' (side drop 45 deg.)	1.28	F3.c Table 3.4.6

† The symbols used for the loadings are defined in Table 2.2.13.

TABLE 3.4.4
MPC RESULTS - MINIMUM SAFETY FACTOR

Load Case I.D.	Load Combination[†,††]	Safety Factor	Location in FSAR ~~Where the Analysis is Performed~~
E1			
	Design internal pressure, P_I	15	E.1.a Lid 3.E.8.1.1 of Docket 72-1008
E1.a		1.326	Baseplate 3.I.8.1 of Docket 72-1008
		1.36	*Shell* Table 3.4.7
		N/A	Supports
		15	E.1.b Lid P_i bounds
	Design external pressure, P_o	1.326	Baseplate P_i bounds
E1.b		1.17	Shell 3.H (Case 4) (buckling) of Docket 72-1008
		N/A	Supports
	Design internal pressure, P_i,		
E1.c	plus Temperature T	1.4	E1.c Table 3.4.8
E2	D + H + (P_i, P_o)	6.5	Lid 3.E.8.1.2 of Docket 72-1008
		1.088	Baseplate 3.I.8.2 of Docket 72-1008
		2.63(stress),	Shell 3.AA (stress) of Docket 72-1008
		1.17(buckling)	3.H (Case 4) (buckling) of Docket 72-1008
		4.58	Supports 3.AA of Docket 72-1008

† The symbols used for the loadings are defined in Table 2.2.13

†† Note that in analyses, bounding pressures are applied, i.e., in buckling calculations P_o is used, and in stress evaluations either P_o or P_i is appropriate

TABLE 3.4.4 (CONTINUED)
MPC RESULTS - MINIMUM SAFETY FACTOR

Load Case I.D.	Load Combination[†,††]	Safety Factor	Location in FSAR ~~Where the Analysis is Performed~~		
E3					
E3.a	(P_i,P_o) + D + H', end drop	2.8	E.a	Lid	3.E.8.2.1-2 of Docket 72-1008
		1.28		Baseplate	3.I.8.3 of Docket 72-1008
		1.21		Shell	3.H (Case 5) (buckling) of Docket 72-1008
		N/A		Supports	
E3.b	(P_i,P_o) + D + H', side drop 0 deg.	2.8	E.b	Lid	end drop bounds
		1.28		Baseplate	end drop bounds
		1.1		*Shell*	Table 3.4.6
		1.18		*Supports*	Table 3.4.6
		~~1.82~~		~~Basket Supports: Appendix 3.Y~~	
E3.c	(P_i,P_o) + D + H', side drop 45 deg.	2.8	E.c.	Lid	end drop bounds
		1.28		Baseplate	end drop bounds
		1.46		*Shell*	*Table 3.4.6*~~Calculation Package~~
		1.56		*Supports*	Table 3.4.6

† The symbols used for the loadings are defined in Table 2.2.13
†† Note that in analyses, bounding pressures are applied, i.e., in buckling calculations P_o is used, and in stress evaluations either P_o or P_i is appropriate

TABLE 3.4.4 (CONTINUED)
MPC RESULTS - MINIMUM SAFETY FACTOR

Load Case I.D.	Load Combination1†, ††	Safety Factor	Location in FSAR
E4	T	Subsection 3.4.4.2 shows there are no primary stresses from thermal expansion.	Subsection 3.4.4.2
E5	D + T* + (P_i*,P_o*)	27.2 1.78 1.08 (buckling);4.16(stress) N/A	Lid 3.E.8.2.1.3 of Docket 72-1008 Baseplate 3.I.8.4 of Docket 72-1008 Shell 3.H (Case 6) (buckling) of Docket 72-1008 3.4.4.3.1.5 (thermal stress) of Docket 72-1008 Supports N/A

† The symbols used for the loadings are defined in Table 2.2.13.

†† Note that in analyses, bounding pressures are applied, i.e., in buckling calculations P_o is used, and in stress evaluations either P_o or P_i is appropriate

TABLE 3.4.5
HI-STORM 100 STORAGE OVERPACK AND HI-TRAC RESULTS - MINIMUM SAFETY FACTORS

Load Case I.D.	Loading†	Safety Factor	Location in FSAR
01	D + H + T + (P_o, P_i)	1.32	Overpack
		N/A	Shell (inlet vent)/Base *3.4.3.5*~~3.D~~
			Top Lid N/A
		2.83 (125 T);2.29 (100 T)	HI-TRAC
			Shell *3.4.3.3; 3.4.3.4*
		2.604 (ASME Code limit)	~~3.AB~~
		1.919 (ASME Code limit)	Pool Lid *3.4.3.8*~~3.AB~~
		N/A	*Transfer Lid* *3.4.3.9*
		5.31; 1.11(optional bolts)	Top Lid *N/A*~~3.AB~~
		~~Tables in 3.4.3~~	Pocket Trunnion *3.4.4.3.3.1*
			~~3.AA; 3.AI~~
			~~Lifting Calculations 3.4.3~~
02			
02.a	D + H' + (P_o,P_i) (end drop/tip-over)	1.36(weld)	Overpack
		1.27 (bolt)	Shell/Base ~~3.M;~~3.4.4.3.2.3
			Top Lid ~~3.K/3.L;~~3.4.4.3.2.2
02.b	D + H' + (P_o,P_i) (side drop)	2.09	HI-TRAC
		1.392	Shell ~~3.Z;~~3.4.9
		1.651	Transfer Lid ~~3.AD;~~3.4.4.3.3.3
			Top Lid ~~3.AH;~~3.4.4.3.3.5
03	D (water jacket)	1.168	~~3.AG;~~ 3.4.4.3.3.4
04	M (small and medium penetrant missiles)	2.65 (Side Strike); 1.35(End strike)	*Overpack* *3.4.8.1*
		1.23 (End Strike)	*HI-TRAC* *3.4.8.2.1*

† The symbols used for the loadings are defined in Table 2.2.13.

TABLE 3.4.6
MINIMUM SAFETY FACTORS FOR MPC COMPONENTS DURING TIP-OVER
45g DECELERATIONS

Component - Stress Result	MPC-24		MPC-68	
	0 Degrees	**45 Degrees**	**0 Degrees**	**45 Degrees**
Fuel Basket - Primary Membrane (P_m)	3.41 (852) ~~[3.T.1]~~	4.88 (852) ~~[3.T.7]~~	3.01 (1603) ~~[3.T.25]~~	4.36 (1603) ~~[3.T.31]~~
Fuel Basket - Local Membrane Plus Primary Bending (P_L+P_b)	1.43 (1012) ~~[3.T.2]~~	1.28 (132) ~~[3.T.8]~~	2.18 (1590) ~~[3.T.26]~~	1.44 (774) ~~[3.T.32]~~
Enclosure Vessel - Primary Membrane (P_m)	6.59 (1642) ~~[3.T.3]~~	6.72 (1766) ~~[3.T.9]~~	6.56 (2393) ~~[3.T.27]~~	6.86 (2377) ~~[3.T.33]~~
Enclosure Vessel - Local Membrane Plus Primary Bending (P_L+P_b)	1.98 (1203) ~~[3.T.4]~~	2.76 (1735) ~~[3.T.10]~~	1.10 (1925) ~~[3.T.28]~~	1.56 (1925) ~~[3.T.34]~~
Basket Supports – Primary Membrane (P_m)	6.73 (1096) ~~[3.T.5]~~	8.95 (1102) ~~[3.T.11]~~	7.15 (1710) ~~[3.T.29]~~	9.37 (1699) ~~[3.T.35]~~
Basket Supports - Local Membrane Plus Primary Bending (P_L+P_b)	3.57 (1096) ~~[3.T.6]~~	4.02 (1083) ~~[3.T.12]~~	1.18 (1715) ~~[3.T.30]~~	1.56 (1704) ~~[3.T.36]~~

Notes:

1. Corresponding ANSYS element number shown in parentheses.
2. ~~Corresponding appendix table shown in brackets (Relocated to Calculation Package).~~

TABLE 3.4.6 (CONTINUED)
MINIMUM SAFETY FACTORS FOR MPC COMPONENTS DURING TIP-OVER
45g DECELERATIONS

Component - Stress Result	MPC-32	
	0 Degrees	45 Degrees
Fuel Basket - Primary Membrane (P_m)	3.51 (715) ~~[3.T.13]~~	4.96 (366) ~~[3.T.19]~~
Fuel Basket - Local Membrane Plus Primary Bending (P_L+P_b)	1.51 (390) ~~[3.T.14]~~	1.28 (19) ~~[3.T.20]~~
Enclosure Vessel - Primary Membrane (P_m)	4.11 (1091) ~~[3.T.15]~~	5.59 (1222) ~~[3.T.21]~~
Enclosure Vessel - Local Membrane Plus Primary Bending (P_L+P_b)	1.11 (1031) ~~[3.T.16]~~	1.46 (1288) ~~[3.T.22]~~
Basket Supports - Primary Membrane (P_m)	3.44 (905) ~~[3.T.17]~~	4.85 (905) ~~[3.T.23]~~
Basket Supports - Local Membrane Plus Primary Bending (P_L+P_b)	1.30 (901) ~~[3.T.18]~~	1.71 (908) ~~[3.T.24]~~

Notes:

1. Corresponding ANSYS element number shown in parentheses.
2. ~~Corresponding appendix table shown in brackets (Relocated to Calculation Package).~~

TABLE 3.4.6 (CONTINUED)
MINIMUM SAFETY FACTORS FOR MPC24E COMPONENTS DURING TIP-OVER
45g DECELERATIONS

Components – Stress Result	*0 Degrees*	*45 Degrees*
Fuel Basket – Primary Membrane (P_m)	-10,050 (3.67)	-7,021 (5.26)
Fuel Basket – Primary Membrane plus Primary Bending ($P_L + P_b$)	31,912 (1.73)	30,436 (1.82)
Enclosure Vessel – Primary Membrane (P_m)	6,586 (6.59)	6,534 (6.65)
Enclosure Vessel – Primary Membrane plus Primary Bending ($P_L + P_b$)	23,100 (2.82)	17,124 (3.80)

Notes: 1. All stresses are reported in psi units and are based on closed gaps (primary stresses only).
2. The numbers shown in parentheses are the corresponding safety factors.

TABLE 3.4.7
STRESS INTENSITY RESULTS FOR CONFINEMENT BOUNDARY - INTERNAL PRESSURE ONLY

Locations (Per Fig. 3.4.11)	Calculated Value of Stress Intensity (psi)	Category	Table 3.1.13 Allowable Value (psi)†	Safety Factor (Allowable/Calculated)
Top Lid				
A	1641	$P_L + P_b$	26,300	16.0
Neutral Axis	20.2	P_m	17,500	866.3
B	1605	$P_L + P_b$	26,300	16.39
C	687	$P_L + P_b$	26,300	38.3
Neutral Axis	731	P_m	17,500	23.9
D	2960	$P_L + P_b$	26,300	8.89
Baseplate				
E	19,683	$P_L + P_b$	30,000	1.5
Neutral Axis	412	P_m	20,000	48.5
F	20,528	$P_L + P_b$	30,000	1.5
G	9,695	$P_L + P_b$	30,000	3.1
Neutral Axis	2,278	P_m	20,000	8.8
H	8,340	$P_L + P_b$	30,000	3.5

† Allowable stress intensity at 500 degrees F (top) and 300 degrees F (bottom)

TABLE 3.4.7 (CONTINUED)
STRESS INTENSITY RESULTS FOR CONFINEMENT BOUNDARY - INTERNAL PRESSURE ONLY

Locations (Per Fig. 3.4.11)	Calculated Value of Stress Intensity (psi)	Category	Table 3.1.13 Allowable Value (psi)†	Safety Factor (Allowable/Calculated)
Canister				
I	6,860	P_m	17,500	2.55
Upper Bending Boundary Layer Region	7,189 7,044	$P_L + P_b + Q$ $P_L + P_b$	52,500 26,300	7.30 3.73
Lower Bending Boundary Layer Region	43,986 10,621	$P_L + P_b + Q$ $P_L + P_b$	60,000 30,000	1.36 2.82

† Allowable stress intensity at 500 degrees F (top) and 300 degrees F (bottom)

TABLE 3.4.8
PRIMARY AND SECONDARY STRESS INTENSITY RESULTS FOR CONFINEMENT BOUNDARY - PRESSURE PLUS THERMAL LOADING

Locations (Per Fig. 3.4.11)	Calculated Value of Stress Intensity (psi)	Category	Allowable Stress Intensity (psi)	Safety Factor (Allowable/Calculated)
Top Lid				
A	1,630	$P_L + P_b + Q$	52,500	32.2
Neutral Axis	22.5	$P_m + P_L$	26,300	1,169.
B	1,604.1	$P_L + P_b + Q$	52,500	32.7
C	696	$P_L + P_b + Q$	52,500	75.5
Neutral Axis	731	$P_m + P_L$	26,300	36.0
D	2,960	$P_L + P_b + Q$	52,500	17.7
Baseplate				
E	19,798	$P_L + P_b + Q$	60,000	3.0
Neutral Axis	410.0	$P_m + P_L$	30,000	73.2
F	20,622	$P_L + P_b + Q$	60,000	2.9
G	4,789.4	$P_m + P_L + Q$	60,000	12.5
Neutral Axis	1,131.8	$P_m + P_L$	30,000	26.5
H	4,139.4	$P_L + P_b + Q$	60,000	14.5

TABLE 3.4.8 (CONTINUED)
PRIMARY AND SECONDARY STRESS INTENSITY RESULTS FOR CONFINEMENT BOUNDARY - PRESSURE PLUS THERMAL LOADING

Locations (Per Fig. 3.4.11)	Calculated Value of Stress Intensity (psi)	Category	Allowable Stress Intensity (psi)	Safety Factor (Allowable/Calculated)
Canister				
I	6,787.4	$P_m + P_L$	30,000	4.4
Upper Bending Boundary	4,200.5	$P_L + P_b + Q$	52,500	12.5
Layer Region	1,729.3	$P_m + P_L$	26,300	15.2
Lower Bending Boundary Layer Region	43,484	$P_L + P_b + Q$	60,000	1.4
	10,498	$P_m + P_L$	30,000	2.9

TABLE 3.4.9
SAFETY FACTORS FROM SUPPLEMENTARY CALCULATIONS

Item	Loading	Safety Factor	FSAR Location Where Details are Provided
HI-*STORM*~~TRAC~~ Top Lid Weld Shear	Tipover	3.326	*3.4.4.3.2.2*~~3.K~~
HI-STORM Lid Bottom Plate	End Drop	2.15	*3.4.4.3.2.3*~~3.M; 3.X~~
HI-STORM Lid Bottom Plate Welds	End Drop	1.36	*3.4.4.3.2.3*~~3.M~~
Pedestal Shi*eld*~~ell~~ Compression	End Drop	1.23	*3.4.4.3.2.3*~~3.M~~
HI-STORM Inlet Vent Plate Bending Stress	End Drop	1.69	*3.4.4.3.2.3*~~3.M~~
HI-STORM Lid Top Plate Bending	End Drop – 100 100S	5.29 1.658	*3.4.4.3.2.3*~~3.M~~
HI-TRAC Pocket Trunnion Weld	HI-TRAC Rotation	4.37	*3.4.4.3.3.1*~~3.AA~~
HI-TRAC 100 Optional Bolts - Tension	HI-TRAC Rotation	1.11	*3.4.4.3.3.1*~~3.AI~~
HI-STORM 100 Shell	Seismic Event	18.6	3.4.7
HI-TRAC Transfer Lid Door Lock Bolts	Side Drop	2.387	*3.4.4.3.3.3*~~3.AD~~
HI-TRAC Transfer Lid Separation	Side Drop	1.392	*3.4.4.3.3.3*~~3.AD~~
HI-STORM 100 Top Lid	Missile Impact	1.3~~35~~	*3.4.8.1*~~3.G~~
HI-STORM 100 Shell	Missile Impact	2.65	*3.4.8.1*~~3.G~~
HI-TRAC Water Jacket –Enclosure Shell Bending	Pressure	1.17	*3.4.4.3.3.4*~~3.AG~~
HI-TRAC Water Jacket – Enclosure Shell Bending	Pressure plus Handling	1.15	~~Subsection~~ 3.4.4.3.3.1
HI-TRAC Water Jacket – Bottom Flange Bending	Pressure	1.434	*3.4.4.3.3.4*~~3.AG~~
HI-TRAC Water Jacket - Weld	Pressure	1.42	*3.4.4.3.3.4*~~3.AG~~
Fuel Basket Support Plate Bending	Side Drop	1.82	*3.4.4.3.1.8*~~3.Y~~
Fuel Basket Support Welds	Side Drop	2.00	*3.4.4.3.1.8*~~3.Y~~
MPC Cover Plates in MPC Lid	Accident Condition Internal Pressure	1.39	*3.4.4.3.1.8*~~3.Y~~
MPC Cover Plate Weld	Accident Condition Internal Pressure	6.04	*3.4.4.3.1.8*~~3.Y~~
HI-STORM Storage Overpack	External Pressure	2.88	*3.4.4.5.2*~~3.AK~~
HI-STORM Storage Overpack Circumferential Stress	Missile Strike	2.49	3.4.8.1~~; 3.B~~
HI-TRAC Transfer Cask Circumferential Stress	Missile Strike	2.54	3.4.8.2.*1*~~; 3.AM~~
HI-TRAC Transfer Cask Axial Membrane Stress	Side Drop	2.09	~~3.Z;~~ 3.4.9.*1*

TABLE 3.4.10
INPUT DATA FOR SEISMIC ANALYSIS OF ANCHORED HI-STORM 100 SYSTEM

Item	Data Used		Actual Value and Reference
Cask height, inch	231.25		231.25" (Dwg. 1495)
Contact diameter at ISFSI pad, inch	146.5		146.5 (Dwg. 3187)
Overpack empty, wt. Kips	270		267.87 (Table 3.2.1)
Bounding wt. of loaded MPC, kips	90		88.135 (Table 3.2.1)
Overpack-to-MPC radial gap (inch)	2.0		2.0' (Dwg. 1495, Sheets 2 and 5)
Overpack C.G. height above ISFSI pad, inch	117.0		116.8 (Table 3.2.3)
Overpack with Loaded MPC - C.G. height above ISFSI pad	118.5		118.5 (Table 3.2.3)
Applicable Response Spectra	Fig. 3.4-31 to 3.4-36		Figures 3.4-30
ZPA:	RG 1.60	Western Plant	
Horizontal 1	1.5	1.45	
Horizontal 2	1.5	1.45	Site-Specific
Vertical	1.5	1.3	
No. of Anchor Studs	28		Up to 28
Anchor Stud Diameter			
Inch	2.0		2.0 (BOM 3189)
Yield stress, ksi	80 (minimum)		Table 1.2.7
Ultimate stress, ksi	125 (minimum)		Table 1.2.7
Free length, inch*	16-42		Site-specific
Pre-load tensile stress, ksi*	55-65		55-65

*For the confirmatory dynamic analyses, bolt spring rates were computed using the maximum length, and the preload stress was slightly above 60.1 ksi. For the static analysis, all combinations were evaluated.

Numerical integration is performed using the Kutta-Merson integrator which offers options for variable or fixed time-step and error bounding.

The Working Model Code is commercially available. Holtec has performed independent QA validation of the code (in accordance with Holtec's QA requirements) by comparing the solution of several classical dynamics problems with the numerical results predicted by Working Model. Agreement in all cases is excellent.

Additional theoretical material is available in the manual: "Users Manual, Working Model, Version 3", Knowledge Revolution, 66 Bovet Road, Suite 200, San Mateo, CA, 94402.

DYNA3D

"DYNA3D" is a nonlinear, explicit, three-dimensional finite element code for solid and structural mechanics. It was originally developed at Lawrence Livermore Laboratories and is ideally suited for study of short-time duration, highly nonlinear impact problems in solid mechanics. DYNA3D is commercially available for both UNIX work stations and Pentium class PCs running Windows 95 or Windows NT. The PC version has been fully validated at Holtec following Holtec's QA procedures for commercial computer codes. This code is used to analyze the drop accidents and the tip-over scenario for the HI-STORM 100. Benchmarking of DYNA3D for these storage analyses is discussed and documented in Appendix 3.A.

3.6.3 ~~Appendices~~ *Appendix* Included in Chapter 3

3.A HI-STORM Deceleration Under Postulated Vertical Drop Event and Tipover

~~3.B HI-STORM 100 Overpack Deformation in Non-Mechanistic Tipover Event~~

~~3.C Response of Cask to Tornado Wind Load and Large Missile Impact~~

~~3.D Vertical Handling of Overpack with Heaviest MPC~~

~~3.E Lifting Trunnion Stress Analysis for HI-TRAC~~

~~3.F Lead Slump Analysis (HI-TRAC Side Drop)~~

~~3.G Missile Penetration Analysis for HI-STORM 100~~

~~3.H Missile Penetration Analysis for HI-TRAC~~

~~3.I HI-TRAC Free Thermal Expansions~~

~~3.J Deleted~~

~~3.K HI-STORM Tipover Lid Analysis~~

~~3.L HI-STORM Lid Top Plate Bolting~~

~~3.M Vertical Drop of Overpack~~

~~3.N Deleted. Information relocated to calculation package Element Listings for MPC24 Basket~~

~~3.O Deleted. Information relocated to calculation package Element Listings for MPC24 Enclosure Vessel~~

~~3.P Deleted. Information relocated to calculation package Element Listings for MPC32 Basket 3.Q Deleted. Information relocated to calculation package Element Listings for MPC32 Enclosure Vessel~~

~~3.R Deleted. Information relocated to calculation package Element Listings for MPC68 Basket 3.S Deleted. Information relocated to calculation package Element Listings for MPC68 Enclosure Vessel3.T Deleted. Information relocated to calculation package ANSYS FEA Results for MPC's~~

~~3.U HI-STORM 100 Component Thermal Expansions MPC 24~~

~~3.V HI-STORM 100 Component Thermal Expansions MPC 32~~

~~3.W HI-STORM 100 Component Thermal Expansions MPC 68~~

~~3.X Calculation of Dynamic Load Factors~~

~~3.Y Miscellaneous Calculations~~

~~3.Z HI-TRAC Horizontal Drop Analysis~~

~~3.AA HI-TRAC 125 Rotation Trunnion Weld Analysis~~

~~3.AB HI-TRAC Pool Lid Stress and Closure Analysis~~

~~3.AC Lifting Calculations~~

~~3.AD 125 Ton HI-TRAC Transfer Lid Stress Analysis~~

~~3.AE Global Analysis of HI-TRAC Lift~~

~~3.AF MPC Transfer from HI-TRAC to HI-STORM 100 Under Cold Conditions of Storage~~

~~3.AG Stress Analysis of the HI-TRAC Water Jacket~~

~~3.AH HI-TRAC Top Lid Separation Analyses~~

~~3.AI HI-TRAC 100 Rotation Trunnion Weld Analysis~~

~~3.AJ 100 Ton HI-TRAC Transfer Lid Stress Analysis~~

~~3.AK Code Case N-284 Stability Calculations~~

~~3.AL HI-TRAC Lumped Parameters for Side Drop Analysis~~

~~3.AM HI-TRAC 100 Transfer Cask Circumferential Deformation and Stress~~

~~3.AN DYNA3D Analyses of HI-TRAC Side Drops and Impact by a Large Tornado Missile~~

~~3.AO Not used.~~

~~3.AP Not used.~~

~~3.AQ HI-STORM 100 Component Thermal Expansions MPC 24E~~

~~3.AR Analysis of Transnuclear Damaged Fuel Canister and Thoria Rod Canister~~

~~3.AS Analysis of Generic PWR and BWR Damaged Fuel Containers~~

3.6.4 Calculation Package

In addition to the calculations presented in Chapter 3 ~~and the Appendices~~, supporting calculation packages have been prepared to document other information pertinent to the analyses.

The calculation packages contain additional details on component weights, supporting calculations for some results summarized in the chapter, and miscellaneous supporting data that supplements the results summarized in the FSAR Chapter 3. All of the finite element tabular data, node and element data, supporting figures, and numerical output for all fuel baskets are contained in the calculation package supplement supporting this revision of the FSAR.